

2014-01-01

Identification And Characterization Of Novel Anti-Leukemia And Anti-Lymphoma Compounds

Yahaira Santiago

University of Texas at El Paso, yahaira.santiago@gmail.com

Follow this and additional works at: https://digitalcommons.utep.edu/open_etd

 Part of the [Biology Commons](#)

Recommended Citation

Santiago, Yahaira, "Identification And Characterization Of Novel Anti-Leukemia And Anti-Lymphoma Compounds" (2014). *Open Access Theses & Dissertations*. 1346.

https://digitalcommons.utep.edu/open_etd/1346

This is brought to you for free and open access by DigitalCommons@UTEP. It has been accepted for inclusion in Open Access Theses & Dissertations by an authorized administrator of DigitalCommons@UTEP. For more information, please contact lweber@utep.edu.

IDENTIFICATION AND CHARACTERIZATION OF NOVEL ANTI-
LEUKEMIA AND ANTI-LYMPHOMA COMPOUNDS

YAHAIRA SANTIAGO VAZQUEZ

Department of Biological Sciences

APPROVED:

Renato J. Aguilera, Ph.D., Chair

Siddhartha Das, Ph.D.

Giulio Francia, Ph.D.

Luis Echevoyen, Ph.D.

Charles Ambler, Ph.D.
Dean of the Graduate School

Copyright ©

by

Yahaira Santiago Vazquez

2014

Dedication

To my family with all my love.

IDENTIFICATION AND CHARACTERIZATION OF NOVEL ANTI-
LEUKEMIA AND ANTI-LYMPHOMA COMPOUNDS

by

YAHAIRA SANTIAGO VAZQUEZ

DISSERTATION

Presented to the Faculty of the Graduate School of

The University of Texas at El Paso

in Partial Fulfillment

of the Requirements

for the Degree of

DOCTOR OF PHILOSOPHY

Department of Biological Sciences

THE UNIVERSITY OF TEXAS AT EL PASO

December 2014

Acknowledgements

I want to thank Dr. Renato J. Aguilera for the opportunity given to me for being part of his lab, for the guidance, and the confidence deposited on me. Additional appreciated guidance and mentoring was provided from Dr. Gudmundur Thordarson, Dr. Siddhartha Das, Dr. Giulio Francia, and Dr. Luis Echegoyen. Cell culture techniques and bioassays were possible thanks to the training offered by Dr. Armando Varela, Dr. Carolina Lema, and Ms. Gladys Almodovar from the Border Biomedical Research Center (BBRC) at the University of Texas at El Paso.

This research was also possible thanks to the collaboration with Dr. Jonathan R. Dimmock, Dr. Swagatika Das, Dr. Umashankar Das, and additional lab research team members at the Drug Discovery and Development Research Group in the College of Pharmacy at the University of Saskatchewan, and additional collaborators of Dr. Jonathan R. Dimmock. Thanks to Dr. Elisa Robles-Escajeda, Ms. Lina Hamdan, Ms. Nora Ortega, Ms. Almendra Muro, and Ms. Karla Parra for their time devoted in collaborating with some biosassays.

I am thankful for the funding provided by NIGMS RISE (training: 5 R25 GM069621-10) and NIGMS (grant: ISC3GM10371, BBRC: 8G12MD007592). Thanks to Dr. Elizabeth Walsh, Ms. Elizabeth Quezada, and the RISE graduate students for the assistance offered in the RISE Program.

Days were full of happiness thanks to Alfredo, Almendra, Jonathan, Jose, Nora, Yoshira, Karla, Ruben, Sarah, Lisett, Diego, and Denisse. Thank you, Alfredo Roman, for helping me edit the dissertation.

Abstract

The anti-cancer properties of curcumin, the natural yellow pigment in the roots of turmeric (*Curcuma longa*), have been extensively described over the last century. It has been shown to interfere with multiple cell signaling pathways, including execution of apoptosis, anti-proliferation, anti-angiogenic, and anti-inflammatory properties. However, curcumin's cytotoxic potential is limited when administered *in vivo*. With the idea of preserving curcumin's characteristics, but improving its bioavailability, analogues have been developed and evaluated in the last decade. Most of the analogues have shown very good anti-cancer activity in various cell lines and one analogue is now in a clinical trial. Nonetheless, this analogue acts through redox-dependent mechanism in MDA-MB-231 human breast cancer cells and DU-145 human prostate cancer cells and causes necrosis in some lymphoid cancerous cells. Thus, the main scope of my research has been the identification and characterization of a lead curcumin analogue, from a library of compounds, as a potent apoptotic agent against leukemia and lymphoma.

Table of Contents

Acknowledgements.....	v
Abstract	vi
Table of Contents.....	vii
List of Tables	xi
List of Figures.....	xii
Chapter 1: Curcumin and its analogues against cancer.....	1
1.1 Brief history of cancer	1
1.2 Chemicals, viruses, bacteria, and lifestyles as etiologic agents of cancer	3
1.3 DNA repair mechanisms during genomic and epigenomic alterations	7
1.4 Tumor suppressor genes and the immune system are allies in getting rid of cancer ..	11
1.5 Past and present cancer statistics	12
1.6 Advances in therapeutic treatments and cancer prevention	13
Chapter 2: Novel 3,5-bis(arylidene)-4-oxo-1-piperidinyl dimers: Structure-.....	24
activity relationships and potent antileukemic and antilymphoma.....	24
cytotoxicity	24
2.1 Introduction	24
2.2 Results.....	26

2.3 Discussion	27
2.4 Conclusions	33
2.5 Experimental	33
2.5.1 Synthesis of series 3-5	33
2.5.2 Statistical analyses	34
2.5.3 Evaluation of 3-5 against Molt4/C8, CEM, HeLa, and L1210 cells	34
2.5.4 Evaluation of 3b, c, e-h, 4b, c, e, f and 5 against some lymphoma, leukemic, breast, prostate and nonmalignant cells	34
2.5.5 Evaluation of 3a-d, g, 4a, c, e, g, i and 5 against a panel of human tumor cells	35
2.5.6 The induction of phosphatidylserine externalization, caspase activation, and depo- rization of the mitochondrial membrane potential in CEM cells by 3f and 4f.....	35
2.5.7 Phosphatidylserine externalization assay	35
2.5.8 Caspase-3 assay	36
2.5.9 Mitochondrial membrane polarization assay	36
2.6 Appendix	47
Kendall's coefficient of concordance.....	56
Chapter 3: A novel curcumin analogue sensitizes leukemia and lymphoma cells to apoptosis via increased TNF- α and DAPK1 expression.....	60
1.1 Introduction	60

3.2	Methods.....	63
3.2.1	Curcumin analogue synthesis and reagents.....	63
3.2.2	Cell lines and culture conditions	63
3.2.3	Screening assays (DNS and MTS)	65
3.2.4	Image acquisition and analysis for DNS assay	66
3.2.5	Generation of dose-response curve and determination of CC50 value	67
3.2.6	Apoptosis assay	67
3.2.7	Mitochondrial membrane potential assay	67
3.2.8	Caspase-3/7 and -8 activity assays	68
3.2.9	RNA extraction and RT-PCR array.....	68
3.2.10	Western blots	69
3.2.11	ELISA assay	70
3.2.12	Statistical Analysis.....	70
3.3.	Results and Discussion	70
3.3.1	Identification of a novel potent curcumin analogue	70
3.3.2	NC2496 induces apoptosis at low micromolar concentrations	71
3.3.3	NC2496 induces programmed cell death through TNF- α and DAPK-1	72
3.4	Conclusions	74
3.5	Appendix.....	83

Summary and conclusions91

Vita101

List of Tables

Table 1.1: Number of new cancer cases and deaths (2014)	21
Source: SEER 2014 Cancer Statistics Factsheets: All Cancer Sites. National Cancer Institute. Bethesda, MD, http://seer.cancer.gov/statfacts/html/all.html	21
Table 2.2: Evaluation of 3a-g, 4a, c, e, g, i and 5 against some human tumor cell lines. a	41
Table 1. Evaluation of 3b,c,e-h, 4b,c,e,f and 5 against various lymphoma and leukemic cell lines ^a	58
Table 2. Evaluation of 3b,c,e-h, 4b,c,e,f and 5 against some breast and prostate cancer cells and nonmalignant cells ^a	59
Table 3.1: Anticancer activity of the analogue against some hematological cancer cell lines ^a ...	75
S. Table 3.1: Regulation of anti-apoptotic and apoptotic genes by NC2496.	84
S. Table 3.2: Regulation of apoptotic and anti-apoptotic genes by NC2496 ^a	87
S. Table 3.3: Primers designed for RT-PCR confirmation.....	90

List of Figures

Figure 1.1: Hypothetical model of the stages in tumor development.	17
Figure 1.2: DNA composition.	18
Figure 1.3: From DNA to protein.	19
Figure 1.4: Hypothetical karyotype in cancer.....	20
Figure 1.5: Apoptosis induction of curcumin analogues compared to curcumin.	22
Figure 1.6: Toxicity of curcumin analogues on normal lymphocytes.	23
Figure 2.1: The structures of the compounds in series 1 and 2.	37
Figure 2.2: The structures of the analogues 3-5.....	38
Figure 2.3: Heat map illustrating the toxicity of the compounds.	40
Figure 2.4: 3f and 4f induce apoptotic cell death in a human CEM T-lymphocyte cell line as detected by phosphatidylserine externalization.	42
Figure 2.5: 3f and 4f induce apoptotic cell death via caspase-3 activation in the CEM T lymphocyte cell line	44
Figure 2.6: 3f and 4f mediated cytotoxicity appears to be initiated via mitochondrial $\Delta\Psi_m$ disruption in CEM T-cells.	46
Figure 3.1: Pharmacophore utilized to synthesize the analogues.	75
Figure 3.2: The effect of NC2496 in Jurkat and Nalm-6 cell lines.....	76
Figure 3.3: Apoptotic cell death indicators.	77
Figure 3.4: Gene-expression profiling during NC2496 and curcumin-induced apoptosis.	79
Figure 3.5: DAPK-1 and TNF- α proteins are the expression products of NC2496 cell death induction.....	80
Figure 3.6: Proposed cell death mechanism of NC2496.....	81

S. Fig. 3.1: Discovery of cytotoxic curcumin analogues against hematological malignancies...83

Chapter 1: Curcumin and its analogues against cancer

This first chapter describes what cancer is and proposes curcumin analogues as therapeutic agents. Before being able to describe cancer treatments, it is essential to first understand the nature of cancer. Furthermore, statistics and developing strategies to fight and prevent cancer are presented.

1.1 Brief history of cancer

The first documented emergence of cancer was back in 1500 B.C. in Egypt, where eight cases of breast lumps and the applied treatment were described on a papyrus [1]. The methods used to destroy the lumps were surgical removal and cauterization. Around 400 B.C., Hippocrates described large masses or lumps protruding from breasts, neck, or nose of people. The lumps resembled the rough exterior and hardness of crabs, thus Hippocrates named the lumps as *karkinos* [2]. Hippocrates hypothesized that an excess of black bile caused these protuberances. He also observed that some masses were not life-threatening. While dissecting and describing breast cancer lumps, Galen of Pergamon (131-201, A.D.), found swollen veins all around the masses. Around 47 B.C., cancer was considered a disease and was Aulus Cornelius Celsus who coined the latin term *karkinoma* to designate it. In antiquity, the causes of cancer and its many types were unknown and observations were only made about one visible stage of the disease.

In modern times, cancer is defined as a broad group of pathologies involving different stages (unregulated cell growth, invasion, and metastasis). The progress of biology throughout the years has revealed that cancer is developed by the accumulation of mutations in the DNA of normal cells. Thus, mutations are responsible for the changes that make the cells grow in an uncontrolled way. These mutations ultimately alter cell receptors, cell signaling pathways, cell division, and survival rates. These combinations of alterations stimulate uncontrolled cell proliferation forming a lump of cells called tumor. Thus, tumors can be classified into malignant

and benign. Malignant tumors invade nearby parts of the body and later spread to more distant parts of the body through the lymphatic system or bloodstream (Fig. 1.1). Benign tumors do not invade neighbor tissues and do not spread throughout the body. Although, benign tumors are not considered cancerous, because they lack the ability to spread; they can become cancerous as well. If a tumor is left untreated, it can spread causing a series of different health complications; for these reasons it is considered that cancer comprehends a group of diseases.

The basis of cancer would not have been able to be elucidated without major previous discoveries made on the genetic material. In 1860, deoxyribonucleic acid (DNA) was first discovered by Friedrich Miescher and later in 1944 Oswald Avery and colleagues proved that DNA is the chemical entity in which the genetic information is carried [3]. Nine years later, Watson and Crick elucidated the double-helical structure of DNA. Interconnected nucleotides form the DNA structure and each nucleotide is formed by a phosphate group, a deoxyribose sugar, and a single nitrogenous base (Fig.1.2). We also know that there are two basic categories of nitrogenous bases: the purines (adenine [A] and guanine [G]), each with two fused rings, and the pyrimidines (cytosine [C], thymine [T], each with a single ring. A decade later, François Jacob and Jacques-Lucien Monod postulated that base sequences in the DNA double helix coded information for the construction of proteins. Also, that the specific sequence of those bases in the DNA precisely determine the sequence of amino acids in proteins [4]. The sequence of amino acids in turn determines the unique structure and function of each type of protein. Therefore, the specification of amino acid sequence, which is accomplished by base sequences in the DNA, provides almost all the information that is required to construct a protein (Fig. 1.3). Only about 1.5% of a mammal's genomic DNA carries sequence information that encodes the structures of proteins and the other 98.5% of DNA is known to be "noncoding" stretches in the genome called junk DNA [5]. Following these discoveries, the discipline of molecular biology grew up delivering solutions to understand how the genetic constitution of cells and organism determines its appearance and function. Thus, molecular biology and genetics offered a better understanding

of how cancer arises. Further findings helped in the understanding of the causative factors of cancer. These findings lead to the conclusion that a small number of alterations in the genetic material are needed for carcinogenesis [6]. Now we better understand that cancer originates with the accumulation of alterations or mutations in our genetic material (Fig. 1.4). Alfred G. Knudson thus postulated in 1971 the “two hit hypothesis” to explain that two mutations are at least necessary to sufficiently affect the genome and promote cancer formation [7]. One of these mutations should be a germ line mutation (inherited from parents and contained in the germ cells) and the other one a somatic mutation (accumulated along our life in any part of the body). The hereditary and nonhereditary forms of cancer entail the same number of events as well. Therefore, cancer can develop when two somatic mutations occur or two germ mutations are inherited. These mutations comprise a wide range of alterations like deletions, translocations, and amplifications of DNA caused by environmental factors, lifestyles, oncogenes, viruses, or bacteria.

1.2 Chemicals, viruses, bacteria, and lifestyles as etiologic agents of cancer

Cancer can originate from the exposure to certain chemicals and environmental agents. This was early noticed by the English physician John Hill, who in 1761 associated the excessive use of tobacco with the development of nasal cancer [8]. Fourteen years later, Percivall Pott, a surgeon in London, reported a considerable number of patients with cancer of the scrotum [9]. All of these patients had worked in their youth as chimney sweepers. Within three years, the Danish sweeper’s organization urged its members to remove well with water and soap the coal tar from their skin. This practice markedly lowered the rate of scrotal cancer in Europe. In 1916, Katsusaburo Yamagiwa, a Japanese pathologist, succeeded in experimentally inducing cancer in rabbits by painting their ears with coal tar [10]. In 1925, British chemists were successful in purifying several components of coal tar that were particularly carcinogenic, as demonstrated by the ability of these compounds to induce cancer on laboratory mice. Additional products of combustion and causative agents of cancer, such as polycyclic aromatic hydrocarbons (3-

methylcholanthrene, benzo[a]pyrene, and 1,2,4,5dibenz[a,h anthracene) were subsequently found in the condensates of cigarette smoke as well [11], [12]. All these discoveries realized at the end of the nineteenth century, made clear that chemical exposure was in part the cause of a number of types of cancer and that even occupational exposure was correlated with specific types of cancer. These findings suggested that certain chemical species that come in contact with the human body could perturb tissues and cells and ultimately induce the emergence of a tumor. Since then, it was also thought that chemical species present naturally in foodstuffs or generated during cooking could also induce cancer. It was not until the 1960's when William Lijinsky decided to test this by broiling steaks in charcoal, ultimately finding 8 micrograms of benzo[a]pyrene per kilogram of broiled steak [12]. Lijinsky continued his research on processed food finding other sorts of carcinogens such as nitrosamides, nitrosamines, and nitrites.

Since 1761, it was determined that certain chemicals were carcinogens, however, the biological explanation for these incidents was unknown until studies in the field of genetics initiated. In 1927, the geneticist Hermann Joseph Muller discovered that exposure of *Drosophila melanogaster* to X-rays induced mutations in the DNA of the flies' cells [13]. This event led Muller to carry out studies on the mechanisms of the gene mutation, thus being able to explain how genes rearranged.

Further epidemiologic correlations made in 1949 and 1950, among smokers and nonsmokers, gave the most compelling association between environmental exposure and cancer incidence. Two groups of epidemiologists reported that individuals who were heavy cigarette smokers were more than twenty times in risk of developing lung cancer than nonsmokers [14], [15]. These findings proved to be critical for subsequent cancer research, since they suggested that cancers often had specific, assignable causes. Indeed, in reports from 1950-2000, epidemiologists identified a variety of environmental and lifestyle factors that were strongly correlated with the incidence of certain cancers; in some of these cases, researchers have been able to discover the specific biological mechanisms through which these factors act to cause

increased incidence of some of these cancers. In order to study the biological reasons for cancer initiation and development, researchers decided to recreate cancer in the laboratory. Thus, cancerous cell lines were established by treating laboratory animals with various carcinogens found in coal tar and petroleum products [16]. Tumors were isolated from the animals and grown *in vitro* in supplemented media. An extensive assortment of cancerous cell lines have also been established from tumors removed from patients. Some of these cell lines are still in use today to study mechanisms of cellular death resistance and for testing chemotherapeutic drugs. It is from these tumor cell lines that we have gained most of our contemporary knowledge of cancer.

Another independent line of research surged during the first decade of the twentieth century to find explanation for the initiation of cancer. These scientists hypothesized that not only chemicals or lifestyles were responsible of cancer, but other agents influenced initiation of cancer as well. Francis Peyton Rous, a pathologist, was one of the pioneers who in 1910 discovered a virus to be a tumor causing agent [17]. A farmer brought him a chicken with a lump in the chest. He removed the tumor and identified it as a sarcoma tumor type that was growing on the chicken. He cleaned the tumor from other cells, minced, and filtered the disrupted cells in saline solution, the isolated filtrate (free from bacteria and cancerous cells) was transferred to another healthy chicken and later the animal developed a tumor. He removed the tumor from this other chicken and repeated the same experiment in other healthy chicken. He repeated this many times discovering that the tumor was more aggressive each time. He concluded that an infectious agent was responsible for the tumors. At this time viruses were not well understood and the causes of cancer were not completely elucidated. Twenty years later, Richard Shope, a colleague of Rous, discovered the papilloma virus in rabbit's warts [18]. It was confirmed that the Papillomavirus (HPV) was responsible of warts. Rous returned to his experiments and was able to isolate the Rous sarcoma virus (RSV) confirming and concluding this was the etiologic agent of sarcoma. After this, a wide variety of viruses able to induce cancer were found. For example, various DNA (i.e. Hepatitis B virus, adenovirus, and herpesvirus) and RNA (i.e. Human T-cell

Leukemia Virus) tumor viruses were discovered. Even a virus with the ability to induce a variety of distinct tumor types was discovered in 1953, and was named Polyomavirus [19].

Viruses are generally simple in structure, composed of nucleic acid (DNA or RNA) wrapped in a protein coat (a capsid) and, in some cases, a lipid membrane surrounds the capsid. When isolated, viruses are metabolically inert. They can multiply only by infecting and parasitizing a suitable host cell. The viral genome, once introduced into the cell, provides the instructions for the synthesis of progeny virus particles. The host cell provides the machinery required for viral replication and transcription. The endpoint of the replication cycle is the production of hundreds, even thousands of progeny virus particles that can then leave the infected cell and proceed to infect other susceptible cells. The way viruses cause tumors is by activation or addition of oncogene copies into the host genome. Viruses can be carriers of oncogenes that were part of a previous host's genome or can insert into the vicinity of a cellular oncogene functioning as a positive transcriptional regulator and thus activating the tumorigenic potential of the cellular gene [20]. This is typically a slow process and requires prolonged and extensive viral replication and integration. In the same way, viruses can affect the proper expression of tumor suppressor genes by inserting and interfering with original DNA sequences [21].

About one-fifth of deaths from cancer worldwide are associated in one way or other with infectious agents [22]. Fifty to seventy-five percent (50-75%) of stomach cancer mortality worldwide is attributable to long-term infections with *Helicobacter pylori* (*H. pylori*), fifty to seventy percent (50-70%) of hepatocellular carcinoma cases worldwide are associated with chronic hepatitis B and C virus infections, and Human Papilloma Virus has been implicated in 99.7% of cervical squamous cell cancer cases worldwide [23], [24], [25]. Cancer can be portrayed as an environmental and/or infectious disease, since the evidence gathered from cancer research asserts that physical, chemical, environmental agents, bacteria, and viruses are causative agents of cancer.

A more concrete example on the dependence of cells on their surrounding is in the case of stomach and intestinal cells in direct contact with normal flora and pathogens. As previously mentioned, *H. pylori*, is considered the most common etiologic agent of infection-related cancers. In some individuals, *H. pylori* colonization does not cause any symptoms, but long-term carriage of *H. pylori* significantly increases the risk of developing gastric cancer. Among infected individuals, approximately 10% develop peptic ulcer disease, and of those 1 to 3% develop gastric adenocarcinoma, and <0.1% develop mucosa-associated lymphoid tissue (MALT) lymphoma [26]. How exactly *H. pylori* causes gastric cancer is by the expression of cytotoxin-associated gene A (CagA) protein that leads to gastric epithelial cell proliferation and carcinoma via the Wnt signaling pathway [26], [27].

The close relationship and dependence of cells on their surroundings have been demonstrated experimentally. This has been nicely illustrated by the behavior of normal cells [26] when they are removed from living tissues and propagated *in vitro*. Even though the liquid medium used to culture normal cells contains all the nutrients required to sustain their growth and division, including amino acids, vitamins, glucose, and salts, such medium, on its own, it does not support the proliferation of normal cells. Instead, cell proliferation depends upon the addition of serum to the medium, usually prepared from the blood of calves or fetal calves [28]. This serum contains the growth factors that promote cellular proliferation. Growth factors, such as cytokines and hormones, convey many of the signals that tie the cells within a tissue together into a single community, all members of which are in continuous communication with their neighbors. Thus, agents surrounding the cells are important to consider as etiologic factors in cancer development.

1.3 DNA repair mechanisms during genomic and epigenomic alterations

Non-cancerous mammalian cells contain well-organized chromosomes which in metaphase visibly consist of two sister chromatids attached at the centromere. The number, sizes, and shapes of the metaphase chromosomes are particular to each pair. In contrast, cancerous cells

exhibit aberrantly structured chromosomes of various sorts (Fig.1.4) [6]. These mutated cells can contain extra copies of chromosomes; can show the loss of entire chromosomes, and the fusion of the arm of one chromosome with another [29]. These changes in chromosomal configuration directly contribute to genetic instability and to the alteration of gene expression [30]. All these sorts of mutations arise and kept on cancerous cells as consequence of inefficient gene regulation and repair mechanisms.

The chromosomes of healthy cells may undergo changes in their structure, but these changes are detected, reverted, and repaired. Endogenous and exogenous events can inflict damage to the cell's genome and can severely compromise its integrity [31]. Thus, to counteract these damaging effects and maintain the genomic integrity, three major conserved cellular pathways have evolved [32]. One is the DNA damage response, which ensures efficient repair of all types of damage. DNA damage can include different sorts of translocations and inversions. Chromosomal translocations result when DNA segments from one chromosomal arm and become fused to the arm of another chromosome [33]. There is another type of chromosomal translocation termed reciprocal translocation that results when chromosomal segments are exchanged between different chromosome pairs and each chromosome receives a segment. A chromosomal segment may also become inverted, which may affect the regulation of genes that are located near the breakage-and-fusion points. The second pathway to correct DNA damage is the chromosome replication pathway which accurately governs the replication of DNA. Single base-pair substitutions, for example, can occur during DNA replication. A well-structured chromosome replication pathway is so essential because only a point mutation in the DNA sequence of a proto-oncogene is all that is required to convert a normal gene into a potent oncogene [34]. Point mutations can affect the structure of proto-oncogene-encoded proteins too, converting them into active oncoproteins. Cellular receptors (which are made of protein) once mutated can be potent causative agents of cancer. Amplification and overexpression of receptor genes can be accomplished also by the insertion of oncogenes or virus in the promoter region of

the gene. In other instances, these receptors are always “ON” continuously transmitting signals for cell division even in the absence of growth factors that turn “ON” the growth receptors. As an important example, there is the epidermal growth factor receptor (EGF-R) that extends from the extracellular space through the plasma membrane of cells into the cytoplasm. Normally, EGF-R, like almost all other 60 similarly structured receptors, in resting state is in an auto-inhibitory conformation and its kinase domain in the inactive form. Presence of its cognate ligand (i.e., EGF protein) in the extracellular space induces receptor mediated dimerization that brings the intracellular domains into close proximity, promoting the association of kinase domains and a signaling cascade is activated in the cell interior [35]. In response to these signals, a gene is transcribed for the production of more EGF proteins for cellular growth. The catalytic activity of EGFR is tightly regulated in normal cells by protein-tyrosine phosphatases, by other protein tyrosine or serine/threonine kinases, and by autoregulatory mechanisms [36]. When the EGFR gene contains point mutations at exons 19 and 21 the coded EGF protein behaves in a different way. These EGFR mutations affect the resting state conformation of the receptor causing receptor dimerization and the auto-activation of the EGFR pathway promoting EGFR-mediated pro-survival signals to downstream targets [37]. The third pathway to correct DNA, is the chromosome segregation pathway which preserves the correct number of chromosomes during cell division. There are occasions in which also the produced DNA copies may be fused head-to-tail forming a chromosomal segment that is termed homogeneously staining region (HSR). A DNA segment may also be cleaved out of a chromosome, replicated as an autonomous extra chromosomal entity, and increase to many copies per nucleus, resulting in the appearance of sub chromosomal fragments termed double minutes (DMs). These latter two changes cause increases in the copy number of genes carried in such segments, resulting in gene amplification [38]. Sometimes, both types of amplification can coexist in the same cell and independently favor the growth of cells by increasing the copy number of growth-promoting genes. All this three cellular

pathways exhibit crosstalk, forming a network in which disruption of one pathway leads to engagement of the others to protect genome integrity while maintaining cell homeostasis.

Further genomic alterations of DNA leading to cancer consist also on the elimination of growth-inhibiting genes (tumor suppressor genes). These can be accomplished by deletions and methylations. When a segment in the middle of a chromosomal arm is discarded and the flanking chromosomal regions are joined, this results in an interstitial deletion (Fig.1.4). Thus, deletions cause incomplete or multiple coding sequences for protein synthesis consequently altering cellular function. This is exemplified by retinoblastomas (RBs), which mRNA transcripts are either markedly reduced in quantity or are abnormal in length. About 40% of RBs are caused by DNA deletions and accordingly affect mRNA transcript [39]. Thus, absence or non-biological functional RB protein leads to cancer.

Additional alterations in gene expression include epigenetic modifications. These are stable alterations in gene expression that takes place during cell proliferation and occur without causing changes in gene sequence. DNA methylations constitute the most commonly occurring epigenetic modification and are also involved in cancer development [40]. DNA methylations are covalent chemical modifications, resulting in the addition of a methyl (CH_3) group at the 5' carbon of the cytosine ring. Methylations in DNA prevent the binding of polymerases for DNA transcription leading to gene silencing. In cancer, tumor suppressor genes are often hypermethylated leading to cell proliferation and ultimately cancer. Tumor suppressor genes are known to be antigrowth genes. Tumor formation seemed to happen when these genes are inactivated by methylations or are deleted. Another recognized cause of oncogenesis is hypomethylation. This epigenetic abnormality, discovered in 1983 and prior to hypermethylation, frequently occur in highly repeated DNA sequences [41]. Hypomethylation of transcription regulatory regions seems to be less frequent than hypermethylation of DNA promoter regions [42], [43]. Nonetheless, hypomethylations frequently take place in transcription control sequences, including heterochromatic DNA repeats, dispersed retro-transposons, and

endogenous retroviral elements [44], [45]. Hypomethylations of these regions may cause a gene's constant expression which can lead to cell proliferation and eventually cancer.

1.4 Tumor suppressor genes and the immune system are allies in getting rid of cancer

As discussed in the previous section, mammalian cells count with an elaborate cellular repair apparatus that continuously monitors the genome integrity and replaces mutant sequences of DNA with appropriate wild-type sequences. This repair apparatus maintains genomic integrity by minimizing the number of mutations that strike the genome of a particular cell [46]. Conversely, no system is infallible and some mistakes in genetic sequences can survive its scrutiny. Genome mistakes can become fixed in a particular cell at a particular time; nonetheless, prior to the repair, mutations can be copied into newly synthesized DNA molecules, and passed on as mutations to progeny cells. In this sense, many of the mutations that accumulate in the genome represent the consequences of occasional oversights made by the repair apparatus. Yet other mistakes are the results of significant damage to the genome that exceeds the capacities of the repair apparatus. Fortunately, there are other systems to get rid of cancer. These systems are the immune system and tumor suppressor genes that can work together to control cancer [47].

Evidence about the immune system's contribution in the elimination of cancerous cells has been rapidly accumulating. Thus, three fundamental roles of the immune system against cancer have been recognized and these are the following: (1) protection against pathogens that induce tumors, (2) elimination of inflammation, and (3). elimination of certain cancerous cells [48]. Not all cancerous cells or all pathogens are eliminated by the immune system, because these employ various strategies to evade detection and elimination. This in turn is aggravated by difficulties associated with the immune system's organization in recognizing what is self and what is strange or not-self [49]. However, there are features of cancerous cells that distinguish them apart from normal cells [50]. Tumors differ fundamentally from normal cells in antigenic composition and biologic behavior. Thus, they have multiple genetic alterations, epigenetic instability, and abnormal expression of growth factors that induce altered density in antigen

levels, inflammation, and ultimately invasion and metastasis. Some of these differences significantly impact the interaction between cancerous cells and the immune system perhaps representing a frailty of cancer, which can be exploited therapeutically.

Under these circumstances, immunological cells, such as Natural killer (NK) cells are able to recognize and kill cancerous cells that do not display normal levels of surface molecules like Major Histocompatibility Complex (MHC) I [51]. Once NK cells identify cancerous cells as targets for elimination, they release IFN- γ in the vicinity of the targeted cells. Released IFN- γ , in turn, elicits several distinct responses [52]. IFN- γ enables the NK cells to call in other types of immune cells to assist in killing targeted cancerous cells, thereby amplifying the immune system's response.

Another, line of evidence supporting the role of the immune system in protecting against cancer is the relationship between immunity and tumor suppressor genes. As an example, there is the tumor suppressor p53, which is well-known for its role in regulating apoptosis and the cell cycle, therefore maintaining the stability of the genome. In recent years, p53 has been adjudicated with additional biological functions including autophagy, fertility, nutritional responses, cell motility/migration, cell-cell communication, and regulation of the human immune system [53]. The expression of p53 upon DNA damage can trigger clearance of damaged cells or tumors via the innate immune system, as evidenced by in vitro and in vivo experiments [54]. Thus, the mechanism for this is still unknown, though believed to occur through NKG2D (Killer cell lectin-like receptor subfamily K, member 1 or CD314) system and up regulation of ULBP2 (NKG2D ligand 2) [55].

1.5 Past and present cancer statistics

In 2008, it was estimated that about 1,437,180 new cancer cases of the top ten cancer types were expected to be diagnosed, and about 565,650 people in the US were projected to die of cancer (SEER statistics, 2008). In 2014, it is estimated that in the US there will be 1,665,540 new cases of the top ten cancer types and an estimated 585,720 people will die of these diseases

(Table 1.1). Thus, there are 228,360 more expected cases and 20,070 more deaths for 2014 than in 2008. In Table 1.1 are shown the most common cancer types in the US and these are prostate, breast, lung, colon, melanoma, bladder, lymphoma, kidney, thyroid, and endometrial cancer. Among these, melanoma and thyroid cancer incidences and deaths account for the rise in cancer incidences and deaths for 2014.

Despite efforts in education, prevention, screenings, and investment on cancer research, statistics are telling us that cancer burden in the US is on the increase. In the US, cancer remains the second most common cause of death, accounting for nearly 1 of every 4 deaths since 2008 statistics (American Cancer Society, 2013). In comparison to the cancer estimates in 1991, an actual estimate has been reduced by about a 20% [56]. This short-lived declining trend could be in part attributed to disadvantages in anticancer therapies, population aging, lifestyle risk factors, (tobacco use, diet, obesity, lack of exercise, alcohol consumption, and excessive exposure to sunlight), environmental and occupational exposures to carcinogens and mutagens, (including chemicals and radiation), infectious agents (*Helicobacter pylori*, hepatitis B virus, hepatitis C virus, human papillomavirus, and Epstein-Barr virus), chronic inflammation, hormone metabolism, family history, ethnicity, and socioeconomic status [57]. Disadvantages of anticancer therapies include poor selectivity and resistance development having major concerns in poor prognosis [58]. Anticancer drugs with poor selectivity toward cancerous cells lead to toxicity and life-threatening negative side effects. Resistance to anticancer drugs originates from diverse genetic alterations evolved on cancerous cells. Therefore, significant reduction in the rates of cancer incidence and mortality requires further global education, lifestyle changes, collaborations among different institutions, and research on prevention, detection and treatment.

1.6 Advances in therapeutic treatments and cancer prevention

Improvements in anticancer therapies have been made possible by successfully combining different traditional therapeutic approaches and by discovering novel therapies. Traditional therapeutic approaches against cancer comprise radiation therapy, surgery, and

chemotherapy [59]. Development of vaccines, combined chemotherapies, and antibodies has been also improving outcomes among certain cancer types. Even more advances in techniques such as magnetic resonance imaging, ultrasonography, immunohistochemistry, and flow cytometry are offering early cancer detection and diagnosis. In addition, there is a growing amount of preventive strategies against cancer based on the discovery of phytochemicals in vegetables, fruits, roots and leaves and outcomes from the performance of physical exercise have also been identified.

The intense scientific studies on the properties of vegetables, fruits, roots, and leaves against cancer initiated around the 1990's [60]. Plant derived products offer antioxidants that act by avoiding oxidative damage of the cell and supporting the immune system [61], [62]. In addition to the benefits from nutrition, studies have shown the positive impact of moderate physical exercises as well for the prevention and survivorship of cancer. Exercise promotes reduced levels of insulin, glucose, sex hormones, and inflammation, and increases intestinal motility and immune system response [63], [64]. Nutritional and exercise strategies to fight cancer should be seriously implemented in our daily routines. In 2014 the World Health Organization (WHO) alerted about a global cancer surge fuelled by alcohol, smoking and obesity projecting a 70% of increase in cancer cases by 2032.

Indeed, novel anticancer drugs and more effective treatments are needed. Although the pharmaceutical industry will undoubtedly continue to develop new therapies against cancer, a contribution from the academic sector to the early drug discovery phases can guarantee the rapid identification of targets [65]. Industry alone cannot support the required breadth of drug discovery efforts, thus only by association with academic institutions can this be accomplished. With the purpose of contributing to anticancer drug discovery, we have evaluated the *in vitro* potential of hundreds of compounds developed by Dr. Jonathan R. Dimmock, Dr. Umashankar Das, Dr. Swagatika Das, and other collaborators. We have discovered that the most cytotoxic compounds among the library to be curcumin-like molecules with novel functional groups that

displayed greater toxicity to leukemia and lymphoma cells than to control non-malignant MCF10A and Hs-27 cell lines. These molecules were also found to exhibit little if any toxicity to other types of cancer cell lines such as those derived from breast, colon, and prostate cancers

1.7 Curcumin and its analogues against cancer

Discoveries of plant-based drugs with the ability of influencing multiple targets and showing reduced normal cell toxicity are desired. These effects may diminish therapy disadvantages and improve patient prognosis. In addition, drugs that are able to induce cancerous cell death at low micromolar concentrations, via apoptosis, and without disturbing normal cells have therapeutic advantages and thus are preferred [66]. These properties reduce drug dose, normal tissue toxicity, and inflammation.

From the dried roots of the *Curcuma longa* (turmeric) plant, we can obtain a class of compounds known as the curcuminoids, comprised of curcumin, demethoxycurcumin, bisdemethoxycurcumin, and cyclocurcumin [67]. Curcuminoids consist of two methoxylated phenols connected by two α , β unsaturated carbonyl groups. Curcumin is naturally available in turmeric as two chemical conformations the keto and enol with the enol conformation being more stable. Curcumin is the principal curcuminoid and comprises approximately 2-5% of turmeric. It is responsible for the yellow color of the spice as well as the majority of turmeric's therapeutic effects.

For years, curcumin has been an attractive natural therapeutic agent. Its value prevails on the interaction and regulation of multiple cellular targets, the ability to modulate growth and transcription factors' expression and activity, induction in the production of inflammatory cytokines, down-regulation of enzymes, and apoptosis induction without affecting non-cancerous cells. Preclinical and clinical trials have revealed that high doses of curcumin are non-toxic to humans or animals. However, phase I clinical trials have shown that curcumin failed as therapy due to its low bioavailability after its digestion [68]. Synthetic modifications to curcumin's molecule or the synthesis of analogues may overcome curcumin's deficiencies as a therapeutic

drug by making a molecule more potent and difficult to metabolize [69]. One of the major problems with curcumin is its low bioavailability *in vivo* [70]. The degradation kinetics and the stability of curcumin under various pH conditions were examined by Wang et al. [71]. Their results show that about 90% of curcumin was decomposed within 30 minutes when incubated in 0.1 M phosphate buffer and serum-free medium, pH 7.2, at 37°C. A series of pH conditions ranging from 3 to 10 were tested and the result showed that decomposition was pH dependent and occurred faster at neutral-basic conditions. Thus, it was found that curcumin is more stable in cell culture medium containing 10% fetal calf serum and in human blood. Under these conditions less than 20% of curcumin decomposed within 1 hr and, after incubation for 8 hrs, about 50% of curcumin still remained. The reasons for curcumin's reduced bioavailability are poor absorption and rapid metabolism severely diminishing its bioavailability as revealed by studies over the past decades [72]. To overcome the aforementioned conditions curcumin analogues have been developed.

The need for curcumin-like compounds with improved bioavailability has led to the chemical synthesis of a series of analogues, using curcumin as the lead structure. One such compound is EF-24, a synthetic curcumin analogue that showed cell cycle arrest and apoptosis by a redox-dependent mechanism in MDA-MB-231 human breast cancer cells and DU-145 human prostate cancer cells [73]. However the effect of EF-24 on lymphoid cancerous cell lines is more necrotic than apoptotic within 24 hrs of incubation. The curcumin analogues that we have characterized are more apoptotic than EF-24 (Fig. 1.5). Although, EF-24 is more bioavailable than curcumin [74], it shows more *in vitro* toxicity to normal peripheral blood mononuclear cells (PBMC's). The same effect has been observed with other curcumin analogues (Fig. 1.6). Thus, *in vivo* experiments on EF-24 or other analogues derived from curcumin show no cytotoxicity in animals [19], [20].

So far, we have characterized the cell death of interesting curcumin-like analogues able to induce significant cytotoxicity at low micromolar concentrations. They do kill cancerous cells through apoptosis and present selectivity for leukemia and lymphoma cells over other types of cancerous and normal cells. The following two chapters will present data on the relationship between structure and activity of 3,5-bis(arylidene)-4-oxo-1-piperidinyl dimmers against leukemia and lymphoma and on a novel curcumin analogue which sensitizes leukemia and lymphoma cells to apoptosis by induction of TNF- α and DAPK1.

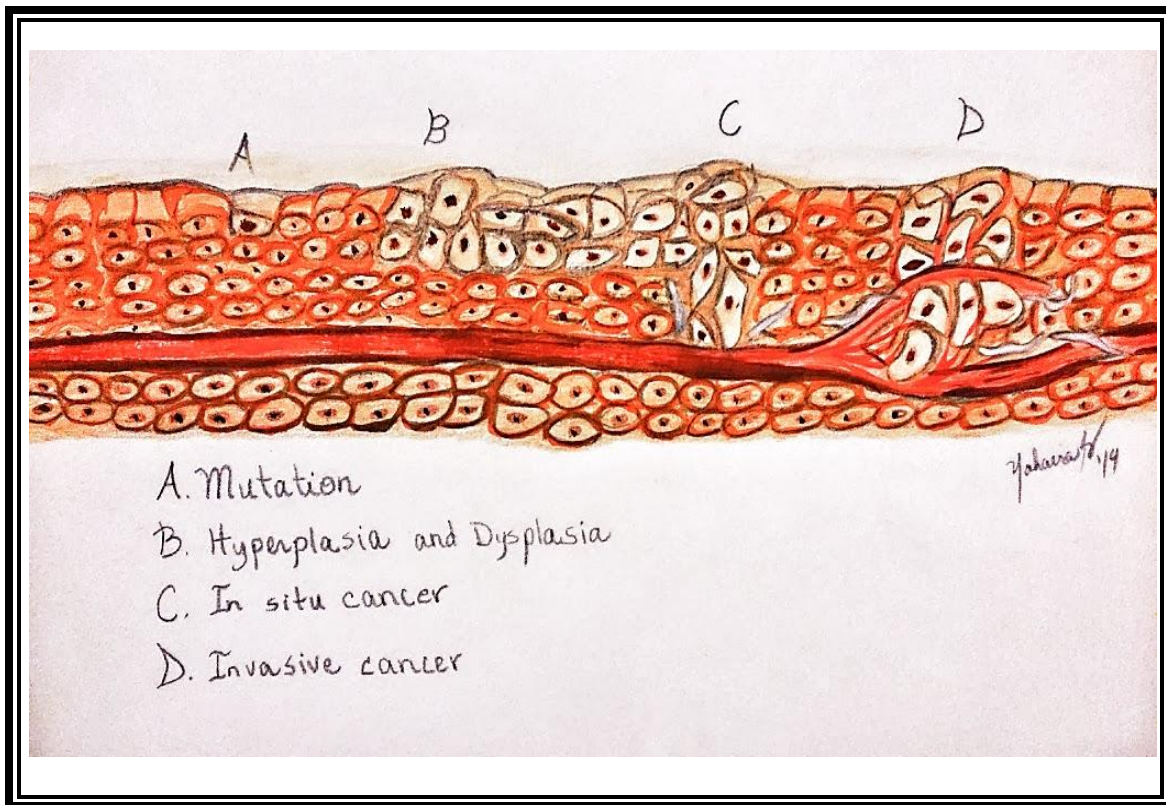


Figure 1.1: Hypothetical model of the stages in tumor development.

A. The tumor begins to develop when a cell experiences an uncorrected mutation. B. The altered cell divides too often (hyperplasia) passing the mutation on to its progeny during cell growth and division. At some point, one of these cells experiences another mutation that further

increases its tendency to divide, thus looking abnormal in appearance (dysplasia). C. If the tumor that has formed from these cells is still contained within its tissue of origin, it is called in situ cancer. In situ cancer may remain contained indefinitely. D. If some cells experience additional mutations and recruit stromal cells (i.e. pericytes or endothelial cells) that allow the tumor to invade neighboring tissues and shed cells into the blood or lymph, the tumor is said to be malignant. The escaped cells may establish new tumors (metastases) at other locations in the body.

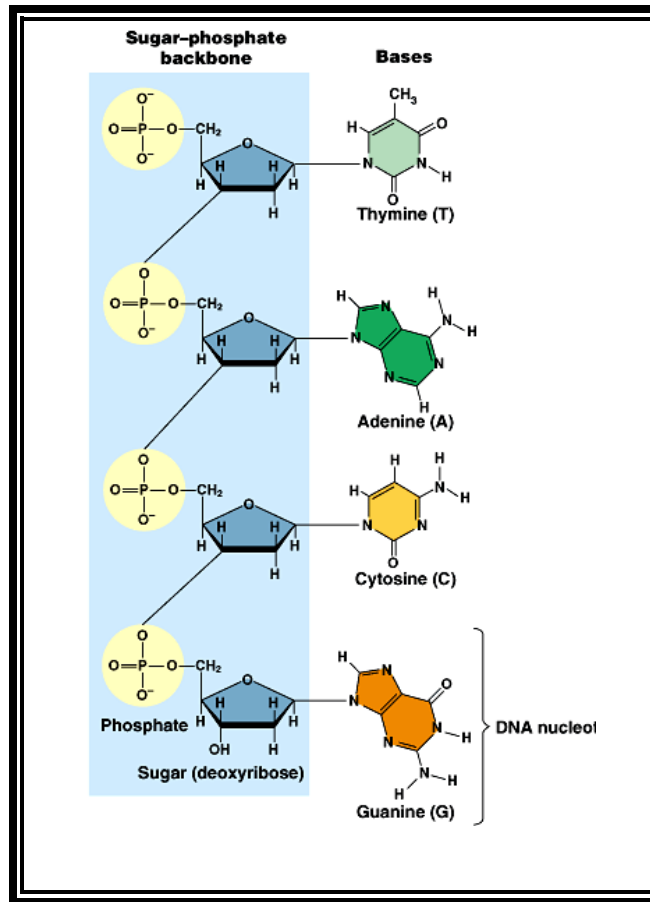


Figure 1.2: DNA composition.

DNA is composed of four different nitrogenous bases bonded to a sugar-phosphate backbone. Thus, bases can be classified into pyrimidines (thymine and cytosine) and purines (adenine and guanine). The nucleotides are covalently linked together in a chain through the

sugars and phosphates, which thus form a “backbone” of alternating sugar-phosphate-sugar-phosphate. Hydrogen bonds between the base portions of the nucleotides hold the two chains together. The three-dimensional structure of DNA, the double helix, arises from the chemical and structural features of its two polynucleotide chains.

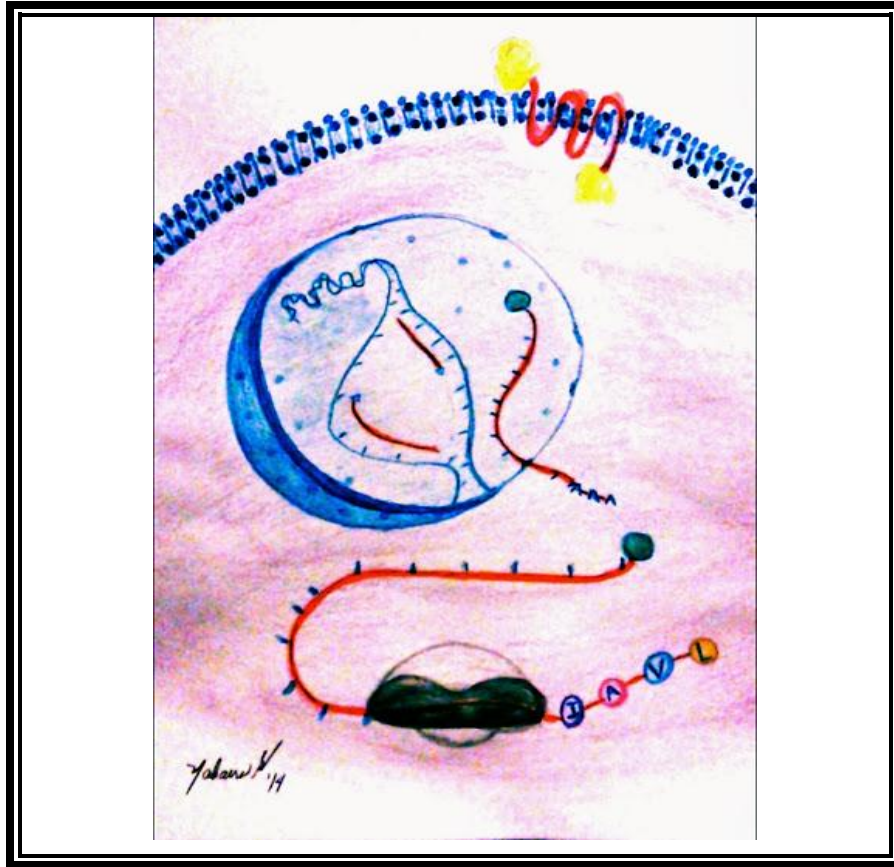


Figure 1.3: From DNA to protein.

Signals from the outside can stimulate cell membrane receptors to trigger cell division or protein synthesis. During cell division, both strands of DNA are replicated and passed to daughter cells. During protein synthesis, one of the strands is transcribed into pre-messenger RNA. Coding and noncoding regions of DNA are transcribed into pre-mRNA. Some regions are removed (introns) during initial mRNA processing. The remaining exons are then spliced together, and the spliced mRNA molecule (red) is prepared for export out of the nucleus through addition of an endcap (green sphere) and a polyA tail. Once in the cytoplasm, the mRNA can be

used to construct a protein. From this Central Dogma of Molecular Biology, it was determined that mutated DNA induces mutated proteins and malfunction of the cell, thus conducting to pathologies.

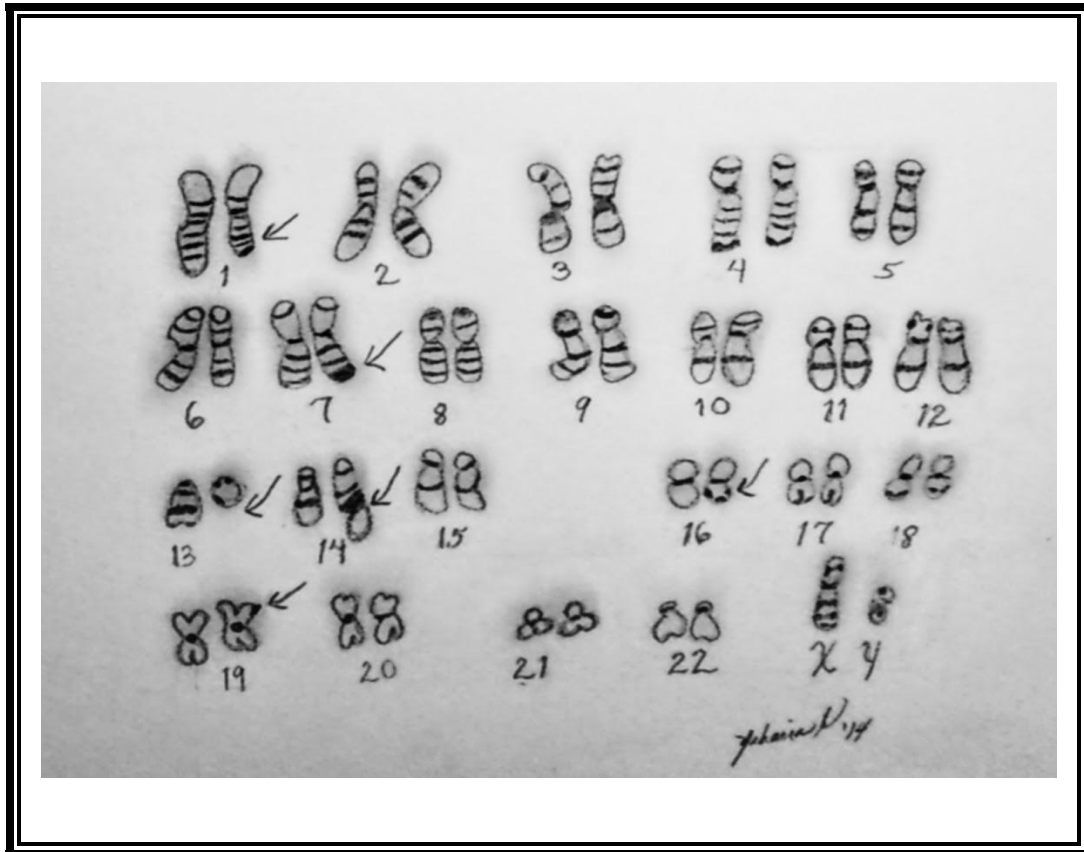


Figure 1.4: Hypothetical karyotype in cancer.

In humans, each cell normally contains 23 pairs of chromosomes, for a total of 46. The number, sizes, and shapes of the chromosomes are particular to each pair. In contrast, when there is extra or missing chromosome material, pathology is suspected. Thus, chromosome imbalances may occur because of a change in the number or structure of the chromosomes. Usually, differences in the amount of chromosome material can affect an individual's growth and development and may cause birth defects and/or mental retardation. In addition, an individual

with aberrantly structured chromosomes of various sorts can present cancer. The arrows indicate aberrant chromosomes with deletions or insertions.

Table 1.1: Number of new cancer cases and deaths (2014)

Common Types of Cancer	Estimated New Cases 2014	Estimated Deaths 2014
Prostate Cancer	233,000	29,480
Breast Cancer (Female)	232,670	40,000
Lung & Bronchus Cancer	224,210	159,260
Colon & Rectum Cancer	136,830	50,310
Melanoma of the Skin	76,100	9,710
Bladder Cancer	74,690	15,580
Non-Hodgkin Lymphoma	70,800	18,990
Kidney and Renal Pelvis Cancer	63,920	1,820
Thyroid Cancer	62,980	1,890
Endometrial Cancer	52,630	8,590
-	-	-
All Cancer Sites	1,665,540	585,720

Source: SEER 2014 Cancer Statistics Factsheets: All Cancer Sites. National Cancer Institute. Bethesda, MD, <http://seer.cancer.gov/statfacts/html/all.html>

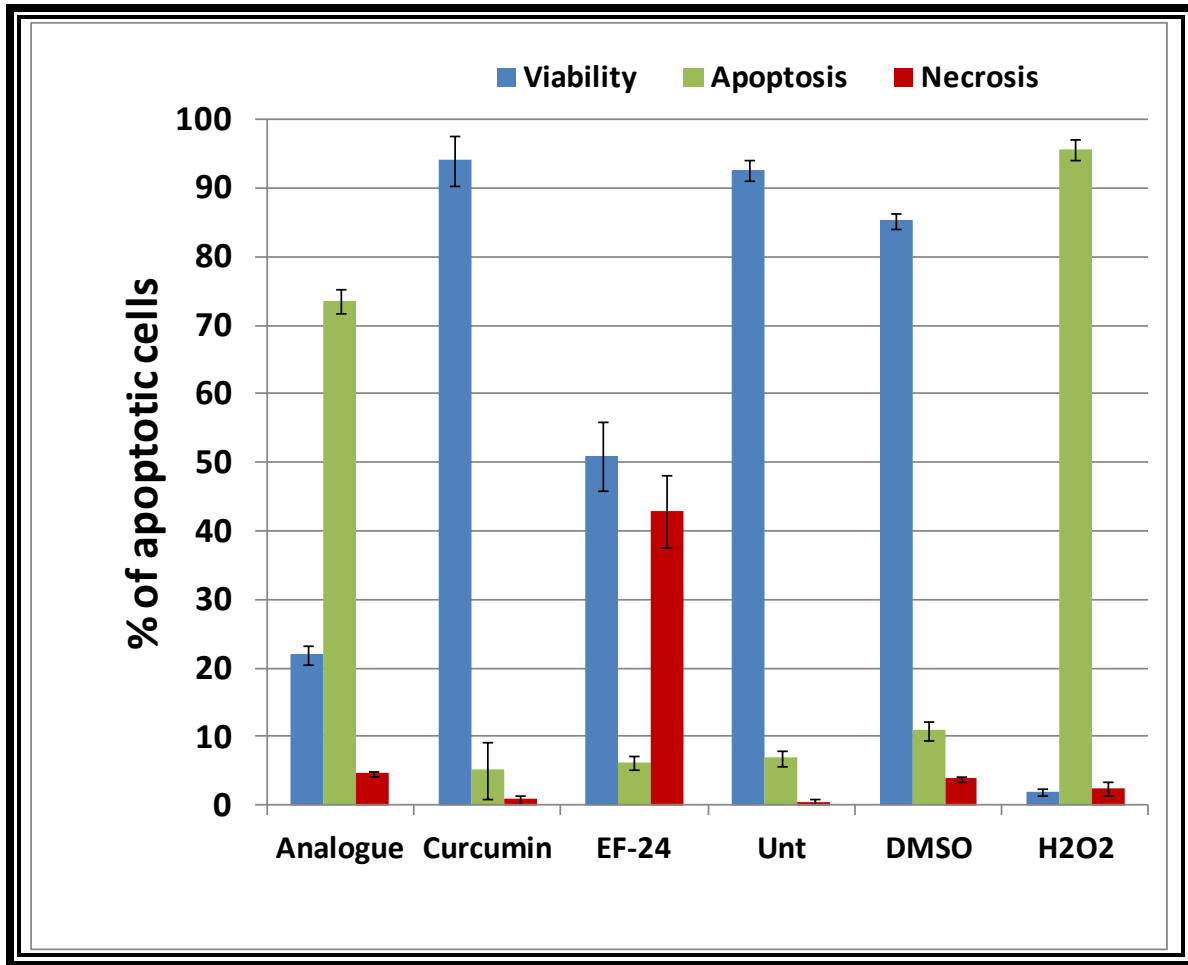


Figure 1.5: Apoptosis induction of curcumin analogues compared to curcumin.

When tested at 1 μ M for 24 hrs curcumin is not effective killing lymphoid cancerous cells. Its analogues EF-24 and an analogue synthesized by Dr. J.R.Dimmock (University of Saskatchewan) show more cytotoxic potential. The analogue synthesized by the group in Saskatchewan show more apoptotic capabilities than EF-24, a known curcumin analogue in clinical trial.

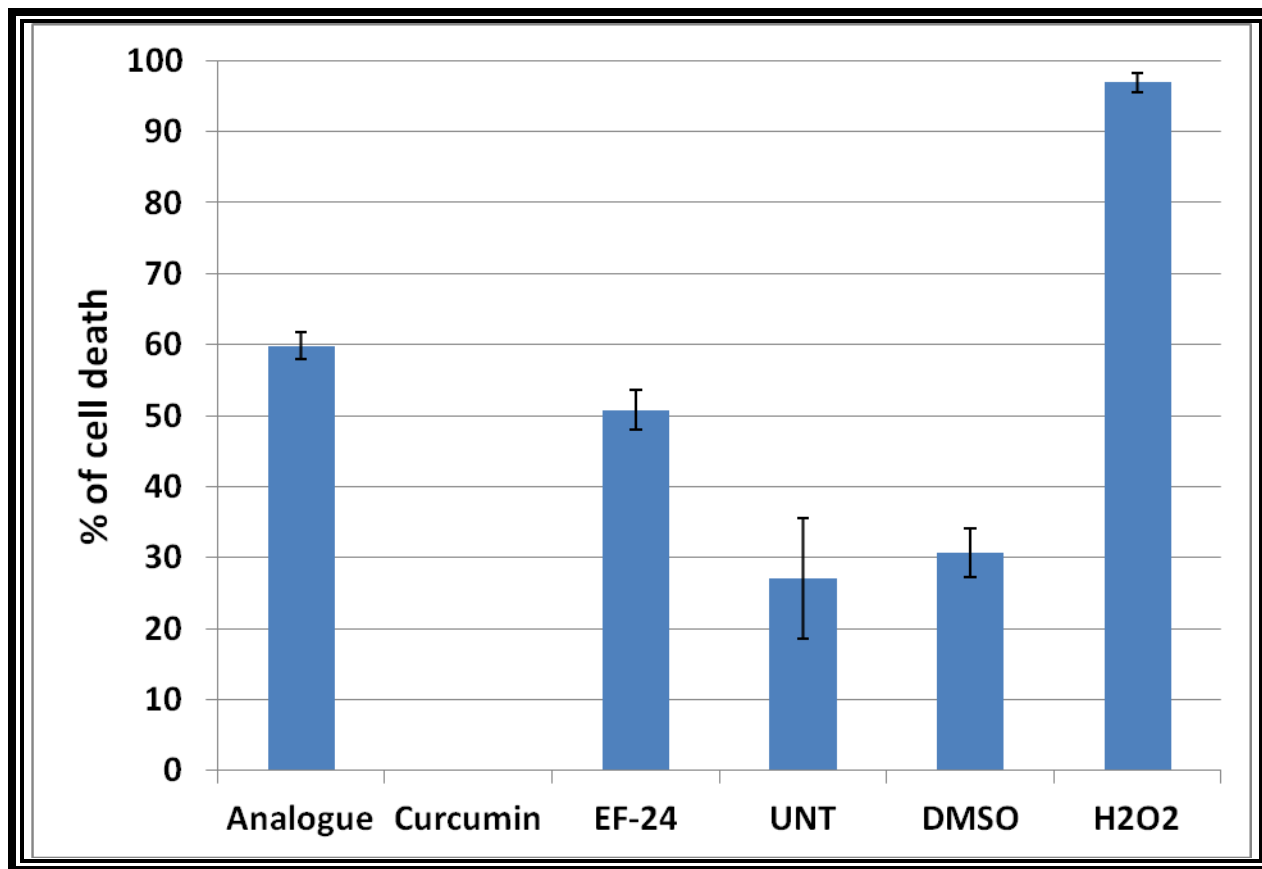


Figure 1.6: Toxicity of curcumin analogues on normal lymphocytes.

When tested at 1 μ M for 24 hrs curcumin shows not toxicity on normal peripheral blood mononuclear cells (PBMC's). However, its analogues EF-24 and an analogue synthesized by Dr. J.R.Dimmock (University of Saskatchewan) induce toxicity to the cells.

Chapter 2: Novel 3,5-bis(arylidene)-4-oxo-1-piperidinyl dimers: Structure-activity relationships and potent antileukemic and antilymphoma cytotoxicity

Novel clusters of 3,5-bis(benzylidene)-4-oxo-1-piperidinyl dimers 3e5 were evaluated against human Molt4/C8 and CEM T-lymphocytes and human HeLa cervix adenocarcinoma cells as well as murine L1210 leukemia neoplasms. Several of these compounds demonstrated IC50 values in the submicromolar and low micromolar range and compounds possessing 4-fluoro, 4-chloro and 3,4,5-trimethoxy substituents in the series 3 and 4 were identified as potent molecules. A heat map revealed the very high cytotoxic potencies of representative compounds against a number of additional leukemic and lymphoma cell lines and displayed greater toxicity to these cells than nonmalignant MCF10A and Hs-27 neoplasms. These dienones are more refractory to breast and prostate cancers. The evaluation of representative compounds in series 3e5 against a panel of human cancer cell lines revealed them to be potent cytotoxins with average IC50 values ranging from 0.05 to 8.51 mM. In particular, the most potent compound 4g demonstrated over 382-fold and 590-fold greater average cytotoxic potencies in this screen than the reference drugs, melphalan and 5-fluorouracil, respectively. A mode of action investigation of two representative compounds 3f and 4f indicated that they induce apoptosis which is due, at least in part, to the activation of caspase-3 and depolarization of the mitochondrial membrane potential.

2.1 Introduction

The principal interest in our laboratories is the design, synthesis and antineoplastic evaluation of conjugated unsaturated ketones. The perceived importance of these compounds is their ability to interact preferentially with thiols in contrast to amino and hydroxyl groups [75], [76] which are present in nucleic acids. Thus the genotoxic properties displayed by various alkylating agents in cancer chemotherapy [77] may well be absent in conjugated enones. Initially

compounds containing one α,β -unsaturated group were prepared which demonstrated cytotoxic and anticancer properties [78]. However, a number of studies showed that an initial chemical insult followed by a second interaction with cellular constituents can be more harmful to tumors than nonmalignant cells [79], [80], [81]. Hence an additional conjugated enone group was introduced into the design of candidate cytotoxins leading to the mounting of the 1,5-diaryl-3-oxo-1,4-pentadienyl pharmacophore onto a number of heterocyclic and carbocyclic scaffolds such as series 1 as indicated in Fig. 2.1. In these compounds the capacity for sequential alkylation of cellular thiols now exists.

In recent years a novel cluster of cytotoxic agents were developed possessing two 1,5-diaryl-3-oxo-1,4-pentadienyl groups which have the general structure 2 as indicated in Fig. 2.1. In this way multiple sequential alkylations of cellular thiols can take place. Most of the compounds displayed micromolar or submicromolar IC₅₀ and CC₅₀ values against various neoplastic cell lines [82], [83]. In general, the greatest potencies were found in those compounds with the shortest linker group X between the two piperidinyl nitrogen atoms. From these studies, two compounds possessing oxalyl and malonyl linkers were identified as the most promising cytotoxic agents and are referred to as 3a and 4a, respectively. An initial study examined the compounds in series 3-5, against HCT116 and HT29 human colon cancer cells [84]. In general, these compounds are potent cytotoxins having IC₅₀ values less than 1 μ M in 78% of the bioassays and are substantially more potent than 5-fluorouracil which is used clinically in treating colon cancers. These encouraging results justify the further bioevaluation of series 3-5.

The next phase of the study was threefold. 1. An examination of the effects of placing different substituents into the aryl rings of 3a and 4a on cytotoxic potencies was proposed. The variations in the electronic, hydrophobic and steric properties of the aryl substituents may enable correlations between these physicochemical properties and cytotoxic potencies to be established. The groups chosen had either positive (+) or negative (-) Hammett σ and Hansch π values namely 4-fluoro, 4-chloro and 3,4-dichloro (+,+), 4-methyl and 4-dimethylamino (-,+), and 3,4-

dimethoxy, 3,4,5-trimethoxy and 4-methoxy (-,-). In addition, there are substantial differences in the sizes of the aryl groups. For example, the molar refractivity (MR) values of the 4-fluoro and 3,4,5-trimethoxy groups are 0.92 and 23.61, respectively [85]. 2. The aspiration was made to gain some idea of the sensitivity of these compounds towards human lymphomas and leukemia cancers and if tumor selectivity compared to normal cells was demonstrated. 3. An investigation was planned to find some of the ways in which promising lead compounds exert their antineoplastic effects.

The overall objective is that these investigations will enable one or more promising prototypic cytotoxic molecules to be identified which will be developed from the prospective of their drug-likeness properties [86] (see Fig. 2.2).

2.2 Results

The syntheses of 3a and 4a has been described previously [82] and a literature method was used for the preparation of 3b-i, 4b-i and 5 [84]. In brief, various aryl aldehydes were condensed with 4-piperidone to produce the corresponding 3,5 bis(benzylidene)-4-piperidones. Acylation of these dienones with oxalyl or malonyl chlorides gave rise to series 3 and 4, respectively. Reaction of 3,5-bis(benzylidene)-4-piperidone with 1,3-dibromopropane led to the synthesis of 5.

The dienones 3aei, 4aeh and 5 were evaluated against human Molt4/C8 and CEM T-lymphocytes, human cervix carcinoma HeLa cells and murine L1210 leukemic cells. These results are presented in Table 1. The results of the cytotoxic evaluation of 3b, c, e-h, 4b, c, e, f and 5 against a number of lymphomas as well as breast and prostate cancer cell lines are presented as a heat map in Fig. 2.3 while a summary of these bioevaluations is portrayed in Appendix Tables S1 and S2. In addition, 3a-d, g, 4a, c, e, g, i, and 5 were evaluated against a panel of human cancer cell lines including human colon cancer and leukemic cell lines and these results are summarized in Table 2.2.

The modes of action of the dienones 3f and 4f in CEM cells were also investigated. Both compounds induce cell death via apoptosis, activate caspase-3 and depolarize the mitochondrial membrane potential. These results are presented in Figs. 4-6, respectively.

2.3 Discussion

The dienones 3a-i, 4a-h and 5 were evaluated against non-adherent Molt4/C8 and CEM T-lymphocytes as well as adherent HeLa adenocarcinoma cells with a view to determine if the compounds displayed efficacy towards human transformed and neoplastic cells. In addition, compounds which are cytotoxic to non-adherent cells may have the potential to inhibit the growth of tumors with metastatic potential. The murine L1210 assay was employed as a number of anticancer drugs are toxic to this cell line [87] and hence this bioassay may point to compounds with clinical utility.

The biodata presented in Table 1 reveals that the majority of the compounds are potent cytotoxins. No less than 39% of the IC₅₀ values are submicromolar and in particular the IC₅₀ figures of 3b, c, g and 4f, g are submicromolar in all four bioassays. In the case of 3b, g and 4a, g, the IC₅₀ values in the Molt4/C8 screen are in the double digit nanomolar range (10^{-8} M) and are clearly lead molecules. Furthermore, the relative cytotoxic potencies of the compounds in series 3 and 4 were verified against the four neoplastic cell lines using Kendall's coefficient of concordance [88]. This nonparametric test is based on ranks and ignores the magnitude of the differences in the potencies of groups of compounds. The derivation of the equation used in these determinations is given in the Appendix Section. The relative potencies of 3a-i are the same in the Molt4/C8, CEM, HeLa and L1210 bioassays since Kendall's coefficient of concordance is 0.9812 ($p = 0.0001$). A similar situation prevails among the analogs 4a-h; in this case, Kendall's coefficient is 0.9315 ($p = 0.0005$). Furthermore, when all of the dienones in series 3 and 4 are considered, the relative potencies are the same as revealed by Kendall's coefficient of 0.9504 ($p < 0.0001$). Thus it is likely that these alkylating agents which are designed to target thiol macromolecules e.g., glutathione, cysteine, thioredoxin reductases and glutathione S-transferase

isozymes appear to act with the same molecular targets in all four cancer cell lines. The variations in potencies include differences in the alignment of the compounds at their binding sites.

In order to make some specific observations regarding the effects of placing different substituents in the aryl rings on cytotoxic potencies, the average IC₅₀ values in the four bioassays presented in Table 1 were computed. Both 3c and 4c possess a para chloro group and display excellent potencies; however the addition of a metachloro atom leading to 3d and 4d brings about 45- and 38-fold decreases, respectively, in the average IC₅₀ values. Very interestingly, the replacement of a para chloro group in 3c and 4c by a methoxy group led to 3h and 4h, respectively that were virtually inactive. On the other hand, the addition of a meta methoxy group to 3h and 4h leading to 3f and 4f increased potencies by 25- and >1038-fold, respectively. Still greater increases in potencies were noted with the 3, 4, 5-trimethoxy analogs 3g and 4g whose average potencies are the highest among the compounds in series 3-5. The replacement of a chloro group in 3c by a fluoro group (3b) in series 3, lead to an increase in the average cytotoxic potency by over 2-fold. The relative cytotoxic potencies of the compounds in series 3 and 4 which have different para substituents are F > Cl > H > CH₃ > OCH₃ and H > Cl > CH₃ > F > OCH₃, respectively. This observation reveals that in addition to the electronic, hydrophobic, and steric properties of the aryl substituents, the nature of the linker groups between the piperidinyl nitrogen atoms influences the magnitude of the IC₅₀ values. This point is further illustrated in comparing the biodata between 4a and 5. Compound 5 which possesses no carboxamide group is 5-fold less potent than 4a, suggesting that the two carbonyl groups in carboxamide group present in 4a contribute to the cytotoxic potencies observed. Linear and semilogarithmic plots between the σ , π , and MR constants of the aryl substituents in series 3 and 4 and the IC₅₀ values generated in each of the four bioassays were undertaken. However no correlations ($p < 0.05$) or trends toward a correlation ($p < 0.1$) were noted. The mean of the average potencies of 3a-h and 4a-h are 16.9 and >53.8 μ M, respectively, revealing that

compounds in series 3 are more potent than the series 4. If the data for the two outliers 3h and 4h are discounted, the relevant figures are 5.39 and 6.66 μM , respectively. Hence the oxalyl linker in series 3 is marginally preferred in terms of potency.

Comparisons were made between the cytotoxic properties of the compounds in series 3-5 and two reference compounds, melphalan and curcumin. Melphalan is an alkylating agent used in cancer treatment, while there is considerable interest at the present time in curcumin as an antineoplastic agent [89]. The IC₅₀ values of 3-5 are lower than the figures for melphalan in 53% of the comparisons made. Curcumin contains an arylidene keto and aryl vinyl groups and therefore bears some structural similarity to the compounds in series 3-5. In 72% of the comparisons made, the IC₅₀ values of 3-5 were lower than the figures for curcumin. In particular, the average IC₅₀ values of 3g and 4g are 13.5 and 14.2 times lower than the figure for melphalan and are 63.8 and 66.8 times more potent than curcumin.

An evaluation of the biodata was undertaken with a view to determine if the compounds varied in their potency towards each of the four cell lines. In other words, is tumor-selectivity observed? The average IC₅₀ values of 3a-g, 4a-g and 5 (the outliers 3h, i and 4h are omitted) towards Molt4/C8, CEM, HeLa and L1210 cells are 2.79, 6.62, 6.24 and 7.70 μM , respectively. Thus clearly Molt4/C8 cells are more sensitive to 3a-g, 4a-g and 5 than CEM, HeLa and L1210 cells while the murine L1210 neoplasms are the most refractory. In general, tumor-selectivity was demonstrated. The importance of this observation is that compounds which vary in their potencies to different cells may have the capacity to display greater toxicity to tumors than nonmalignant cells.

The biodata in Table 1 are encouraging and thus the extent to which representative compounds are effective against other neoplasms was addressed. Many of the analogs in series 3-5 are effective against Molt4/C8 and CEM T-lymphocytes and L1210 leukemic cells. Hence the cytotoxic potencies of representative compounds against T-cell derived lymphoma and leukemic cell lines (Jurkat, CEM, SUP-T, HUT-102, Molt-3 and EL-4) were compared with B-

cell derived lymphoma and leukemic cells (Nalm-6, Raji, Ramos and BJAB). In addition, the YT neoplasm, which is a natural killer-like leukemic cell line, was included in the array of cell lines. In view of the high mortalities caused by breast and prostate cancers, the efficacy of various analogs against several of these neoplastic cell lines was considered viz breast (MCF-7, MDA-231 and HCC70) and prostate cancers (DU145, 22rv1 and LAPC4). Two non-transformed cell lines were also utilized in order to observe the relative toxicity towards nonmalignant tissues namely breast epithelial cells (MCF10A) and foreskin fibroblasts (Hs-27). The cells are of human origin except for murine EL-4 cells and are non-adherent except for the breast, prostate and Hs-27 cell lines which are adherent in nature.

The results obtained for representative compounds in series 3-5 are presented as a heat map in Fig. 3 while specific figures are available in Appendix Tables 2.1 and 2.2. The following figures in parentheses are the average of the percentage of dead cells caused by 3b, c, e-h, 4b, c, e, f and 5 towards one or more cell lines. The following generalizations of the data obtained were made. First, Fig. 2.3 reveals clearly the greater lethality of the compounds towards lymphoma and leukemic cell lines (49.8) than either breast (11.9) or prostate (19.7) cell lines. The most sensitive cells are Jurkat (81.9), CEM (78.3) and Ramos (76.9). In addition, the compounds are more effective against B-cells (59.0) than T-cells (48.6). Secondly, the cytotoxic potencies of the lymphatic and leukemic cells (49.8) and to a lesser extent the DU145, 22rv1 and LAPC4 prostate cancers (19.7) compare favorably with the non-toxic effects of the compounds on the non-transformed Hs-27 control cell line (7.33). On the other hand, the toxicity of the compounds towards MCF-7, MDA -231 and HCC70 breast cancer cells (11.9) is similar to the effect on the MCF10A cell lines (8.50). Thirdly, somewhat surprising is the extent of cell death of the lymphoma and leukemic cells being influenced more by the cell line than the structures of the compounds as may be observed in Fig. 3. Thus the average percentage of dead lymphoma and leukemic cells was within the relatively narrow range of 43.0e58.3. The most potent compounds towards leukemia and lymphoma cells are 3f (58.3), 4e (56.4), 4f (53.4) and 3g (52.5) suggesting

the importance of the 3,4-dimethoxy aryl substitution pattern present in 3f and 4f to cytotoxicity. One may also note that the two most potent compounds towards prostate cancers are 3f (39.8) and 4f (30.0). In summary, the compounds are toxic against a range of leukemic and lymphoma cells which are non-adherent and therefore these compounds may have the capacity to combat metastasis. In addition, the relatively low toxicity towards nonmalignant MCF10A and Hs-27 cells is encouraging.

The data generated in this study for the compounds in series 3-5 is that a number of these dienones display marked cytotoxic potencies for various leukemia and lymphoma cell lines. A previous study indicated that many of these compounds are very toxic towards human HCT116 and HT29 colon cancer cells [87]. Thus the next phase of the current investigation consisted of examining additional colon cancers and leukemic cells in order to confirm their potency to these tumors. Representative compounds in series 3-5 were evaluated against approximately 59 human tumor cell lines from nine different neoplastic conditions, viz leukemia, melanoma and non-small cell lung, central nervous system, colon, ovarian, renal, prostate, and breast cancers [84]. Some of these data are presented in Table 2.2.

The results obtained confirm the marked cytotoxic potencies of most of the compounds towards colon cancer cells. With regard to the IC₅₀ values towards the five colon cancer cell lines, no less than 86% are submicromolar and 29% are in the double digit nanomolar range. The most potent compounds are 3g and 4g displaying average IC₅₀ values of 70 and 60 nM, respectively, which are 121 and 141 times lower, respectively, than 5-fluorouracil which is used clinically in treating colon cancers. The same compounds have marked antileukemic properties as the data in Table 2 reveals. In this case, the IC₅₀ values are submicromolar and in the double digit nanomolar range in 86% and 50% of the bioassays, respectively. The most potent compounds are also 3g and 4g with average IC₅₀ figures of 40 and 30 nM, respectively, which are 1418 and 1890 times lower than the average IC₅₀ value of melphalan which is used in

treating various leukemias. In addition, 4c is a useful antileukemic lead compound displaying an average IC₅₀ value of 40 nM indicating that 4c has more than double the potency of 3c.

The final segment of this investigation was directed to gaining some ideas of the way in which representative compounds caused cytotoxicity. The dienones 3f and 4f were chosen which have the same aryl substituents but differ in the nature of the X-linker group. Many antineoplastic agents exert their cytotoxicity by causing apoptosis [85]. Hence in order to explore this possibility, CEM cells were treated with 3f and 4f for 24 h and the results were determined by flowcytometry using annexin-FITC and Propidium stains. The results, which are portrayed in Fig. 4, revealed that both 3f and 4f induce apoptosis and to a lesser extent necrosis. One may also note that the extent of apoptosis and necrosis caused by 3f and 4f differs which may contribute to some of the variations in the cytotoxic potencies of these two compounds.

There are two principal apoptotic signaling pathways, namely the intrinsic mitochondrial and extrinsic death receptor routes. In the case of the mitochondrial pathway, apoptosis can be induced by different mechanisms some of which involve activation of caspases while others do not [90]. After incubation of CEM cells with either 3f or 4f, a cell permeable caspase-3 fluorogenic dye was employed. The intensity of the stain reveals the extent of caspase-3 activity in cells with intact cell membranes. The result is presented in Fig. 2.5 which reveals that both compounds activate caspase-3 which is an important way by which apoptosis takes place.

Apoptosis can also be caused by compounds affecting the mitochondrial membrane potential (MMP). In the absence of any cytotoxic effects, the MMP is polarized. If 3f and 4f act via the mitochondrial pathway, disruption of the MMP can take place leading to depolarization which may be detected using the JC-1 dye. Fig. 2.6 reveals that both 3f and 4f cause significant depolarization of CEM cells which indicates that these compounds cause apoptosis, at least in part, via the mitochondrial pathway.

In summary, while the ways in which 3f and 4f exert their bioactivity are likely multifactorial, this study has revealed that the compounds cause apoptosis by processes which

include phosphatidylserine translocation, caspase-3 activation and disruption of the MMP which is one the biochemical hallmarks of apoptosis.

2.4 Conclusions

This study has led to the discovery of a novel group of potent antineoplastic agents which demonstrate toxicity to a diverse array of human tumors. The aryl substitution pattern has a profound effect on cytotoxic potencies and in general the 4-fluoro, 4-chloro and 3,4,5-trimethoxy analogs have the lowest IC₅₀ values. The bioevaluations against a wide range of tumors revealed that leukemias (Tables 2.1 and 2.2, Fig. 2.3), lymphomas (Table 2.1, Fig. 2.3) and colon cancers (Table 2.2) are the most sensitive to these compounds while breast and prostate cancers are more refractory (Fig. 2.3). Encouragingly, some of the representative compounds in series 3-5 displayed only marginal toxicity to nonmalignant MCF10A and Hs-27 cells. The cytotoxicity of two representative compounds 3f and 4f towards CEM T-lymphocytes is caused, inter alia, by interfering with the mitochondrial intrinsic pathway. Future studies include in vivo evaluations of the promising lead molecules against different human leukemias, lymphomas and colon cancer xenografts. New analogs and prodrugs based on series 3-5 possessing suitable pharmacokinetic properties [91], [92] will be developed. The objective is to obtain one or more preclinical candidates to treat conditions for which there are considerable unmet medical needs.

2.5 Experimental

2.5.1 Synthesis of series 3-5

The preparation of the compounds in series 3e5 has been described previously [82], [84]. The detailed characterization data for 3a-i, 4a-i and 5 and the ¹H and ¹³C NMR spectra of three representative compounds (one from each series) namely 3e, 4e and 5 are provided in the Appendix Section.

2.5.2 Statistical analyses

Linear and semilogarithmic plots were made between the IC₅₀ values of 3a-i in the Molt4/C8, CEM, HeLa and L1210 bioassays which are presented in Table 1 and the σ , π and MR values of the aryl substituents using a commercial software package [93]. The same evaluation was undertaken with the analogs 4a-h.

A description of the derivation of Kendall's coefficient of concordance is presented in the Appendix Section.

2.5.3 Evaluation of 3-5 against Molt4/C8, CEM, HeLa, and L1210 cells

A literature procedure was utilized to evaluate the compounds in series 3-5, melphalan and curcumin against Molt4/C8, CEM, HeLa and L1210 cells [90]. In brief, different concentrations of the compounds were incubated with the appropriate cell line in RPMI 1640 medium at 37°C for 72 h (Molt4/C8, CEM T-lymphocytes and HeLa cells) or 48 h (L1210 cells). Cell survival was determined using a Coulter counter. The IC₅₀ values are expressed as the mean + SD from the concentration -response curves of at least three independent experiments.

2.5.4 Evaluation of 3b, c, e-h, 4b, c, e, f and 5 against some lymphoma, leukemic, breast, prostate and nonmalignant cells

A number of compounds were evaluated against some lymphoma, leukemic, breast, prostate cancers and nonmalignant cells using a published procedure [94]. In brief, solutions of the dienones in dimethylsulfoxide were added to different cell lines in RPMI media except in the case of Hs-27 fibroblasts, DMEM was used. After 24 h incubation at 37°C, cytotoxicity was noted by the disruption of the cell membrane using Propidium iodide. The average cytotoxicity of three independent experiments was expressed as the percentage of dead cells. These results are presented in Appendix Tables 2.1 and 2.2.

2.5.5 Evaluation of 3a-d, g, 4a, c, e, g, i and 5 against a panel of human tumor cells

The data in Table 2 was obtained by a literature procedure [95]. The GI50 figures are IC50 values except for 3d (the IC50 values using four cell lines are greater than 32.4 μ M) and 5-fluorouracil (for three of the cell lines the IC50 values are in excess of 2.512 mM). All of the data for the colon cancers and leukemic cells are IC50 values. The compounds were evaluated against 59 cell lines except for 3a (60 cell lines) as well as 5 and 5-fluorouracil (57 cell lines).

2.5.6 The induction of phosphatidylserine externalization, caspase activation, and depolarization of the mitochondrial membrane potential in CEM cells by 3f and 4f

CEM cells (ATCC, Manassas, VA) were grown in RPMI-1640 medium (HyClone, Logan, UT) supplemented with 10% heatinactivated fetal bovine serum (HyClone), 100 U/mL penicillin and 100 μ g/mL streptomycin (Lonza, Walkersville, MD). Cells grown exponentially were counted and seeded into 24-well plate formats at a density of 50,000 cells in 500 μ L culture media per well. The dienones 3f and 4f were dissolved in dimethylsulfoxide and aliquots were added to the plates containing the CEM cells in the culture media. All incubation conditions were conducted in a humidified 5% carbon dioxide atmosphere at 37°C. To guarantee high viability, the cells were prepared and cultured as described previously [96]. All treatment and controls were undertaken in triplicate.

2.5.7 Phosphatidylserine externalization assay

The evaluation of the ability of 3f and 4f to induce apoptosis in CEM cells was undertaken as follows. CEM T-lymphocytes were incubated with 1 μ M of 3f or 4f for 24 h and then the cells from each well were collected in a pre-chilled cytometric tube, washed and processed essentially as described previously [97]. In brief, cells were stained with a solution of Annexin V-FITC and Propidium iodide (PI) in 100 μ L of binding buffer (Beckman Coulter, Miami, FL). After 15 min of incubation on ice in the dark, 400 μ L of ice-cold binding buffer was added to cell suspensions and immediately analyzed by flow cytometry (Cytomics FC 500, Beckman Coulter, Miami, FL). These results are presented in Fig. 2.4.

2.5.8 Caspase-3 assay

The activation of caspase-3 by 3f and 4f was demonstrated using the following methodology. The CEM cells were seeded in 24-well plates *vide supra* and treated with 1 μ M of 3f or 4f for 8 h. Caspase-3 activation was determined using a fluorogenic NucView 488 caspase-3/7 substrate for living cells (Biotium, Hayward, CA) following the Vendor's instructions. This substrate is permeable to cells with intact plasma membranes and the emission of a green fluorescent signal indicates caspase-3 activation in real-time via flow cytometry (Cytomics FC 500). The results obtained are portrayed in Fig. 2.5.

2.5.9 Mitochondrial membrane polarization assay

The depolarization of the mitochondrial membrane potential in CEM cells by 3f and 4f was demonstrated by the following methodology. Using a concentration of 1 μ M, the dienones were added to CEM cells and after incubation for 8 h, the cells were stained with 2 μ M of the JC-1 fluorophore (5,5',6,6'-tetrachloro-1,1',3,3'-tetraethylbenzimidazoly- carbocyanine iodide, MitoProbe, Life Technologies, Grand Island, NY) following the manufacturer's protocol. This result is presented in Fig.2.6.

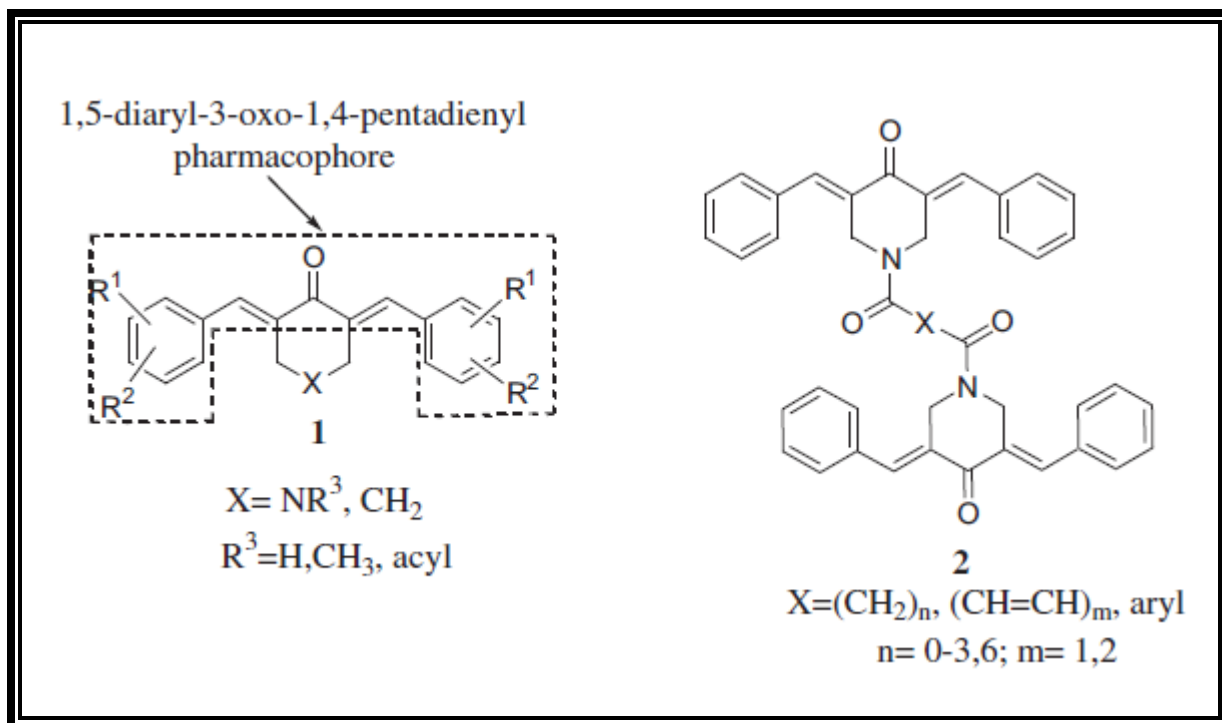


Figure 2.1: The structures of the compounds in series 1 and 2.

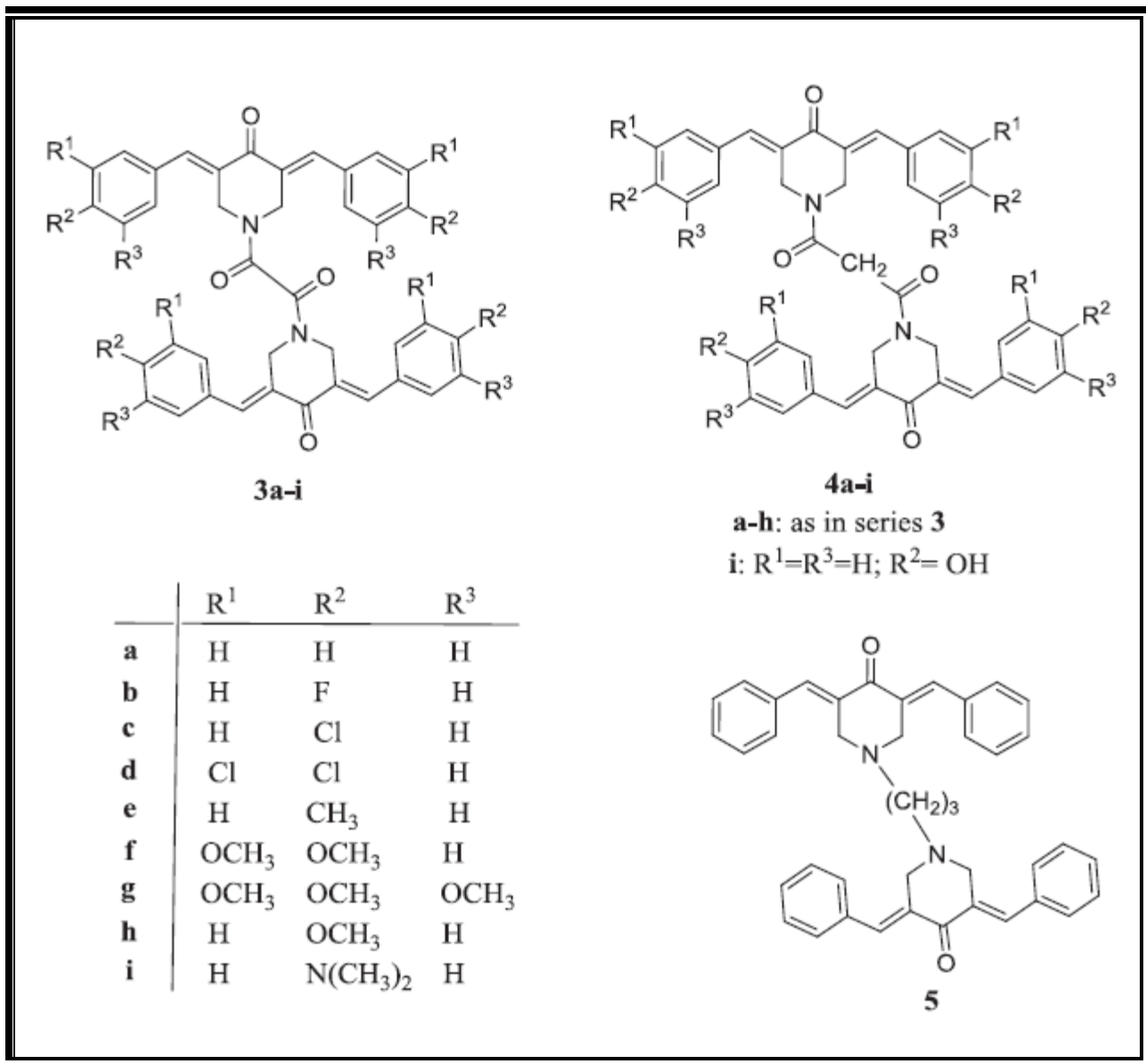


Figure 2.2: The structures of the analogues 3-5.

Table 2.1: Evaluation of 3a-i, 4a-h, and 5 against Molt4/C8, CEM, HeLa, and

L1210 cells.

Compound	IC50 (μM) ^a				Average
	Molt4/C8	CEM	HeLa	L1210	
3a	0.46 ± 0.11	0.75 ± 0.16	1.0 0± 0.10	4.46 ± 0.23	1.67
3b	0.08 ± 0.04	0.22 ± 0.14	0.38 ± 0.04	0.42 ± 0.23	0.28
3c	0.29 ± 0.01	0.79 ± 0.01	0.65 ± 0.44	0.55 ± 0.28	0.57
3d	8.46 ± 2.01	24.6 ± 4.20	27.00 ± 24.3	42.0 ± 5.40	25.5
3e	1.66 ± 0.21	7.72 ± 0.91	3.79 ± 3.29	9.09 ± 1.43	5.57
3f	0.78 ± 0.10	4.36 ± 3.06	4.43± 0.22	6.31 ± 3.46	3.97
3g	0.05 ± 0.02	0.33± 0.06	0.25 ± 0.16	0.18± 0.01	0.20
3h	33.1 ± 2.50	95.1± 69.10	59.90± 45.6	202 ± 16.00	97.5
3i	437 ± 8.00	276± 25.00	>500	297 ± 4.00	>378
4a	0.07 ± 0.01	0.20 ± 0.17	0.91 ± 0.07	1.23 ± 0.38	0.60
4b	1.58 ± 0.04	2.75 ± 0.67	5.61 ± 3.72	11.0 ± 2.5	5.24
4c	1.05 ± 0.62	1.06 ± 0.39	0.82 ± 0.17	0.85 ± 0.36	0.95
4d	23.5 ± 1.0	49.9± 17.7	39.80± 27.0	30.4 ± 8.8	35.9
4e	1.89 ± 0.03	3.44± 1.44	2.88 ± 2.72	5.38 ± 0.78	3.40
4f	0.39 ± 0.07	0.35 ± 0.06	0.37 ± 0.06	0.38 ± 0.18	0.37
4g	0.06 ± 0.02	0.28 ± 0.05	0.22 ± 0.17	0.21 ± 0.08	0.19
4h	449 ± 4.00	369± 45.00	219 ± 17.00	>500	>384
5	1.45 ± 0.06	2.52 ± 1.24	5.54 ± 3.67	2.98 ± 1.81	3.12
Melphalan	2.81 ± 0.33	1.44 ± 0.20	1.70 ± 0.44	4.85 ± 0.87	2.70
Curcumin	6.46 ± 1.41	8.16± 1.66	21.20± 16.1	15.1 ± 1.6	12.7

^aThe IC50 values are the concentrations required to inhibit tumor cell proliferation by 50%.

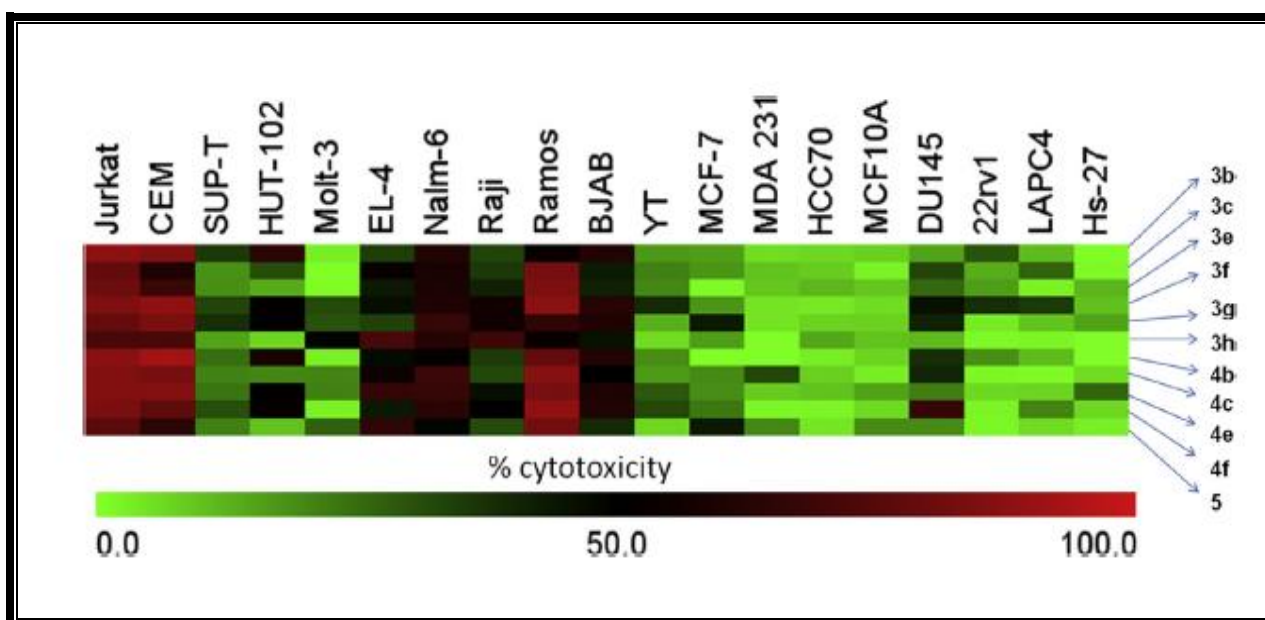


Figure 2.3: Heat map illustrating the toxicity of the compounds.

The final tested concentration of 3b, c, e-h, 4b, c, e, f, and 5 compounds was $1\mu\text{M}$ towards 19 cell lines after 24 h of treatment. The data was generated from three independent determinations. MeV software was utilized to construct the heat map.

Table 2.2: Evaluation of 3a-g, 4a, c, e, g, i and 5 against some human tumor cell lines. a

Compound	All cell lines, IC50 (mM) ^c	Colon cancer cells, IC50 (mM) ^b						Leukemic cells, IC50 (mM) ^b				
		COLO 205	HCC-2998	HCT-15	KM12	SW-620	Ave	HL-60 (TB)	K-562	RPMI-8226	SR	Ave
3a ^a	0.31	0.36	0.19	0.3	0.04	0.07	0.19	0.2	0.2	0.03	0.02	0.11
3b	0.58	0.63	0.62	0.16	0.3	0.32	0.41	1.12	0.28	0.12	0.16	0.42
3c	0.22	0.16	0.31	0.14	0.21	0.18	0.2	0.19	0.13	0.05	0.02	0.1
3d	8.51	12.3	16.6	5.89	11.2	3.8	9.96	13.2	5.89	1.17	1.78	5.51
3g	0.06	0.07	0.1	0.07	0.06	0.03	0.07	0.07	0.03	0.02	0.02	0.04
4a ^a	0.24	0.16	0.17	0.17	0.13	0.05	0.14	0.29	0.05	0.13	0.03	0.13
4c	0.09	0.08	0.13	0.06	0.16	0.03	0.09	0.11	0.03	0.02	0.01	0.04
4e	0.19	0.17	0.3	0.08	0.17	0.15	0.17	0.23	0.1	0.03	0.05	0.1
4g	0.05	0.06	0.1	0.03	0.04	0.05	0.06	0.04	0.03	0.05	0.01	0.03
4i	1.66	1.66	1.74	1.17	0.69	0.76	1.2	1.74	0.53	0.35	0.46	0.77
5	0.19	0.19	0.18	0.2	0.16	0.06	0.16	0.25	0.04	0.04	0.04	0.09
5-Fluorouracil	29.5	3.39	5.75	6.61	7.94	18.6	8.46	85.1	126	3.55	60.3	68.7
Melphalan	19.1	32.4	52.5	36.3	57.5	26.9	41.1	0.38	195	28.2	3.24	56.7

^a The data for 3a and 4a have been published previously [83]. ^b The IC50 values are the concentrations of the compounds which inhibit tumor cell growth by 50%. ^c As indicated in the experimental section, the IC50 values of 3d and 5-fluorouracil towards a few cell lines were not generated due to their being somewhat refractory to the compounds.

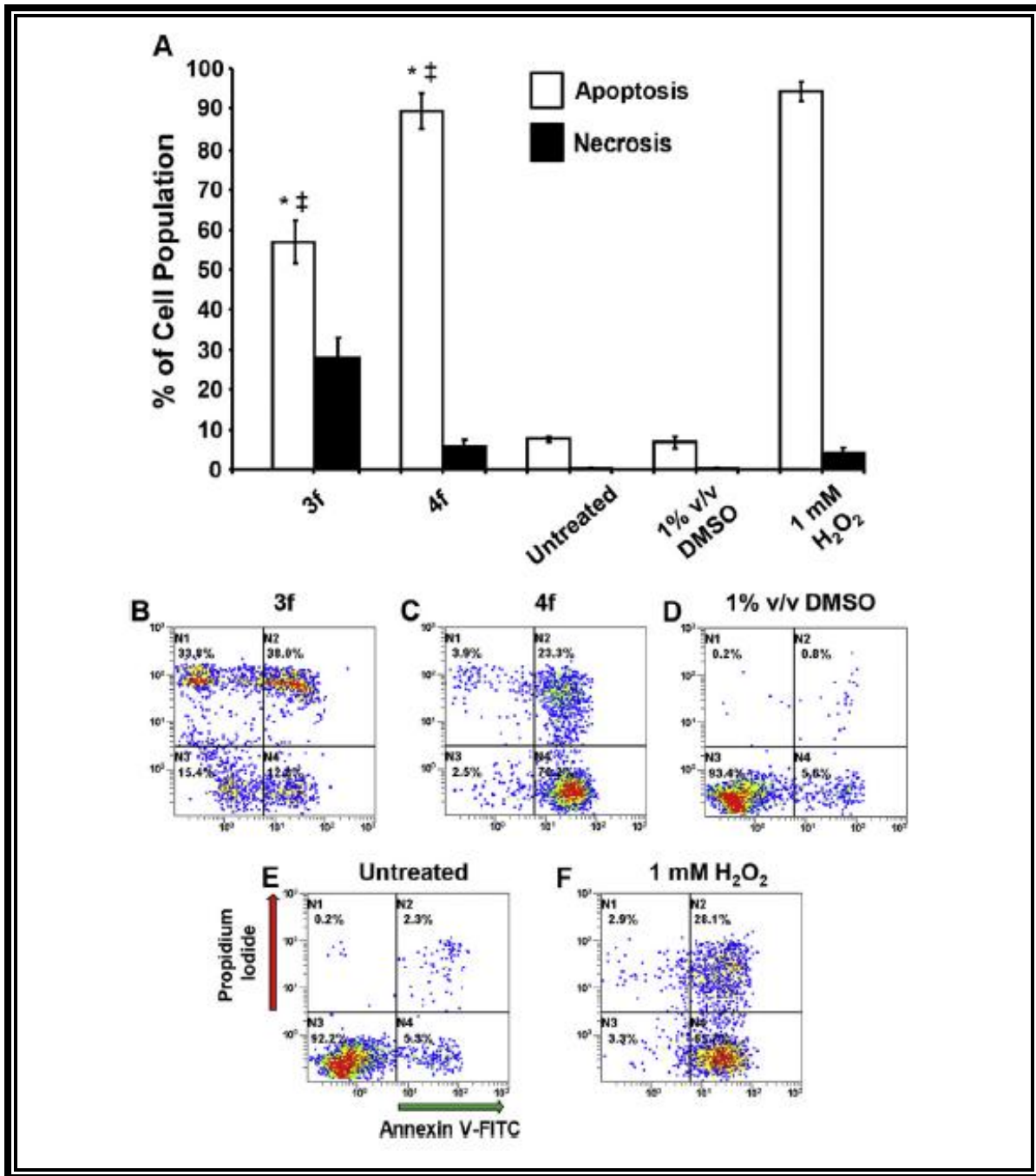


Figure 2.4: 3f and 4f induce apoptotic cell death in a human CEM T-lymphocyte cell line as detected by phosphatidylserine externalization.

The CEM cell line was treated with 1 μ M concentration of 3f and 4f and controls (media alone, 1% v/v DMSO, or 1 mM H₂O₂) for 24 h and the level of apoptosis induction was measured by flow cytometry via Annexin V-FITC binding and Propidium iodide (PI) staining.

(A) Apoptotic cell distribution is expressed as the sum of the percentages of both early and late phases of apoptosis (Annexin V-FITC positive; white bars), whereas cells that were stained by PI but without FITC signal were considered necrotic cells (black bars). Analysis using the two-tailed Student's paired t-test of experimental compounds against untreated (*) and DMSO (+/+) controls was consistently at the level of $p < 0.001$, respectively. Each bar represents the standard deviation of the mean of three independent experiments. Panels B to F are representative flow cytometric analyses utilized to estimate the distribution of apoptosis/necrosis cells, where the FL1 or FL2 detectors settings were accommodated on the x- and y-axes, respectively. Data analysis from quadrant regions in the dot plots are interpreted as follows: the N1 quadrant represents necrotic cells (PI positive); N2 represents cells undergoing late apoptosis (PI and Annexin V-FITC positive); N3 represents unstained viable cells; and N4 represents cells in early apoptosis (Annexin V-FITC positive). Approximately, 3000 events were acquired and analyzed using CXP software (Beckman Coulter).

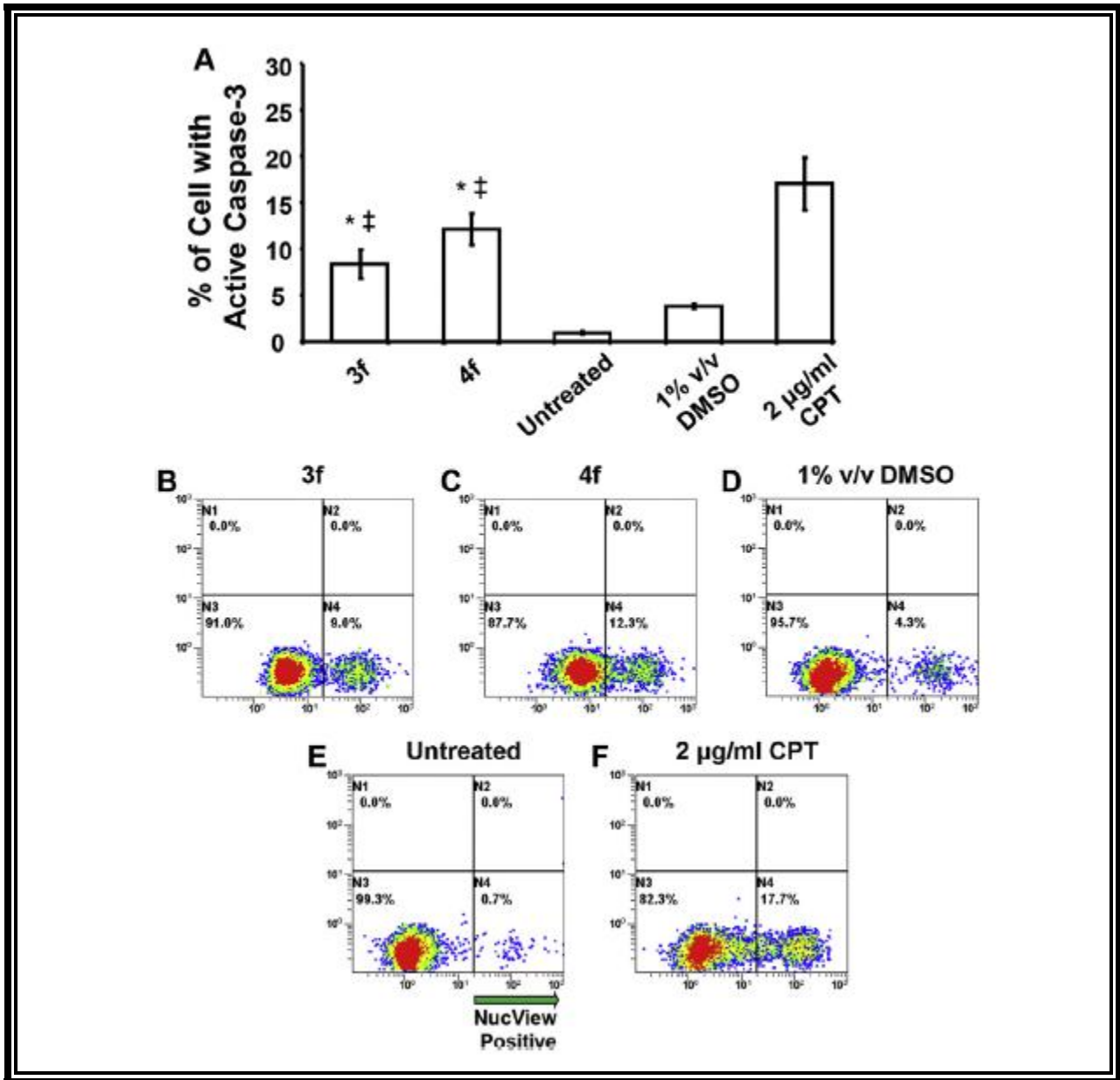


Figure 2.5: 3f and 4f induce apoptotic cell death via caspase-3 activation in the CEM T lymphocyte cell line

Cells were incubated with compounds (1 μ M each) for 8 h and then labeled with NucView 488 caspase-3 substrate and examined via flow cytometry. In panel A, the total numbers of cells with active caspase-3 are graphed along the y axis, whereas different treatments are plotted along the x-axis. Each bar represents the standard deviation of the mean of three independent experiments. Analysis using the two-tailed Student's paired t-test of the

experimental compounds against untreated (*) and DMSO (+/+) controls was consistently $p < 0.01$, respectively. Panels B to F are representative flow cytometric analyses dot plots used to determine the distribution of cells with active caspase-3, where the FL1 and FL2 detectors settings were set on the x and y-axes, respectively. Cells exposed to 2 mg/ml of camptothecin (CPT) were used as positive controls. Untreated and DMSO solvent treated cells were analyzed concurrently. Approximately, 10,000 events were acquired and analyzed using CXP software (Beckman Coulter).

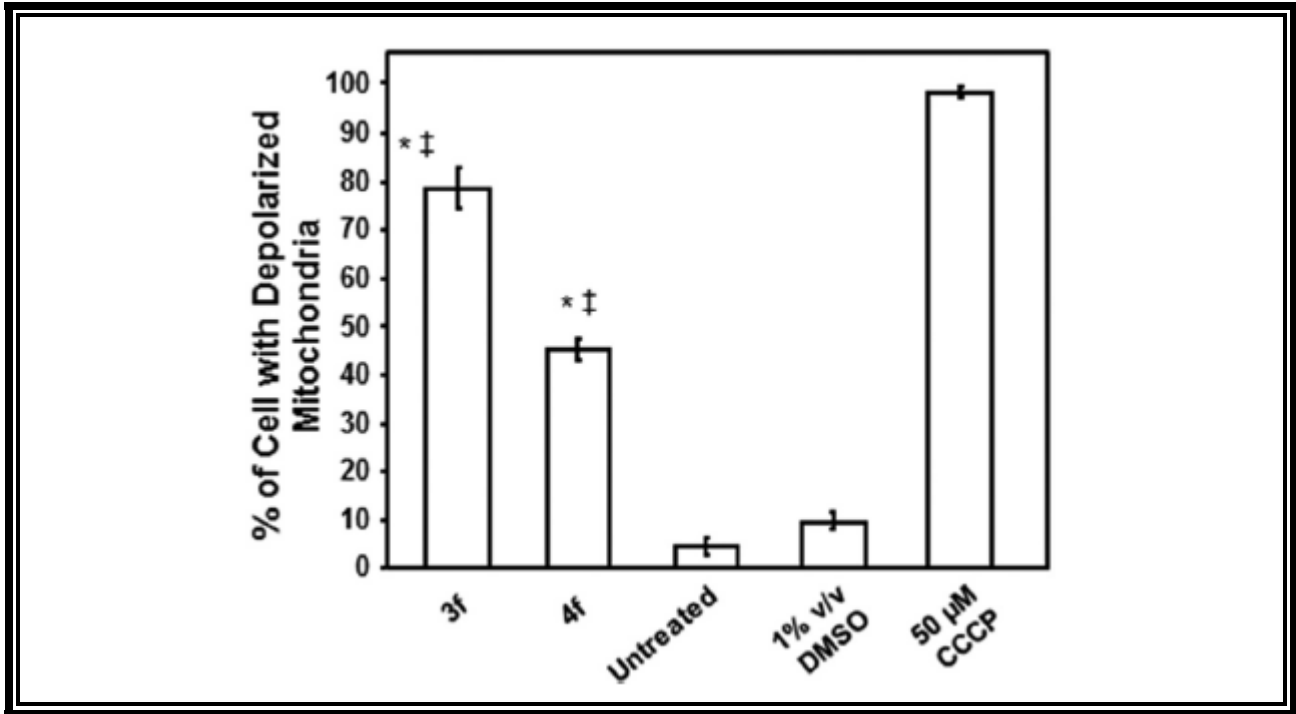


Figure 2.6: 3f and 4f mediated cytotoxicity appears to be initiated via mitochondrial $\Delta\Psi_m$ disruption in CEM T-cells.

Cells were treated for 8 h with the compounds (1 μM) and changes in the mitochondrial $\Delta\Psi_m$ were determined by staining with the aggregate forming lipophilic cationic fluorophore JC-1 and monitored via flow cytometry. After dissipation of mitochondrial $\Delta\Psi_m$, the JC-1 reagent emitted a green fluorescence signal, whereas cells with polarized mitochondrial membrane emitted a red signal. Cells emitting a green fluorescence signal (y-axis) versus treatment type (x-axis) are depicted. Analysis using the two-tailed Student's paired t-test of the experimental compounds against untreated (*) and DMSO (+/+) controls was consistently at the level of $p < 0.001$, respectively. Each bar represents the standard deviation of the mean of three independent assays. Cells exposed to the mitochondrial stressor CCCP (50 μM) were used as positive controls. DMSO solvent and untreated controls were also analyzed in parallel. Approximately 10,000 events were captured and analyzed per sample using CXP software (Beckman Coulter).

2.6 Appendix

Characterization of 3,5-bis(arylidene)-4-piperidone dimers (3a-i, 4a-i and 5)

Melting points were determined on a Gallenkamp instrument and are uncorrected. ¹H and ¹³C NMR were recorded using a Bruker Avance 500 MHz spectrometer equipped with a 5mm BBO probe. Chemical shifts (δ) are reported in ppm. Elemental analyses were undertaken using an Elementer CHNS analyzer. The ¹H and ¹³C NMR spectra of three representative compounds (one from each series) namely 3e, 4e and 5 are presented.

1,2-bis[3,5-bis(Benzylidene)-4-oxo-piperidin-1-yl]ethane-1,2-dione (3a)1

Yield: 62%; mp (chloroform/methanol) 246 °C; ¹H NMR(500 MHz, DMSO-d₆): δ 7.72(s, 2H, 2×=CH), 7.56 (s, 2H, 2×=CH), 7.53(t, 4H, Ar-H), 7.49(d, J=7.07 Hz, 2H, Ar-H), 7.45(m, 6H, Ar-H), 7.39(m, 8H, Ar-H), 4.48(d, J=23.28Hz, 8H, 4×NCH₂); ¹³C NMR (125MHz, DMSO-d₆):184.7, 162.6, 137.9, 137.5, 134.4, 134.1, 131.4, 131.0, 130.9, 130.7, 130.2, 130.1, 129.3, 129.2, 46.4, 41.6.; MS (ESI) m/z: 627 (M+Na)⁺. Anal.calcd for C₄₀H₃₂N₂O₄.H₂O: C 77.17; H 5.14; N 4.50, found: C 77.05; H 4.87; N 4.42.

1,2-bis[3,5-bis(4-Fluorobenzylidene)-4-oxo-piperidin-1-yl]ethane-1,2-dione (3b)2

Yield: 67%; mp (chloroform/methanol) 253 °C; ¹H NMR (500 MHz, CDCl₃): δ 7.73(s, 2H, 2×=CH), 7.57 (s, 2H, 2×=CH), 7.37(q, 4H, Ar-H), 7.25 (q, 4H, Ar-H), 7.18 (t, 4H, Ar-H), 7.098(t, 4H, Ar-H), 4.63 (s, 4H, 2×NCH₂), 4.51 (s, 4H, 2×NCH₂). Anal.calcd for C₄₁H₂₆Cl₈N₂O₄.H₂O: C 53.93; H 3.09; N 3.07 %, found: C 53.84; H 2.98; N 2.74%.

1,2-bis[3,5-bis(4-Chlorobenzylidene)-4-oxo-piperidin-1-yl]ethane-1,2-dione (3c)2

Yield: 61%; mp (methanol) 289 °C; ¹H NMR (500 MHz, CDCl₃): δ 7.72(s, 2H, 2×=CH), 7.54 (s, 2H, 2×=CH), 7.46 (d, J=8.40 Hz, 2H, Ar-H), 7.37(d, J=8.37 Hz, 2H, Ar-H),

7.31(d, J=8.42 Hz, 4H, Ar-H), 7.20(d, J=8.38 Hz, 4H, Ar-H), 4.62 (s, 4H, 2×NCH₂), 4.52 (s, 4H, 2×NCH₂). Anal.calcd for C₄₀H₂₈Cl₄N₂O₄·3 H₂O: C 60.26; H 3.54; N 3.51 %, found: C 60.35; H 3.70; N 3.15%.

1,2-bis[3,5-bis(3,4-Dichlorobenzylidene)-4-oxo-piperidin-1-yl]ethane-1,2-dione (3d)₂

Yield: 64%; mp (chloroform/methanol) 271 oC; ¹H NMR (500 MHz, CDCl₃): δ 7.68 (s, 2H, 2×=CH), 7.55 (s, 1H, =CH), 7.53 (s, 1H, =CH), 7.46 (d, J=8.15 Hz, 6H, Ar-H), 7.41(d, J=1.71 Hz, 2H, Ar-H), 7.20 (dd, J=1.67Hz, J=1.71Hz, 2H, Ar-H), 7.05 (dd, J=1.71 Hz, J=1.77 Hz, 2H, Ar-H), 4.67 (s, 4H, 2×NCH₂), 4.56 (s, 4H, 2×NCH₂). Anal.calcd for C₄₀H₂₄Cl₈N₂O₄: C 54.58; H 2.75; N 3.18 %, found: C 54.52; H 2.90; N 2.95 %.

1,2-bis[3,5-bis(4-Methylbenzylidene)-4-oxo-piperidin-1-yl]ethane-1,2-dione (3e)₂

Yield: 53%; mp (chloroform/methanol) 275 oC; ¹H NMR (500 MHz, CDCl₃): δ 7.79(s, 2H, 2×=CH), 7.65 (s, 2H, 2×=CH), 7.29 (d, J=7.70 Hz, 8H, Ar-H), 7.18(q, 8H, Ar-H), 4.53 (d, J=15.61 Hz, 8H, 4×NCH₂), 2.44 (s, 6H, 2×CH₃), 2.28 (s, 6H, 2×CH₃). ¹³C NMR (125 MHz, CDCl₃): δ 185.04(CO), 162.73(CON), 140.31(C=C-Ph), 140.22(C=C-Ph), 139.15(C=C-Ph), 138.29(C=C-Ph), 131.57(Ar-C), 131.07(Ar-C), 130.67(Ar-C), 130.33(Ar-C), 129.72(Ar-C), 129.62(Ar-C), 129.46(Ar-C), 129.00(Ar-C), 46.07(CH₂NCO), 42.05(CH₂NCO), 21.53(CH₃), 21.43(CH₃). Anal.calcd for C₄₄H₄₀N₂O₄·1.5 H₂O: C 76.76; H 6.30; N 4.07 %, found: C 76.46; H 6.39; N 3.93%.

1,2-bis[3,5-bis(3,4-Dimethoxybenzylidene)-4-oxo-piperidin-1-yl]ethane-1,2-dione (3f)₂

Yield: 60%; mp (chloroform/methanol) 282 oC; ¹H NMR (500 MHz, CDCl₃): δ 7.71(s, 2H, 2×=CH), 7.42 (s, 2H, 2×=CH), 6.99 (d, J=8.47 Hz, 4H, Ar-H), 6.94(d, J=8.08 Hz, 2H, Ar-H), 6.80(m, 6H, Ar-H), 4.70 (s, 4H, 2×NCH₂), 4.64 (s, 4H, 2×NCH₂), 4.00 (s, 6H, 2×OCH₃),

3.96 (d, 12H, 4×OCH₃), 3.74 (s, 6H, 2×OCH₃). Anal.calcd for C₄₈H₄₈N₂O₁₂.H₂O: C 66.75; H 5.84; N 3.24 %, found: C 66.31; H 5.62; N 3.06%.

1,2-bis[3,5-bis(3,4,5-Trimethoxybenzylidene)-4-oxo-piperidin-1-yl]ethane-1,2-dione (3g)₂

Yield: 57%; mp (ethanol) 273 °C; ¹H NMR (500 MHz, CDCl₃): δ 7.63(s, 2H, 2×=CH), 7.44 (s, 2H, 2×=CH), 6.66 (s, 4H, Ar-H), 6.49 (s, 4H, Ar-H), 4.75 (s, 4H, 4×NCH₂), 4.68 (s, 4H, 4×NCH₂), 3.96 (s, 12H, 4×OCH₃), 3.94 (s, 9H, 3×OCH₃), 3.88 (s, 9H, 3×OCH₃), 3.84 (s, 6H, 2×OCH₃). Anal.calcd for C₅₂H₅₆N₂O₁₆ : C 64.72; H 5.85; N 2.90 %, found: C 64.95; H 6.16; N 2.78%.

1,2-bis[3,5-bis(4-Methoxybenzylidene)-4-oxo-piperidin-1-yl]ethane-1,2-dione (3h)₂

Yield: 71%; mp (chloroform/methanol) >300 °C; ¹H NMR (500 MHz, CDCl₃): δ 7.74(s, 2H, 2×=CH), 7.58 (s, 2H, 2×=CH), 7.35 (d, J=8.65 Hz, 4H, Ar-H), 7.22 (d, J=8.63 Hz, 4H, Ar-H), 6.98 (d, J=8.71 Hz, 4H, Ar-H), 6.91 (d, J=8.67 Hz, 4H, Ar-H), 4.60 (s, 4H, 2×NCH₂), 4.53 (s, 4H, 2×NCH₂), 3.90 (s, 6H, 2×OCH₃), 3.76 (s, 6H, 2×OCH₃). Anal.calcd for C₄₄H₄₀N₂O₈ : C 72.91; H 5.56; N 3.86 %, found: C 72.57; H 5.94; N 3.75%.

1,2-bis[3,5-bis(4-(N,N-Dimethylamino)benzylidene)-4-oxo-piperidin-1-yl]ethane-1,2-dione (3i)₂

Yield: 46%; mp (chloroform/methanol) >300 °C; ¹H NMR (500 MHz, CDCl₃): δ 7.75(s, 2H, 2×=CH), 7.65 (s, 2H, 2×=CH), 7.33 (d, J=8.75 Hz, 4H, Ar-H), 7.21(d, J=8.71 Hz, 4H, Ar-H), 6.73 (d, J=16.93 Hz, 8H, Ar-H), 4.58 (s, 4H, 2×NCH₂), 4.54 (s, 4H, 2×NCH₂), 3.08 (s, 12H, 4×NCH₃), 2.95 (s, 12H, 4×NCH₃). Anal.calcd for C₄₄H₄₀N₂O₄.1.5 H₂O: C 76.76; H 6.30; N 4.07 %, found: C 76.46; H 6.39; N 3.93%.

1,3-bis-[3,5-bis(Benzylidene)-4-oxo-piperidin-1-yl]propane-1,3-dione (4a)₁

Yield: 65%; mp (acetone) 201 oC; ¹H NMR (500 MHz, DMSO-d₆): δ 7.72(s, 2H, 2×=CH), 7.57(s, 2H, 2×=CH), 7.53(d, J=4.18Hz, 8H, Ar-H), 7.47 (m, 12H, Ar-H), 4.62(d, J=21.13Hz, 8H, 4×NCH₂), 3.46(s, 2H, CH₂); ¹³C NMR (125MHz, DMSO-d₆):186.3, 165.9,136.6, 136.5, 134.7, 134.5, 132.6, 132.5, 131.0, 130.9, 130.1, 130.0, 129.3, 129.2, 47.0, 42.4; MS (ESI) m/z: 641 (M+Na)⁺. Anal.calcd for C₄₁H₃₄N₂O₄.H₂O: C 77.27; H 5.65; N 4.39, found: C 77.31; H 5.50; N 4.47.

1,3-bis-[3,5-bis(4-Fluorobenzylidene)-4-oxo-piperidin-1yl]propane-1,3-dione (4b)2

Yield: 56%; mp (chloroform/methanol) >300 oC; ¹H NMR (500 MHz, CDCl₃): δ 7.81 (s, 2H, 2×=CH), 7.75 (s, 2H, 2×=CH), 7.49(q, 4H, Ar-H), 7.33 (q, 4H, Ar-H), 7.18 (t, 4H, Ar-H), 7.12 (t, 4H, Ar-H), 4.84 (s, 4H, 2×NCH₂), 4.79 (s, 4H, 2×NCH₂), 3.22 (s, 2H, CH₂). Anal.calcd for C₄₁H₃₀F₄N₂O₄.H₂O: C 69.42; H 4.27; N 3.95 %, found: C 69.58; H 4.30; N 3.71%.

1,3-bis-[3,5-bis(4-Chlorobenzylidene)-4-oxo-piperidin-1yl]propane-1,3-dione (4c) 2

Yield: 58%; mp (chloroform/methanol) 260 oC; ¹H NMR (500 MHz, DMSO-d₆): δ 7.64 (s, 2H, 2×=CH), 7.60 (s, 2H, 2×=CH), 7.57 (d, J=11.46 Hz, 4H, Ar-H), 7.54 (d, J=7.60 Hz, 4H, Ar-H), 7.49 (q, 8H, Ar-H), 4.62 (d, 8H, J=10.15 Hz, 4×NCH₂), 3.51 (s, 2H, CH₂). Anal.calcd for C₄₁H₃₀Cl₄N₂O₄.2.5 H₂O: C 61.38; H 3.77; N 3.49 %, found: C 61.10; H 3.69; N 3.30%.

1,3-bis-[3,5-bis(3,4-Dichlorobenzylidene)-4-oxo-piperidin-1yl]propane-1,3-dione (4d) 2

Yield: 65%; mp (chloroform/methanol) 236 oC; ¹H NMR (500 MHz, CDCl₃): δ 7.71 (s, 2H, 2×=CH), 7.63 (s, 2H, 2×=CH), 7.56 (q, 8H, Ar-H), 7.51 (d, J=8.29 Hz, 2H, Ar-H), 7.30 (d, J=1.45 Hz, 2H, Ar-H), 7.31 (dd, J=1.45 Hz, J=1.53 Hz, Ar-H), 7.15 (dd, J=1.48 Hz, 2H, Ar-H), 4.78 (d, 8H, J=6.72 Hz, 4×NCH₂), 3.30 (s, 2H, CH₂). Anal.calcd for C₄₁H₂₆Cl₈N₂O₄. H₂O: C 53.93; H 3.09; N 3.07 %, found: C 53.84; H 2.98; N 2.74%.

1,3-bis-[3,5-bis(4-Methylbenzylidene)-4-oxo-piperidin-1yl]propane-1,3-dione (4e) 2

Yield: 43%; mp (chloroform/methanol) 251 oC; ¹H NMR (500 MHz, CDCl₃): δ 7.81 (s, 2H, 2×=CH), 7.74 (s, 2H, 2×=CH), 7.40 (d, J=7.90 Hz, 4H, Ar-H), 7.27 (d, J=7.60 Hz, 4H, Ar-H), 7.21(q, 8H, Ar-H), 4.89 (s, 4H, 2×NCH₂), 4.65 (s, 4H, 2×NCH₂), 3.15 (s, 2H, CH₂), 2.43 (s, 6H, 2×CH₃), 2.41(s, 6H, 2×CH₃). ¹³C NMR (125MHz, CDCl₃): δ 186.39(CO), 165.30(CON), 140.31(C=C-Ph), 140.17(C=C-Ph), 138.62(C=C-Ph), 137.34(C=C-Ph), 131.86(Ar-C), 131.39(Ar-C), 130.88(Ar-C), 130.53(Ar-C), 130.45(Ar-C), 130.39(Ar-C), 130.33(Ar-C), 129.68(Ar-C), 129.61(Ar-C), 128.77(Ar-C), 46.79(CH₂NCO), 43.85(CH₂NCO), 40.54 (COCH₂CO), 21.53(CH₃). Anal.calcd for C₄₅H₄₂N₂O₄.H₂O: C 77.94; H 6.40; N 4.04 %, found: C 77.94; H 6.63; N 3.98%.

1,3-bis-[3,5-bis(3,4-Dimethoxybenzylidene)-4-oxo-piperidin-1yl]propane-1,3-dione (4f) 2

Yield: 65 %; mp (chloroform/methanol) >300 oC; ¹H NMR (500 MHz, DMSO-d₆): δ 7.86 (s, 4H, 4×=CH), 7.17 (s, 4H, Ar-H), 7.13 (s, 8H, Ar-H), 4.54 (s, 8H, 4×NCH₂), 3.84 (d, J=7.27 Hz, 24H, 8×OCH₃), 3.48 (s, 2H, CH₂). Anal.calcd for C₄₉H₅₀N₂O_{12.7} H₂O: C 59.69; H 6.54; N 2.84 %, found: C 59.82; H 6.18; N 2.71%.

1,3-bis-[3,5-bis(3,4,5-Trimethoxybenzylidene)-4-oxo-piperidin-1yl]propane-1,3-dione (4g) 2

Yield: 53%; mp (chloroform/methanol) 115 oC; ¹H NMR (500 MHz, CDCl₃): δ 7.78 (s, 2H, 2×=CH), 7.74 (s, 2H, 2×=CH), 6.72 (s, 4H, Ar-H), 6.58 (s, 4H, Ar-H), 4.96 (s, 4H, 2×NCH₂), 4.90 (s, 4H, 2×NCH₂), 3.92 (d, J=15.37 Hz, 30H, 10×OCH₃), 3.86 (s, 6H, 2×OCH₃), 3.37 (s, 2H, CH₂). Anal.calcd for C₅₃H₅₈N₂O₁₆.H₂O: C 63.83; H 6.07; N 2.81 %, found: C 63.84; H 6.27; N 2.51%.

1,3-bis-[3,5-bis(4-Methoxybenzylidene)-4-oxo-piperidin-1yl]propane-1,3-dione (4h) 2

Yield: 61%; mp (chloroform/methanol) 245 oC; ¹H NMR (500 MHz, CDCl₃): δ 7.80 (s, 2H, 2×=CH), 7.73 (s, 2H, 2×=CH), 7.48 (d, J=8.6 Hz, 4H, Ar-H), 7.29 (d, J=10.17 Hz, 2H, Ar-H), 6.98 (d, J=8.49 Hz, 4H, Ar-H), 4.85(s, 4H, 2×NCH₂), 4.72 (s, 4H, 2×NCH₂), 3.88 (d, J=7.72 Hz, 12H, 4×OCH₃), 3.22 (s, 2H, CH₂). Anal.calcd for C₄₅H₄₂N₂O_{8.4} H₂O: C 66.59; H 5.22; N 3.45 %, found: C 66.68; H 5.38; N 3.27%.

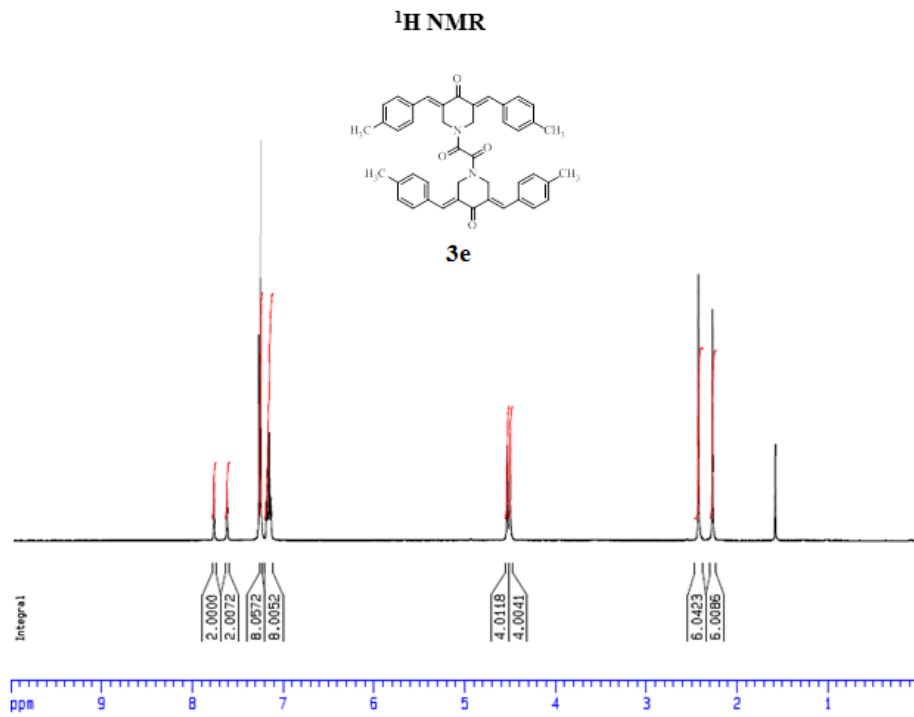
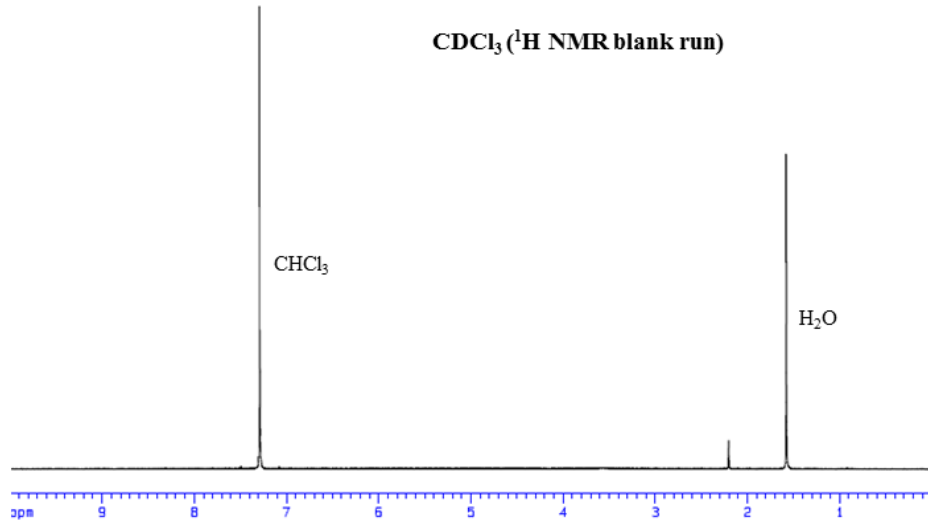
1,3-bis-[3,5-bis(4-Hydroxybenzylidene)-4-oxo-piperidin-1yl]propane-1,3-dione (4i) 2

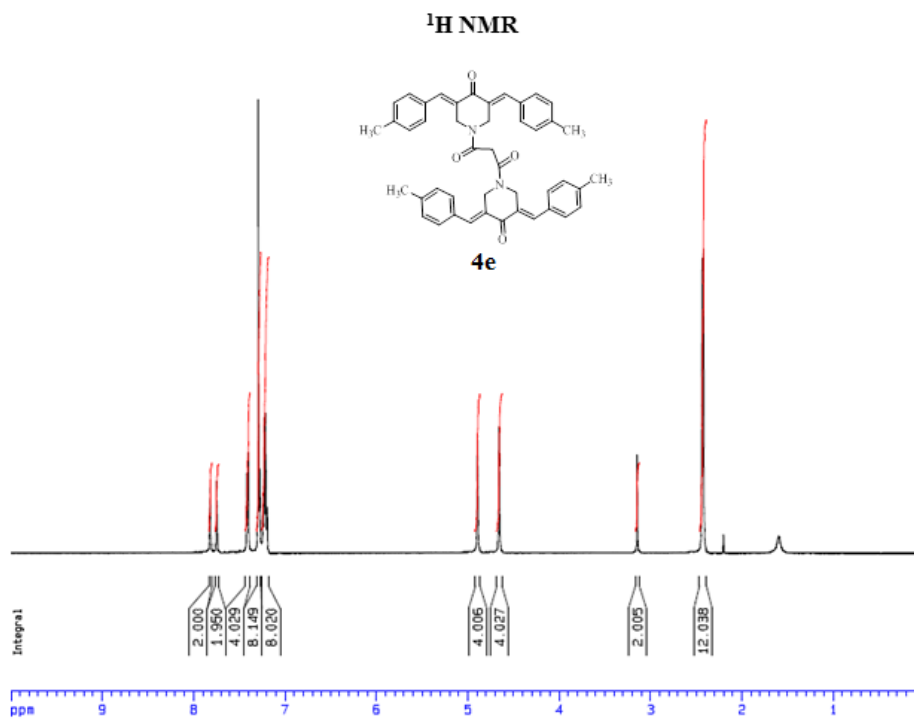
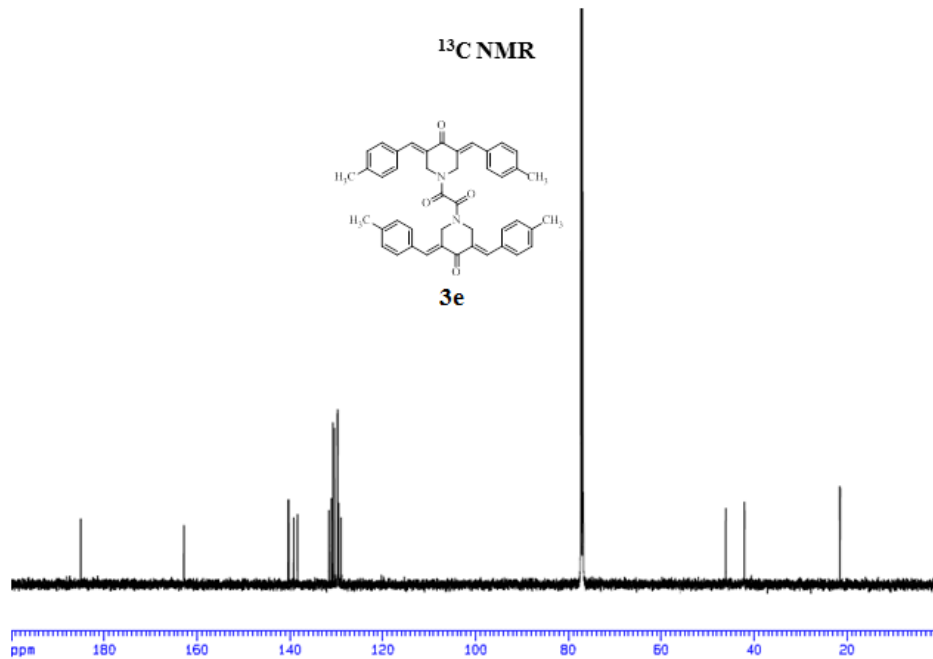
Yield: 56%; mp (chloroform/ethanol) >300 oC; ¹H NMR (500 MHz, DMSO-d₆): δ 7.64 (s, 2H, 2×=CH), 7.60 (s, 2H, 2×=CH), 7.57 (d, J=11.46 Hz, 4H, Ar-H), 7.54 (d, J=7.60 Hz, 4H, Ar-H), 7.49 (q, 8H, Ar-H), 4.62 (d, 8H, J=10.15 Hz, 4×NCH₂), 3.51 (s, 2H, CH₂). Anal.calcd for C₄₁H₃₄N₂O_{8.4.5} H₂O: C 64.46; H 5.68; N 3.67 %, found: C 64.59; H 5.31; N 3.59%.

1,3-bis-[3,5-bis(benzylidene)-4-oxo-piperidin-1yl]propane (5) 2

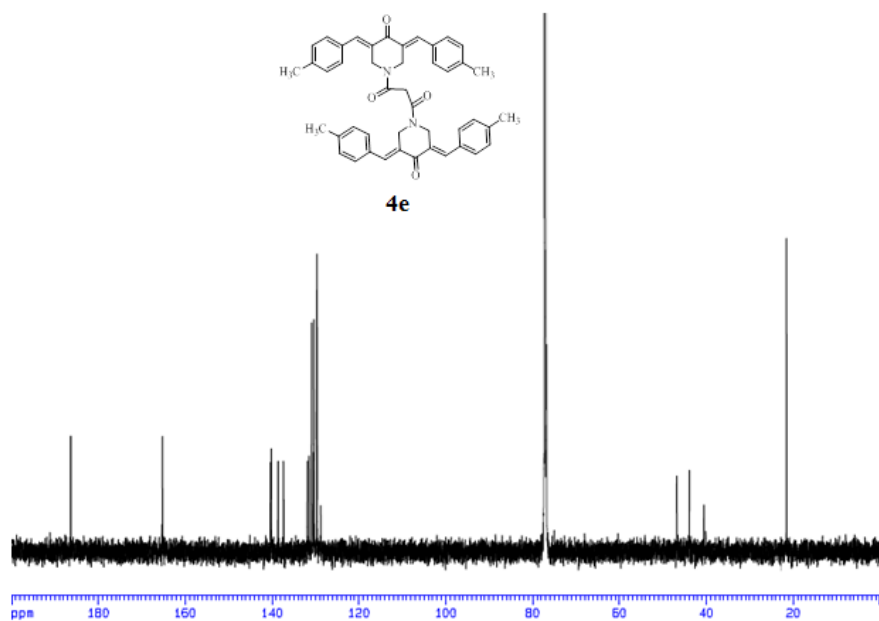
Yield: 63 %; mp (acetone) 135 oC; ¹H NMR (500 MHz, CDCl₃): δ 7.81(s, 4H, 4×=CH), 7.39 (m, 20H, Ar-H), 3.78 (s, 8H, 4×NCH₂), 2.54 (t, 4H, 2×CH₂), 1.60 (p, 2H, CH₂). ¹³C NMR (125 MHz, CDCl₃): δ 187.34 (CO), 136.57 (C=C-Ph), 135.20 (C=C-Ph), 133.11 (C=C-Ph), 130.40 (Ar-C), 129.05 (Ar-C), 128.60(Ar-C), 55.38 (NCH₂CH₂), 54.97 (NCH₂-piperidone), 25.91 (CH₂). Anal.calcd for C₄₁H₃₈N₂O₂: C 83.36; H 6.48; N 4.74 %, found: C 83.74; H 6.79; N 5.05%.

¹H and ¹³C NMR spectra for representative compounds from the series 3-5

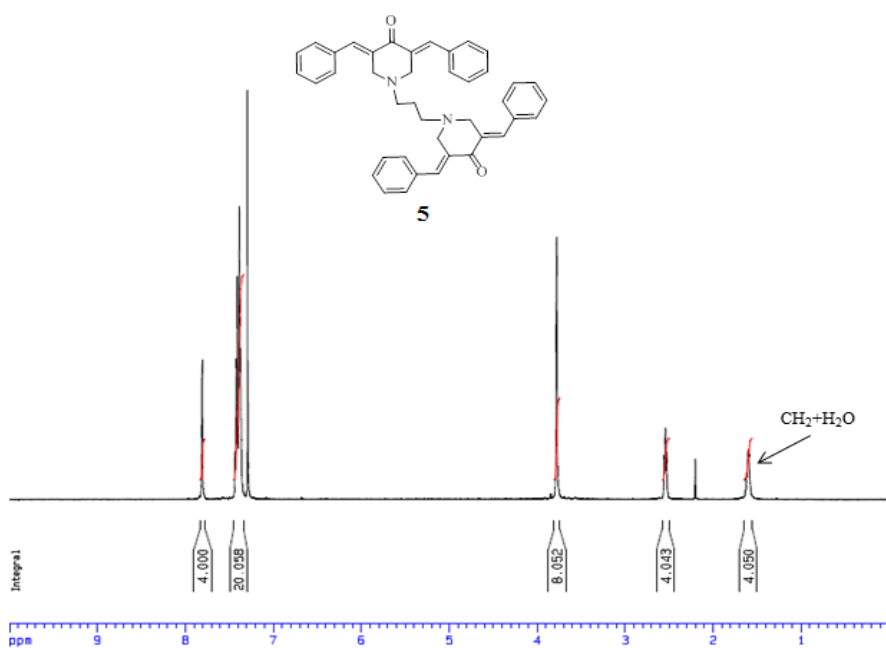




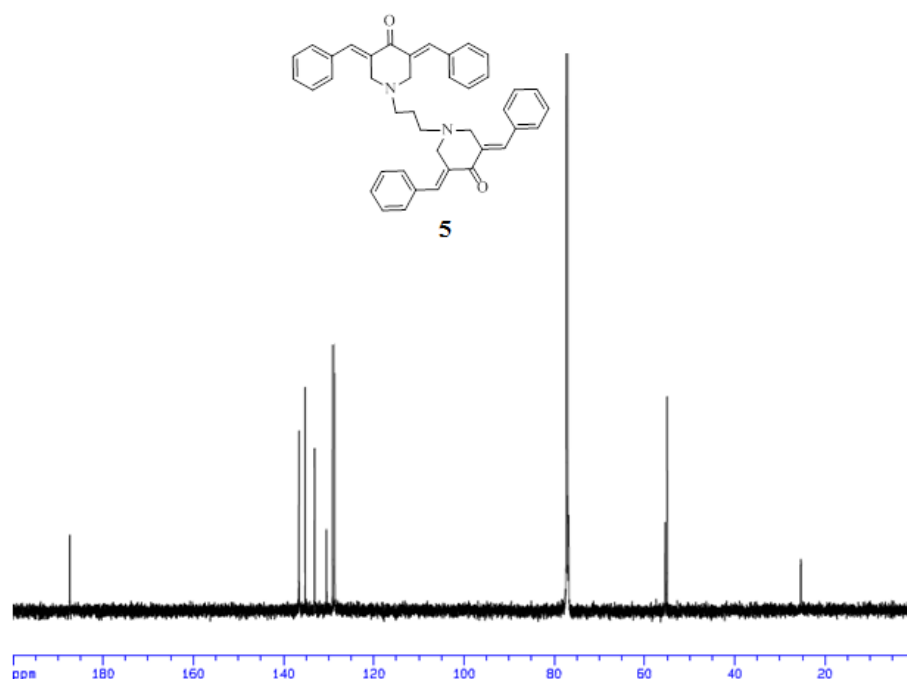
¹³C NMR



¹H NMR



¹³C NMR



Kendall's coefficient of concordance

The equation used to obtain the coefficient of concordance is derived as follows. In this case the cytotoxin i is given the rank r_{ij} where j is the cell line, and there are N cytotoxins and M cell lines. Thus the total rank R given to cytotoxin i is $R_i = \sum_{j=1}^M r_{i,j}$, and the mean value of these ranks is $\bar{R} = \frac{1}{2}m(n + 1)$.

The sum of the squared deviations, (S), is defined as: $\sum_i^N (R_i - \bar{R})^2$.

Kendall's coefficient of concordance (W) is: $W = \frac{12S}{M^2(N^3 - N)}$ (1) If all the cell lines produce identical rankings, then W is 1. If there is no agreement, then W is 0.

When two or more compounds have the potencies (i.e., there are ties in the rankings), then equation 1 will understate the degree of concordance and must be adjusted. The correction factor (T_j) is defined as $T_j = \sum_{i=1}^{g_j} (t_i^3 - t_i)$, in which t_i is the number of tied ranks in the i^{th} group of tied ranks (the number of cases of equal potency at a specific IC₅₀ value) and g_j is the number

of tie values. If there are no tied ranks for cell line j then this will be 0. Using this correction for ties, Kendall's coefficient of concordance as: $W = \frac{12 \sum_{i=1}^N (R_i^2) - 3M^2 N(N+1)^2}{M^2 N(N^2-1) - M \sum_{j=1}^M (T_j)} \dots(2)$.

Table 1. Evaluation of 3b,c,e-h, 4b,c,e,f and 5 against various lymphoma and leukemic cell lines^a

Compound	% dead cells											Average
	Jurkat	CEM	SUP-T	HUT-102	Molt-3	EL-4	Nalm-6	Raji	Ramos	BJAB	YT	
3b	87.8	85.3	35.6	64.4	3.1	34.7	61.6	33.5	53.3	61.8	17.1	48.9
3c	78.5	59.9	18.1	31.4	0.4	52.5	59.0	35.7	82.9	43.1	21.5	43.9
3e	80.7	68.4	18.8	13.9	0.8	43.5	59.5	41.5	84.4	41.5	20.1	43.0
3f	84.8	88.1	33.0	50.9	31.8	46.5	60.7	56.3	87.4	62.8	39.2	58.3
3g	78.7	84.1	38.2	50.5	30.3	33.8	67.6	55.7	65.1	60.9	13.0	52.5
3h	72.0	71.9	15.2	6.7	49.6	71.7	62.6	69.1	53.7	45.8	5.8	47.7
4b	87.1	92.4	24.9	58.5	2.6	47.7	51.9	35.3	78.6	61.2	19.2	50.9
4c	85.3	83.0	21.1	20.4	20.6	55.4	68.6	32.7	86.3	49.9	16.8	49.1
4e	85.5	85.7	23.6	50.9	21.3	66.9	67.6	46.5	83.0	60.2	29.1	56.4
4f	83.9	77.6	31.0	51.6	2.6	43.7	63.9	50.8	88.6	61.0	32.3	53.4
5	76.3	64.5	21.2	10.0	27.4	65.3	49.2	31.9	82.1	39.4	6.6	43.1
Average	81.9	78.3	25.5	37.2	17.3	51.1	61.1	44.5	76.9	53.4	20.1	49.8

^aA concentration of 1 μ M of each compound was incubated with different cell lines for 24 h at 37° C. The figures of the percentage of dead cells are the average of three independent experiments.

Table 2. Evaluation of 3b,c,e-h, 4b,c,e,f and 5 against some breast and prostate cancer cells and nonmalignant cells^a

Compound	% dead cells									
	MCF-7	MDA231	HCC70	Average	MCF10A	DU145	22rv1	LAPC4	Average	Hs-27
3b	16.2	5.5	6.6	9.43	7.7	15.2	30.1	11.3	18.9	0.6
3c	17.8	10.0	8.4	12.1	2.2	33.1	13.6	27.0	24.6	0.0
3e	0.0	9.3	11.9	7.07	9.3	26.0	16.2	2.4	14.9	12.0
3f	17.7	4.6	3.9	8.73	5.8	45.7	38.2	35.4	39.8	10.2
3g	43.2	4.7	7.3	18.4	7.6	41.3	3.4	9.7	18.1	15.4
3h	16.2	0.6	14.7	10.5	9.9	11.4	0.0	1.9	4.43	0.6
4b	0.2	0.4	3.1	1.23	7.0	38.4	18.8	11.1	22.8	0.3
4c	19.5	32.7	7.8	20.0	3.1	40.3	1.7	1.0	14.3	5.7
4e	19.1	8.6	10.1	12.6	15.4	21.9	6.3	7.0	11.7	26.5
4f	23.0	1.8	2.1	8.97	6.1	67.4	2.0	20.6	30.0	6.4
5	43.5	20.1	4.3	22.6	19.4	19.4	1.7	5.7	8.93	2.9
Average	19.7	8.94	7.29	11.9	8.50	32.7	12.0	12.1	19.7	7.33

^a A concentration of 1 μ M of each compound was incubated with different cell lines for 24 h at 37° C. The figures of the percentage of dead cells are the average of three independent experiments.

Chapter 3: A novel curcumin analogue sensitizes leukemia and lymphoma cells to apoptosis via increased TNF- α and DAPK1 expression

Using different cell death assays, we have identified a curcumin-like analogue with potent activity against hematological malignancies. The analogue was developed from recently discovered novel class of curcumin-like molecules designed by structure-based chemical modifications of 1,5-diaryl-3-oxo-1,4-pentadienyl pharmacophore. The cell death mechanism was determined to be mediated by apoptosis through detection of phosphatidylserine externalization, mitochondrial depolarization, and caspase activation. RT-PCR experiments revealed a time-dependent upregulation of Death Associated Protein Kinase-1 (DAPK-1), Tumor Necrosis Factor- α (TNF- α), and Fas-Associated Death Domain (FADD). ELISA and western blots further confirmed the upregulation of the DAPK-1 and TNF- α proteins. Interestingly, cell death regulation among T and B cell lines resulted different and probably this can be a promising therapeutic advantage that needs to be verified in the future.

1.1 Introduction

Recently, we have published about the discovery of a new class of curcumin-like molecules selective against hematological malignancies [98], [82]. The overall objective of these investigations was the development of at least one promising prototypic cytotoxic molecule identified to possess drug-likeness properties. A candidate cytotoxic compound was now identified based on its ability to broadly induce cell death against a panel of hematological cancers at low micromolar concentrations. Characterization of this promising compound has revealed cell death mediated by apoptosis, as evidenced by phosphatidylserine externalization, mitochondrial depolarization, and caspase activation. RT-PCR experiments demonstrated time-dependent upregulation of Death Associated Protein Kinase-1 (DAPK-1), Tumor Necrosis Factor- α (TNF- α), and Fas-Associated Death Domain (FADD). ELISA and western blots further confirmed the upregulation of the DAPK-1 and TNF- α . Publications about curcumin have also shown the upregulation of DAPK-1, but have not evidenced TNF involvement [99]. This is the

first report about a curcumin-like compound inducing both cell death regulators in Jurkat cells. Further, it is evidenced here that Nalm-6 cells die also through DAPK-1. Nonetheless, other genes different than TNF, but related to cell death receptor pathway, such as FADD, are upregulated in Nalm-6 cells in response to this novel curcumin-like analogue.

The expression of DAPK is found to be epigenetically suppressed in several tumors and its death-inducing function has been demonstrated by its over-expression in cell lines [100], [101]. Thus, DAPK-1 has been characterized as a calcium/calmodulin-regulated serine/threonine kinase and considered a potential therapeutic target and important tumor suppressor in deciding the fate of cellular functions such as cell death, survival, motility, and autophagy [102], [103], [104]. Studies by Wu, B. et al have shown that DAPK-1 was required for curcumin-induced cell cycle arrest and apoptosis. This was approached by siRNA knockdown showing attenuation of curcumin-induced inhibition of STAT3 and NF- κ B and diminished curcumin-induced caspase-3 activation [105]. In addition, DAPK-1 expression and activity has been found to be dysregulated in blood malignancies, non-small cell lung, pancreatic, head and neck carcinomas to mention a few [100, 106], [107], [108], [109], [110]. Especially, DAPK silencing occurs with more frequency in B-cell lymphomas [111], [112]. As a tumor suppressor, DAPK-1 down-regulates XIAP and Nuclear Factor-kappa B (NF- κ B), and as a pro-apoptotic kinase, contains a death domain that participates in multiple apoptotic signaling pathways, including the Tumor Necrosis Factor- α (TNF- α), Fas, and Interferon- γ (IFN- γ) pathways [113], [105], [114]. The down-regulation of DAPK-1 by transfecting siRNA in Jurkat cells resulted in reduced susceptibility to Fas-induced apoptosis suggesting the involvement of DAPK-1 in the extrinsic apoptosis pathway in lymphocytes [115].

DAPK-1 is found associated with actin microfilaments and its activation can occur through dephosphorylation of Ser-308 by TNF- α [116], [117], [118]. Induction of TNF- α occurs in response to various stimuli, including lipopolysaccharide (LPS) or small-molecules and can result in apoptosis, increased survival, or inflammatory processes [119], [120], [121]. The

apoptotic pathway of TNF- α occur when this cytokine binds to the extracellular domain of Tumor Necrosis Factor Receptor-1 (TNFR-1) promoting the release of Silencer Of Death Domain (SODD) for the trimerization of TNFR-1 with TNFR-associated death domain (TRADD) [122], [123], [124]. This in turn recruits the receptor interacting protein (RIP), TNFR-associated factor 2 (TRAF-2), and Fas-Associated Death Domain (FADD) [125], [126]. These adaptor proteins recruit pro-caspase-8, which is subsequently activated and induces mitochondrial depolarization and downstream caspases [67], [127]. The survival and inflammatory activity of TNF- α is under the control of TNFR-1 and TRAF-2 [128]. The binding of TRAF-2 to TNFR-1 can result in the activation of Mitogen-Activated Protein Kinase (MAPK) and c-Jun N-terminal Kinase (JNK) [129], [130]. Another major signaling event is the activation of NF- κ B that takes place after TRAF-2 and RIP binding [131]. MAPK, NF- κ B and JNK are known to induce transcription of inflammatory, immunomodulatory, anti-apoptotic, and proliferative genes such as Bcl-2 and XIAP [132]. Nonetheless, DAPK-1 antagonizes TNF- α pro-inflammatory and survival signaling by inhibition of NF- κ B activation [133]. Upon the blockade of NF- κ B, TNF- α can stimulate a strong pro-apoptotic signal inducing internalization of FADD and caspase-8 recruitment leading to the activation of the caspase cascade and apoptosis [134]. Thus, DAPK-1 possesses potential therapeutic capabilities regulating cell death signals which can offer opportunities for the development of anti-cancer drugs.

DAPK-1 has been recently found to be induced by curcumin, a known anticancer compound that unfortunately has low systemic bioavailability that lowers its potential therapeutic and chemopreventive effects [105], [68], [72]. To overcome this limitation, analogues of curcumin's have been synthesized that show promising anti-cancer activity [69], [135]. In this study, a curcumin-like analogue was found to have potent activity against hematological malignancies. Exposure of Jurkat and Nalm-6 human lymphoid cells to the analogue resulted in differential upregulation of TNF- α and DAPK-1, as well as several other pro-apoptotic genes. We utilized a commercial RT-PCR array system (Human Apoptosis RT² Profiler PCR Array,

Qiagen, MD) to detect the effects of the analogue on 84 apoptosis-related genes in Jurkat and Nalm-6 cells at several time points. In addition, western blot analysis to detect the gene products of some of the activated proteins revealed that the up regulation of the genes resulted in an increase in protein levels of DAPK-1. This analysis detected the highest levels of DAPK1 by 8 hrs of treatment with the analogue.

3.2 Methods

3.2.1 Curcumin analogue synthesis and reagents

A new series of curcumin analogues were synthesized and obtained from Dr. J.R. Dimmock (University of Saskatchewan, Saskatchewan, Canada). The compounds were received in powder and prepared as 1 mM stock solution dissolved in DMSO and kept at -20°C. Final solvent concentrations on the cultured cells were 1% (v/v), which had negligible effect on any of the parameters studied. Hoechst 33342 (Hoechst; Invitrogen, Eugene, OR); and Propidium iodide (PI; MP Biomedicals, Solon, OH) stock solutions were prepared in PBS, diluted with cell culture medium, and added to each experimental well at a final concentration of 1 µg/ml for each dye. Annexin V-FITC (Beckman Coulter, Marseille, France), JC-1 dye (Molecular Probes, OR, U.S.), and DEVD-NucView™ 488 substrate (Biotium, Inc., Hayward, CA) were diluted according to the respective manufacturer instructions.

3.2.2 Cell lines and culture conditions

Eleven lymphoid cancer cell lines and two normal non-transformed cell line were utilized to test the cytotoxic potential of the analogue. Each lymphoid cancer cell line selected for this study was a representative hematological malignancy with their unique genetic heterogeneity. The lymphoid cancer cell lines were: Jurkat, SUP-T1, HuT 102, MOLT-3, and CCRF-CEM human T-cell lymphomas and leukemias (obtained from ATCC, Manassas, VA, USA); Nalm-6 (DSMZ, Braunschweig, Germany), Raji, Ramos, and BJAB human B –cell lymphomas and

leukemias (ATCC, Manassas, VA, USA); YT Nk-Like1 human natural killer leukemia cell line (DSMZ, Braunschweig, Germany); and EL4 mouse T -cell lymphoma (ATCC, Manassas, VA, USA). The culture medium for the lymphoid cancer cells was Roswell Park Memorial Institute (RPMI; HyClone). The normal non-transformed cell lines were Hs27 and MCF-10A, obtained from normal human foreskin fibroblasts (ATCC, Manassas, VA, USA) and normal mammary gland (ATCC, Manassas, VA, USA), respectively. Non-transformed cell lines were selected to test the cytotoxicity of the analogue on tissues from normal origin. Growth media for Hs27 was Dulbecco's Modified Eagle Medium (DMEM; HyClone, Logan, UT) and DMEM/F12 supplemented with EGF (100 mg/ml), Hydrocortizone (1mg/ml), CholeraToxin (1mg/ml) and Insulin (10mg/ml) for MCF-10A. All types of culture media were supplemented 10% heat inactivated serum and with 100U/ml penicillin, 100 µg/ml streptomycin, and 0.25 µg/ml amphotericin B (Lonza, Walkersville, MD). The incubation conditions for the cells were 37°C in humidified 5% carbon dioxide (CO₂) atmosphere, in a regular water jacketed incubator.

To prepare the experimental multi-well plates and to guarantee high viability, the Hs27 and MCF-10A cells were washed with fresh media to eliminate cell debris and floating dead cells. Hs27 and MCF-10A cells were harvested from culture flasks by adding 2 ml of 0.25% trypsin solution (Invitrogen, Carlsbad, CA), diluted in serum free DMEM, and incubated for approximately 15 min at 37°C. Trypsin was neutralized by addition of culture media with 10% serum. Cells were then centrifuged to remove the neutralized trypsin and transferred to a new culture flask and replenished with complete growth media. When necessary, the viability of the lymphoid cancer cells was increased by using Ficoll-Paque™PLUS density gradient [136]. After centrifugation at 400xg for 20 min at 25°C, live cells at the interface between the Ficoll-Paque and the cell suspension were collected and washed with fresh culture media. These lymphoid cancer cells were then expanded by starting a new culture. Only cultures containing cell viabilities of 95% or higher were used for the cytotoxicity studies. This was assured by Flow cytometry by staining the cells with PI.

3.2.3 Screening assays (DNS and MTS)

The Differential Nuclear Staining (DNS) screen is a high-throughput screening technique that uses two differential dyes to identify cytotoxic compounds [137]. Hs27, MCF-10A, and lymphoid cancer cells were seeded in black flat-bottomed plastic 96-well assay plates (BD Biosciences, Rockville, MD) at densities of 5,000 cells/well for adherent cell lines and 10,000 cells/well for suspension cells in 100 μ l of culture media/well. The analogue was tested at the final concentration of 1 μ M (diluted in 1% v/v DMSO) per well according to CC50 values previously examined by cytotoxicity assays. The compound was dispensed into the wells via a robotic pipette (epMotion 5070, Eppendorf, New York, NY). As a positive control for cytotoxicity, cells were treated with 300 μ M final concentration of H₂O₂ and not commercial drugs. This was required to achieve constancy in every cytotoxicity assay, since images are segmented based on controls. Commercial drugs are not useful as positive controls in this type of assay, because they are not always toxic or do not have the same cytocidal effects on certain cancer cells lines in vitro. As negative control and for normalization purposes cells were treated with 1% v/v DMSO. Untreated cells were also included as negative controls and as an indicator of cell viability during the incubation period. Cells exposed to the experimental compounds, plus their controls were incubated for a total of 20hr under the conditions described above, and immediately followed by image acquisition. One hour prior imaging, the mixture of Hoechst 33342 and PI was added. Three times overall standard deviation in the assay was used as a cutoff threshold for assessing cytotoxicity of the compounds. All screening was carried out in triplicates.

MTS assay (CellTiter 96 AQueousOne Solution Cell Proliferation Assay; Promega, Madison, WI) was effectuated to confirm the results obtained by DNS assay. Adherent cells were seeded at a density of 5,000 cells/well in 100 μ L medium. The number of cells seeded per well was in accordance with the manufacturer's instructions. For suspension cells, the number of seeded cells per well was 10,000 cells/well. The analogue was tested at the same final

concentration (1 μM) in presence of 1% v/v DMSO and dispensed into the wells with the same robotic pipette utilized for the DNS assay. After 69 hr of incubation, 20 μl of the MTS reagent were added to each well and subsequently incubated for additional 3 hr, completing 72 hr of incubation. The length of incubation period and the amount of MTS reagent added were in accordance with the manufacturer's instructions. Absorbance was read at 490 nm with a reference wavelength of 650 nm using a microplate reader (VERSAmax tunable microplate reader, MDS, Inc., Toronto, Canada). Control wells containing 100 μL of culture medium and MTS reagent were used as blank to subtract background absorbance. Data were expressed as percentage of cell viability relative to DMSO (solvent control) treated cells. The results were expressed as percentages of dead cells. Compounds with cytotoxicity lower than three times overall SD in the assay were considered.

3.2.4 Image acquisition and analysis for DNS assay

The BDPathway 855 Bioimager system and its associated AttoVision v1.6.2 software (BD Biosciences, Rockville, MD) were utilized for image collection and analysis. After Hoechst and PI dye mixture addition and incubation, images were captured with a 380/10 nm 535 LP nm for Hoechst and 555/28 nm 645/75 nm for PI excitation/emission filter sets. Images from each well were acquired using a 10x/ NA 0.75 dry objective. In order to obtain sufficient cell numbers for statistically robust data, images from nine (3x3 montage) contiguous fields were obtained per well. Under these settings the images were subsequently analyzed using the AttoVision software. To define nuclei as individual units or regions of interest (ROIs), pre-processing filters and intensity thresholds were applied for image segmentation. Segmented images were subjected to data classification by the use of the AttoVision software. The percentage of dead cells was calculated from the total number of ROIs per well. Cell nuclei emitting fluorescence signal from both Hoechst and PI (fluorescence co-localization) were considered as dead/dying cells, while cells emitting only Hoechst signal were counted as live cells. Data was classified by the use of the AttoVision software to identify compounds with

cytotoxic activity. Heat maps were constructed using the MeV Multiexperiment Viewer Software v.4.9.

3.2.5 Generation of dose-response curve and determination of CC50 value

The CC50 was defined as the in vitro compound concentration causing 50% of cell population death as compared to solvent treated cells after 20hr of incubation. The same type of cancerous lymphoid cell lines and non-transformed cell lines were plated into black bottom 96-well plates at same densities and conditions used in the DNS assay. The CC50 values were obtained as previously described by Elie, BT. et al [94]. To create dose-response curves and determine the 50% cytotoxic concentration (CC50), the identified hit was tested at several concentrations. Data was normalized by subtracting from each experimental value the average percentage of dead cells from six wells treated with 1% v/v DMSO. The compound's concentrations closest to the 50% cytotoxicity value were plotted and using the linear regression equation exact CC50 value was determined.

3.2.6 Apoptosis assay

Apoptosis assays were performed on lymphoid cancerous cell lines to test whether or not the analogue was killing the cancerous cells by apoptosis. Apoptosis detection was by Flowcytometry (FC 500 Series Beckman Coulter) using Annexin V-FITC (Beckman Coulter, Marseille, France) in combination with PI. Manufacturer's protocol was followed. Untreated cells, 1 μ M Curcumin, 1 μ M EF-24, 300 μ M H₂O₂, and 1% v/v DMSO were included as controls and incubated for a total of 24 hrs.

3.2.7 Mitochondrial membrane potential assay

JC-1 dye (Molecular Probes, OR, U.S.) was used to study the involvement of mitochondria during early stages of apoptosis. Jurkat cells were seeded in 24-well-plates at a density of 3x10⁴ cells in 1 mL of media per well. Cells treated with 1 μ M analogue, 1 μ M Carbonyl cyanide 3-chlorophenylhydrazone (CCCP), 1% v/v DMSO, and untreated cells were

incubated for different time points (4, 7, and 12 hrs). Then, the cells were transferred to Flow cytometry tubes. JC-1 stock solution was prepared at 200 μM concentration and 1.5 μL were added to each Flowcytometry tube. After 15 min incubation at 37 $^{\circ}\text{C}$, the tubes were processed by Flowcytometry (FC 500 Series Beckman Coulter).

3.2.8 Caspase-3/7 and -8 activity assays

Jurkat cells were seeded at a density of 100 cells/ μL in 2.5 mL of media in 24-well-plates. The analogue was tested in a final concentration of 1 μM . As positive controls, 20 μM Camptothecin and 10 μM Curcumin were used. These compound's concentrations were used according to previously determined CC50 values. As negative controls, 1% v/v DMSO-treated and untreated cells were included. For the caspase-3/7 and -8 assays, time-course experiments were designed from 0-20 hr in the presence of DEVD-NucViewTM 488 substrate (Biotium, Inc., Hayward, CA) or fluorescein active caspase-8 staining kit (Abcam, Cambridge, MA) according to the instructions of each manufacturer. Caspase-3/7 and-8 activity was analyzed by Flowcytometry (FC 500 Series Beckman Coulter) and data was analyzed with CXP software (Beckman Coulter).

3.2.9 RNA extraction and RT-PCR array

Jurkat and Nalm-6 cells (1×10^7) were treated with 1 μM analogue, 10 μM curcumin, and 1% v/v DMSO for different time points. Total RNA was extracted from cells using the RNeasy Mini Kit (Qiagen, Austin, TX, USA) and quantified using NanoDrop-1000 Spectrophotometer. Total RNA (1 μg) per sample was converted into cDNA by using the RT2 First Strand Kit (Qiagen, Austin, TX, USA). RT2 Profiler PCR Arrays for human apoptosis (PAHS-012Z) and RT2 Fluor SYBR Green (Qiagen, Austin, TX, USA) were utilized in accordance to manufacturer's instructions to study the expression of 84 apoptotic genes. The RT-PCR was carried out in an iCycler Real-Time PCR Detection System (Bio-Rad, Hercules, CA) using the following conditions: 95 $^{\circ}\text{C}$ for 10 min, followed by 40 cycles of 95 $^{\circ}\text{C}$ for 15 sec, 60 $^{\circ}\text{C}$ for 1 min, 95 $^{\circ}\text{C}$ for 1 min, 55 $^{\circ}\text{C}$ for 1 min, followed by melt curve analysis 80 cycles of 55 $^{\circ}\text{C}$ +0.5 $^{\circ}\text{C}$ per

cycle for 10 min, finally hold at 4°C. RT-PCR results were confirmed by designing specific custom-made primers (Supp.Table:3.3) and using them instead of using the primers in the RT2 Profiler PCR Arrays. The same RT-PCR cycling conditions and buffers contained in the kits where used.

3.2.10 Western blots

Jurkat cells were grown on T-75 bottles in the conditions described before. Cell viability was assured by staining cells with PI and processing them through Flowcytometry. When necessary, viability was optimized via Ficol-Paque™. Cells (1×10^6 per treatment) were incubated for different time-points with $1 \mu\text{M}$ NC2496, $10 \mu\text{M}$ curcumin, and 1% v/v DMSO. Treated cells were collected, washed once with cold PBS and resuspended in 100 μl of Lysis buffer. Following cell lysis, total protein was quantified using NanoDrop-1000 Spectrophotometer. Measurements were done in triplicate and calculations for protein normalization were done. Samples were mixed with Laemmli sample loading buffer (Bio-Rad, Hercules,CA) and boiled for 3 min at 95°C. Whole cell lysates extracts (50 μg protein/sample) were subjected to a 12% SDS polyacrylamide gel electrophoresis and electroblotted onto PVDF membrane. Membrane was blocked overnight at 4°C with 5% BSA (Sigma-Aldrich,St. Louis, MI). The membrane was then incubated with the primary antibodies: rabbit monoclonal anti-human DAPK-1 (1:1000, no. TA310390, OriGene, Rockville, MD), rabbit anti-human Bcl-2 (1:1000, no. 2870, Cell Signaling Technology, Danvers, MA), or mouse anti-human GAPDH (1:10000, no.10r-g109a, Fitzgerald Industries International, North Acton, MA). To normalize the results, membranes were blotted for GAPDH. Proteins were detected with horseradish peroxidase-linked secondary antibodies (1:5,000) and SuperSignal West Pico Chemiluminescent Substrate (Pierce, Rockford, IL). WCIF ImageJ software (<http://www.uhnresearch.ca/facilities/wcif/index.htm>) was used for densitometry analysis.

3.2.11 ELISA assay

Jurkat cells (1×10^7) were treated with $1 \mu\text{M}$ analogue, $10 \mu\text{M}$ curcumin, and 1% v/v DMSO for different time points. Cells and media were collected and centrifuged at 13,000 rpm x10 min at 4°C . Human TNF- α Elisa Kit (Thermo Scientific, Rockford, IL) was utilized to detect in the media of treated and control cells the levels of TNF- α . The assay was performed in triplicates and in accordance to the manufacturer's instructions.

3.2.12 Statistical Analysis

All experiments were performed in biological triplicates. Averages and standard deviations were calculated in Excel (Microsoft). Outliers, student's t-test, and p values were calculated using Graph Pad software.

3.3. Results and Discussion

3.3.1 Identification of a novel potent curcumin analogue

The cytotoxic potential of 19 curcumin analogues was evaluated by DNS using a panel of 13 cell lines (Supp.Fig.3.1a). Jurkat, Nalm-6, CEM and Ramos were the most sensitive cell lines as indicated by red and black squares which represent 50-100% cytotoxicity. Less sensitive cell lines were Sup-T1, Molt-3, YT, MCF-10A, and Hs27 as represented by green and black squares. To further confirm previous findings obtained by using DNS assay, an MTS assay was carried out (Supp.Fig.3.1b). Non-cancerous foreskin fibroblasts (Hs27 cell line) and non-cancerous breast cell line (MCF-10A) were used for DNS and MTS assays. MTS assay with a long (72 hrs) incubation time, was needed to determine if the difference in cytotoxicity seen between the adherent cell lines and the non-adherent blood cancer cells for some of the compounds, might be explained simply on the basis of slower proliferation rate of the adherent cells. This effect is well-known for certain chemotherapeutic agents that show an apparent preferential targeting of highly proliferating cells [138]. As shown in Supplementary Figure 3.2b, certain compounds demonstrated a higher toxicity for the non-cancerous Hs27 and MCF-10A cells when administered for an extended period of time. However, other compounds showed selectivity for

blood cancerous cells when comparing DNS versus MTS. Thus, there were few analogues with selective toxicity for blood cancerous cells. Among these analogues, NC2496 was selected based on its selectivity for blood cancerous cell lines and broad range cytotoxic spectrum against these malignancies.

3.3.2 NC2496 induces apoptosis at low micromolar concentrations

We have identified a novel cytotoxic compound potent against hematological malignancies (Fig. 3.1). The potency of the analogue is shown by its low CC50 ($\leq 1 \mu\text{M}$), broad spectrum against different types of hematological malignancies, and selectivity towards neoplasms (Table 3.1 and S. Fig. 3.1). Phosphatidylserine externalization assays carried out in Jurkat and Nalm-6 cells revealed apoptosis occurrence at 24 hrs of incubation with the analogue (Fig. 3.2). Incubation of Jurkat and Nalm-6 cells with $1 \mu\text{M}$ concentration of the analogue induced more than 50% of apoptosis in Jurkat and Nalm-6 cell populations (Fig. 3.2a & 3.2b). Further apoptotic cell death indicators such as caspase-3/7 and -8 (Fig. 3.3b & 3.3c) and mitochondrial assessment (Fig.3.3a) were realized to confirm apoptosis occurrence. The optimal time for mitochondrial depolarization occurrence in Jurkat cells was determined by time-point experiments (data not shown). Incubation of the cells for 6-8 hrs with $1 \mu\text{M}$ concentration of the analogue was enough to induce 80% of mitochondrial depolarization in Jurkat cells (Fig. 3.3a).

To assess caspase-3/7 and caspase-8 activity, Jurkat cells were treated with $1 \mu\text{M}$ NC2496 or left untreated (controls) for different time points. The study revealed caspase-8 activation at a maximum of 6-8 hr in the presence of the analogue (Fig. 3.3b). Caspase-3/7 activation was found greatest at 20 hr incubation with the analogue (Fig. 3.3c).

In summary, these findings suggested apoptosis occurrence through up-stream effectors at 8 hrs of treatment up to 20hrs when caspase-3/7 is activated. Activation of caspase-8 was hypothesized to occur through cell death receptors which induce caspase-8, mitochondrial depolarization, and ultimately caspase-3 activation.

3.3.3 NC2496 induces programmed cell death through TNF- α and DAPK-1

After identifying apoptosis occurrence induced by NC2496, we decided to characterize in deep the apoptotic cell death pathway induced by the compound in Jurkat and Nalm-6 cells. We carried out RT-PCR arrays to screen changes in gene expression upon incubation with the analogue. RT-PCR arrays were carried out at different time points (4, 8, 12 hrs) and showed up-regulation of apoptotic genes and down-regulation of anti-apoptotic genes (Fig. 3.4, Supp. Table 3.1, & Supp. Table 3.2).

Significant up-regulated genes were DAPK-1, TNF, and FADD; while XIAP and Bcl-2 variants were down-regulated (Supp. Table 3.1 & Supp. Table 3.2). Comparison of the RT-PCR results from Jurkat and Nalm-6 revealed differences among the expression levels of some genes (Supp. Table 3.2). Consequently, we hypothesize that differences in gene expression among different cell types in response to the insult of the compound, are due to the distinctive inalienable features of each cell type. Realization of additional RT-PCRs but with custom-made primers confirmed the identified up-regulated genes (Fig.3.4 & Supp. Table 3.3). Our results showed that NC2496 exhibits apoptosis triggered by signals from the exterior of the cell by members of TNF superfamily death receptors (Fig. 3.6). Death receptor activation was evidenced by TNF, Fas-Associated protein with Death Domain (FADD), and Tumor necrosis factor receptor type 1-associated DEATH domain (TRADD) up-regulation (Fig. 3.4), and by caspase-8 activation (Fig.3b). Up-regulation of TNF death receptors has been proven to be beneficial for tumor regression and/or tumor growth delay as demonstrated in experiments of mice xenotransplanted with BJAB and Jurkat cancer cell lines [139]. In addition, we assessed the TNF- α expression levels through ELISA assays and it was confirmed elevated levels of the cytokine (Fig.3.5a). Although implicated in inflammation, TNF- α can induce apoptosis mediated by antagonists like DAPK-1.

Since we have previously observed up-regulation of DAPK-1 gene, we confirmed its expression through westernblot. We have found in this study timely-dependent induction of DAPK-1 by NC2496. This was demonstrated by RT-PCR (Fig. 3.4 & Supp. Tables 3.1 & 3.2)

and by western blot (Fig.3.5b). The anti-inflammatory and apoptotic role of DAPK-1 induced by NC2496 was confirmed through the down-regulation of Bcl-2 (Fig. 3.5b) and through down-regulation of XIAP (Supp. Table 3.1). DAPK-1 apoptotic role has been confirmed previously by its involvement in the interferon-induced apoptosis through the induction of Fas or TNF [140], [141], [103], [142], [143]. Furthermore, overexpression of DAPK-1, have shown to induce apoptotic morphological changes, such as cell rounding, shrinkage, and blebbing [103], [144], [145]. In addition to apoptosis-promoting activity, several evidences indicate that DAPK-1 plays an important role in tumor suppression. First, the expression of DAPK is frequently lost in various tumor cell lines and tissues such as B cell lymphomas [146], [147]. Second, DAPK is capable of suppressing c-myc, Bcl-2, E2F-induced oncogenic transformation or anti-apoptotic genes [148]. Third, in an experimental metastasis model, the expression level of DAPK-1 was inversely correlated with the metastatic activities of the tumors, and reintroduction of DAPK-1 into the highly metastatic tumors suppressed their ability to form metastases in mice [141]. In addition, a study demonstrated that DAPK-1 is capable of activating p53-mediated apoptotic pathway through a mechanism that requires p19 ARF [148]. In summary, DAPK-1 apoptotic and anti-inflammatory activity has been demonstrated by many studies. In accordance, it was demonstrated by us the apoptotic and anti-inflammatory roles of DAPK-1 over TNF- α through the down-regulation of inhibitors of apoptosis (Supp. Table 3.1, Fig. 3.4 & 3.5) and through the involvement of downstream effectors achieving apoptosis (Fig.3).

Another important aspect that deserves to be pointed out is the observed difference among Jurkat (T-cell) and Nalm-6 (B-cell) cell lines when treated with the analogue. In Supplementary Figure 2 can be noted differences among the expression levels of TNF in Jurkat and Nalm-6 cell lines. Jurkat cells showed double amount of TNF expression levels than Nalm-6 cells. In addition, many more types of TNF receptors were upregulated in Jurkat than in Nalm-6 cells. It is also important to notice the expression levels of caspase-8 and caspase-2/RIPK1 domain containing adaptor with death domain that were induced in Nalm-6 cells. Highly

expressed levels of NOL3 (nucleolar protein 3 (apoptosis repressor with CARD domain)) could possibly repress death receptor effectors and the mitochondrial pathways in Nalm-6 cells. NOL3 has the ability to antagonize both with the extrinsic (death receptor) and the intrinsic (mitochondria/ER) death pathways [149], [150], [151]. Although the upregulation of NOL3, this was unable to detract the apoptotic activity of the analogue in Nalm-6 cells. Apparently, different pathways of cell death can follow after the administration of the analogue and this seems can be given by distinctive features of the cell lines.

3.4 Conclusions

Our findings suggest that NC2496 offers potent cytotoxic advantages over curcumin. The in vitro cytotoxic response of NC2496 is achieved at 1 μ M in 24 hrs vs. 10 μ M curcumin in 24 hrs. The potency and selectivity of NC2496 is given by the recruitment of cell death receptor members and pro-apoptotic regulators. Although, curcumin regulates many apoptotic signaling pathways, it does not stimulate TNF. The activation of this potent cytokine can produce negative effects, but under proper regulation can induce potent cytotoxic responses. We have discovered a curcumin analogue capable of inducing upregulation of DAPK-1, a potent kinase considered a tumor suppressor in charge of deciding the fate of cell death. This novel analogue efficiently engages the execution of apoptosis by TNF under the guidance of DAPK-1, thus achieving targeted elimination of hematological cancerous cells. Discovery of compounds with novel structures and cytotoxic pathways can be an opportunistic way of fine-tuning cancerous cells who escape from death.

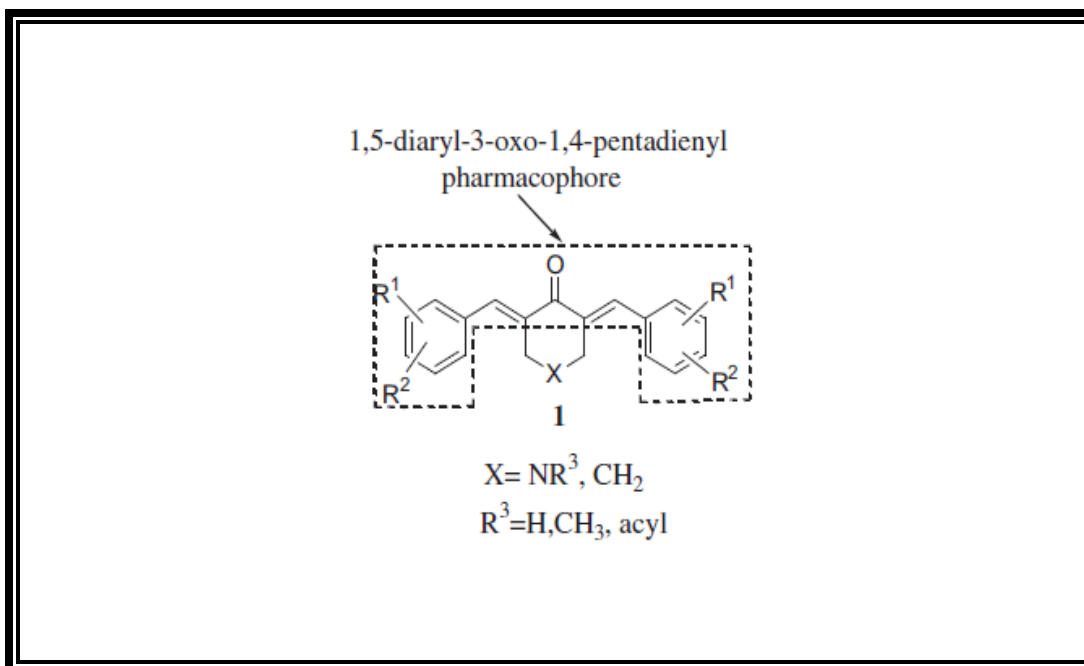


Figure 3.1: Pharmacophore utilized to synthesize the analogues.

Table 3.1: Anticancer activity of the analogue against some hematological cancer cell lines ^a

CC50 ± SD [μM] ^b							
Compound	Jurkat	CEM	Ramos	Nalm-6	Hs27	MCF-10A	OCD-112
NC2496	0.45 ± 0.00	0.59 ± 0.03	0.71 ± 0.01	0.86 ± 0.03	4.78 ± 0.30	15.60 ± 0.14	4.68 ± 0.83
EF-24	0.60 ± 0.04	0.93 ± 0.06	0.94 ± 0.05	0.69 ± 0.04	2.95 ± 0.25	5.00 ± 0.40	0.50 ± 0.42
Curcumin	10.80 ± 0.00	10.6 ± 0.06	9.72 ± 0.00	11.00 ± 0.20	15.27 ± 0.38	14.06 ± 0.66	15.8 ± 0.13

^a The analogue, EF-24 and curcumin

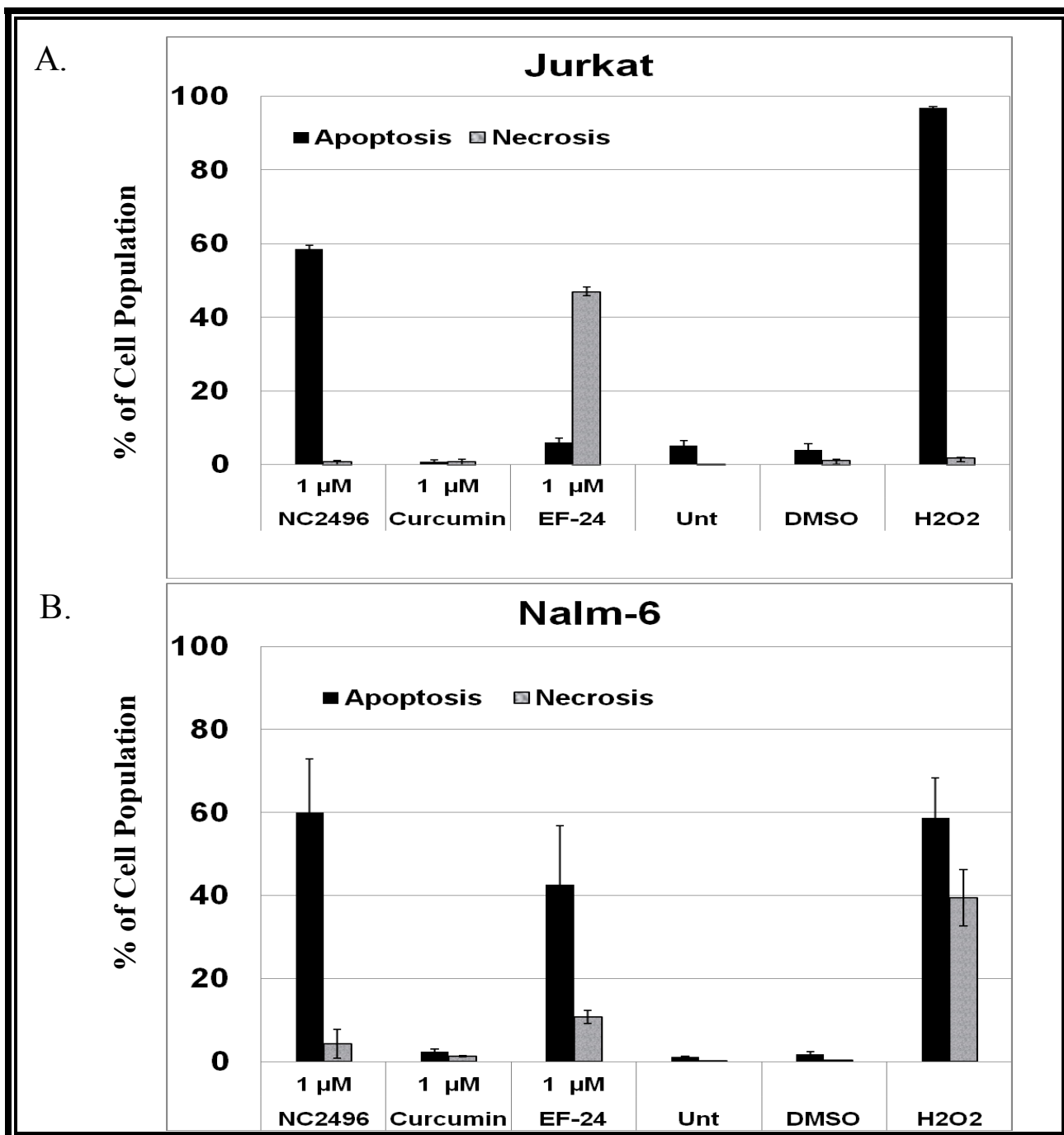


Figure 3.2: The effect of NC2496 in Jurkat and Nalm-6 cell lines.

Apoptosis induction in Jurkat (A) and Nalm-6 (B) was assessed at 24 hrs of incubation with 1 μ M of the analogue. Curcumin and EF-24 were included as reference compounds. 1% v/v DMSO and 1mM H2O2 were included as negative and positive controls, respectively.

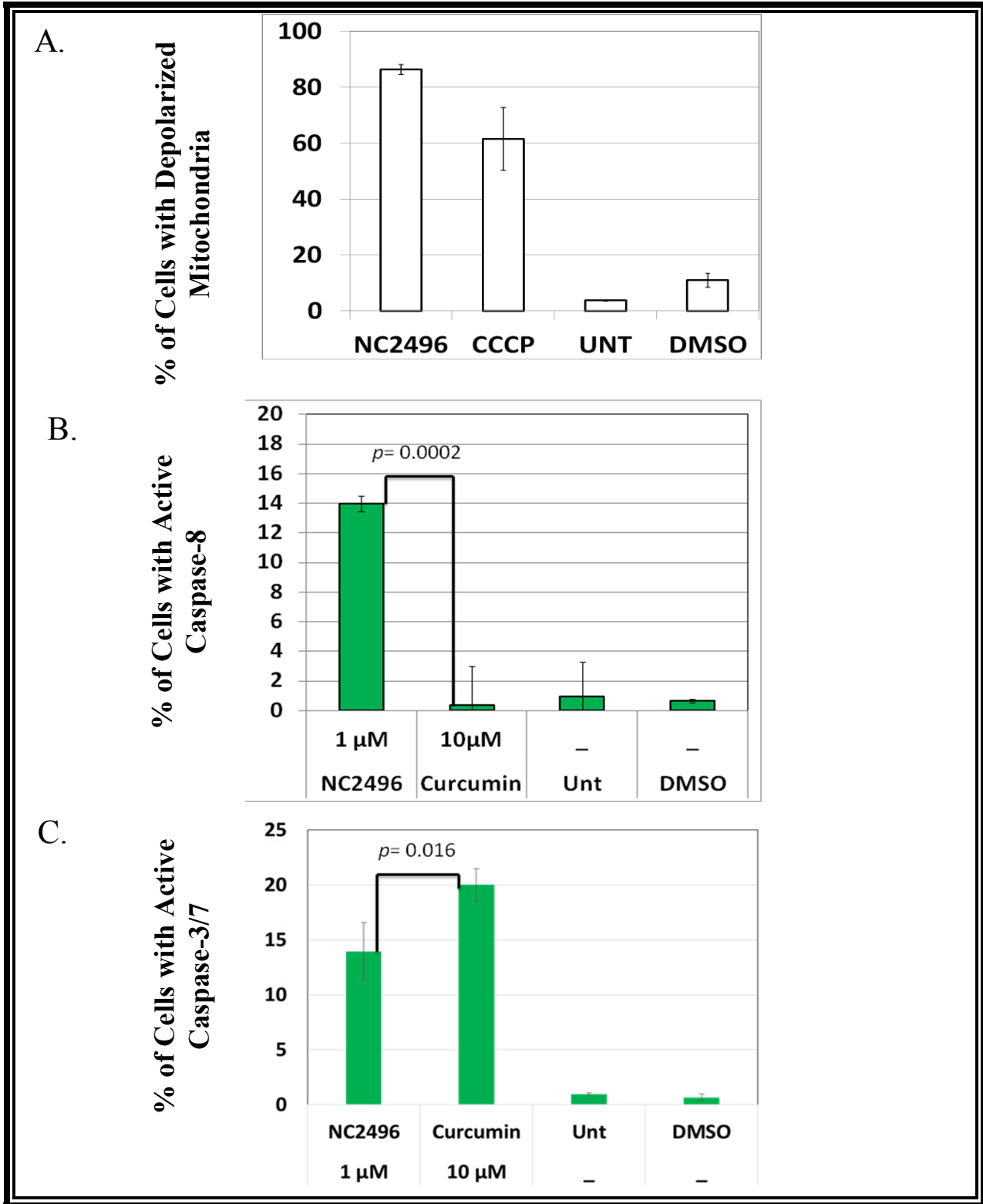


Figure 3.3: Apoptotic cell death indicators.

Mitochondrial depolarization (A), caspase-8 (B), and caspase-3/7 assays (C) were performed as indicators of apoptotic cell death occurrence in Jurkat cells. The assays were performed at different time points and different reference compounds were used in each assay. In all three assays 1 μ M NC2496, 1%V/V DMSO, and 1mM H₂O₂ were utilized. CCCP was utilized at a concentration of 50 μ M. Curcumin was utilized at the determined CC50 concentration of 10 μ M.

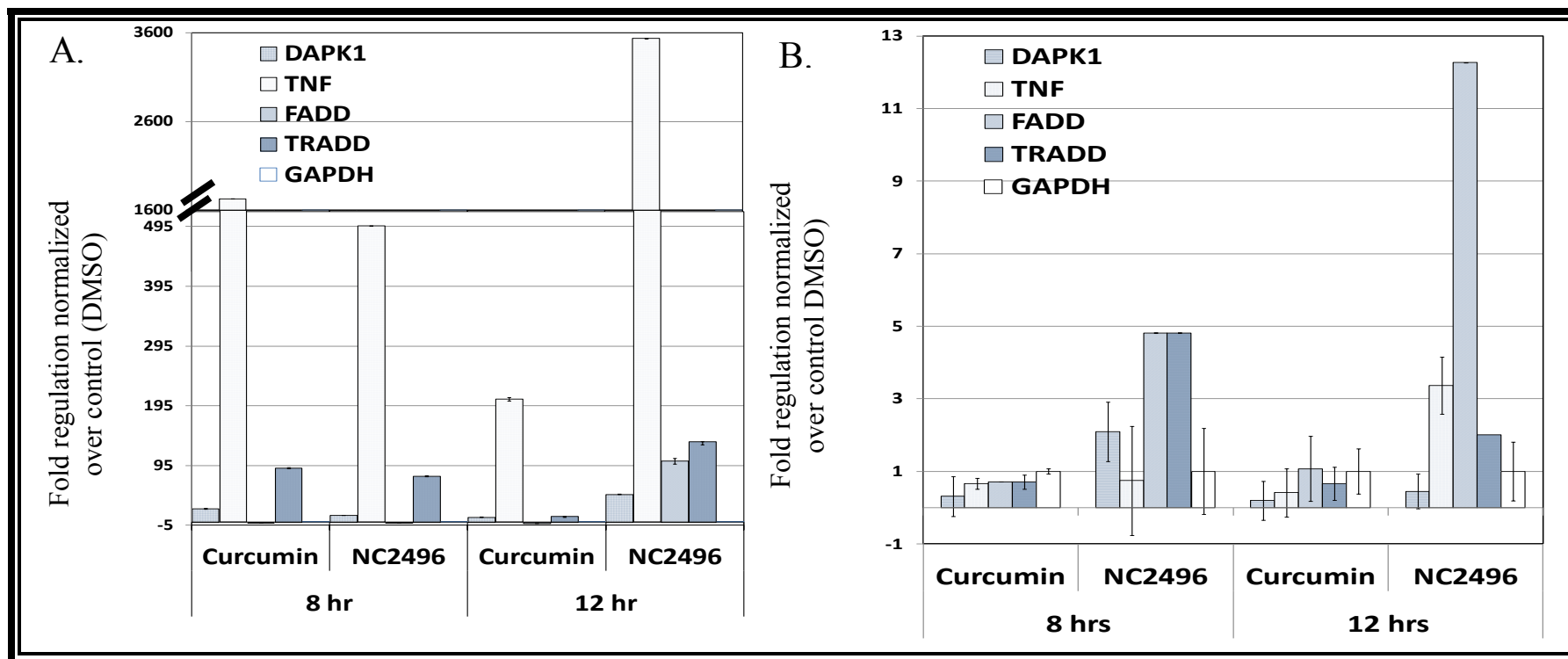


Figure 3.4: Gene-expression profiling during NC2496 and curcumin-induced apoptosis.

Jurkat (A) and Nalm-6 (B) cells were treated for 8 and 12 hrs with 1 μ M NC2496, 10 μ M curcumin and 1% V/V DMSO. Profiling results are the mean of three independent assays. Expression levels of GAPDH were used as the internal housekeeping gene control and to normalize variability between samples. In addition, expression values obtained with the analogue or curcumin were normalized to the values obtained with cells treated with DMSO.

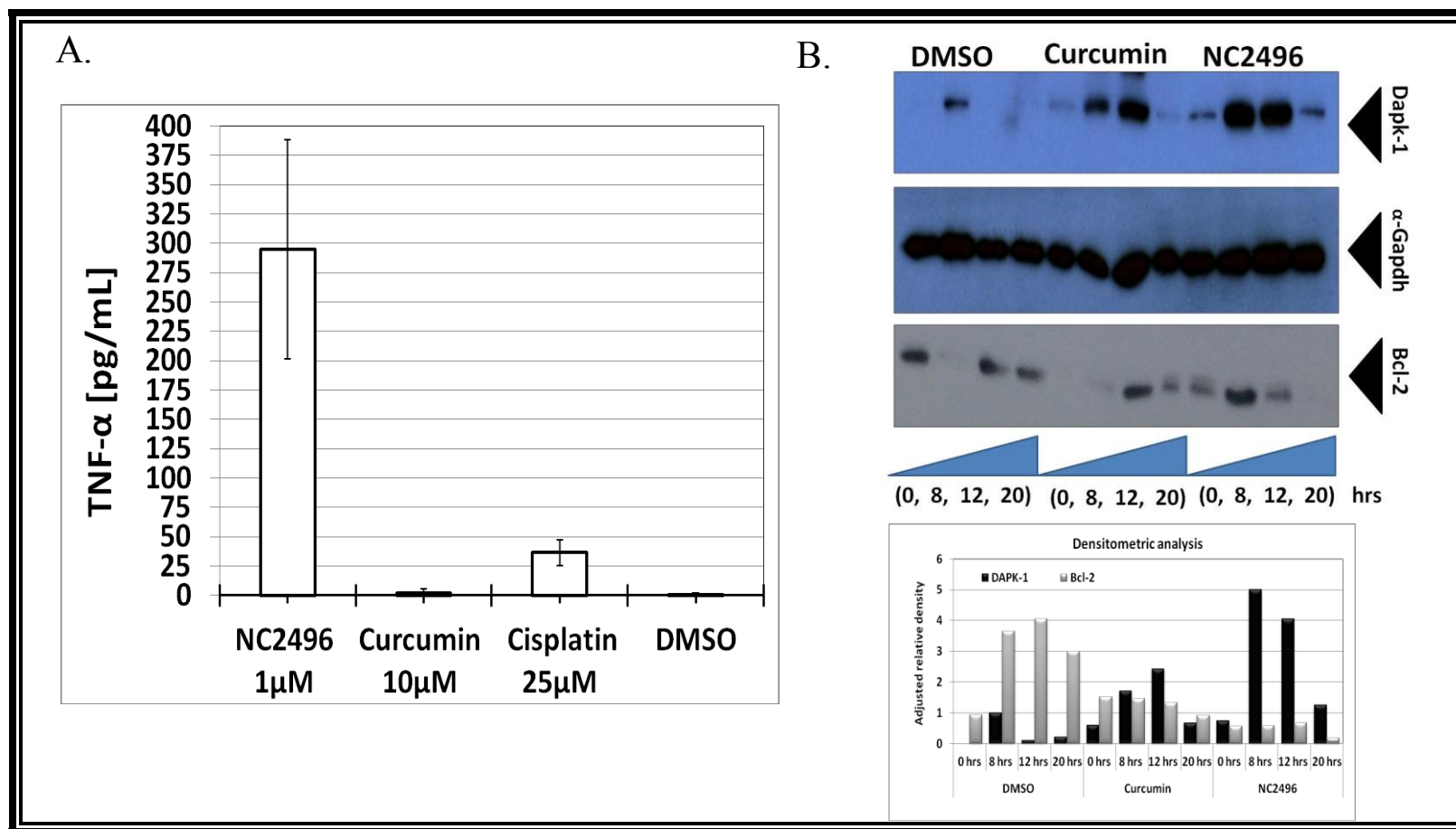


Figure 3.5: DAPK-1 and TNF- α proteins are the expression products of NC2496 cell death induction.

A. ELISA assay was performed to confirm the expression levels of TNF- α at 12 hrs of treatment with 1 μ M NC2496, 10 μ M curcumin, 25 μ M Cisplatin, and 1% V/V DMSO. B. DAPK-1 expression was confirmed by western blot. Bcl-2 expression was found

to be reduced by treatment of curcumin and the analogue for 12 hrs. α -Gapdh was used as loading control for westernblot. ImageJ software version 1.47q (Wayne Rasband, National Institutes of Health, USA) was used for the densitometry analysis.

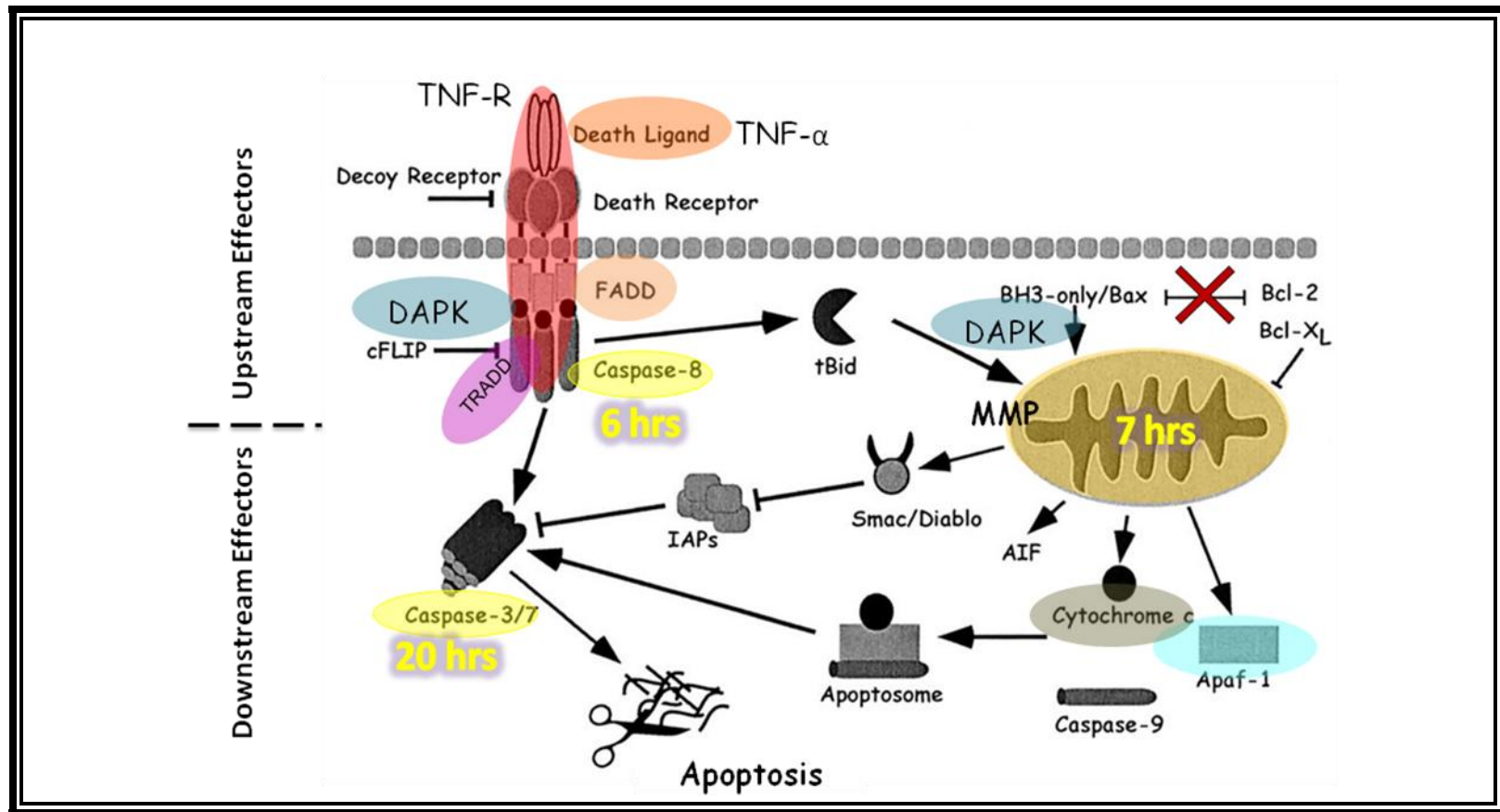
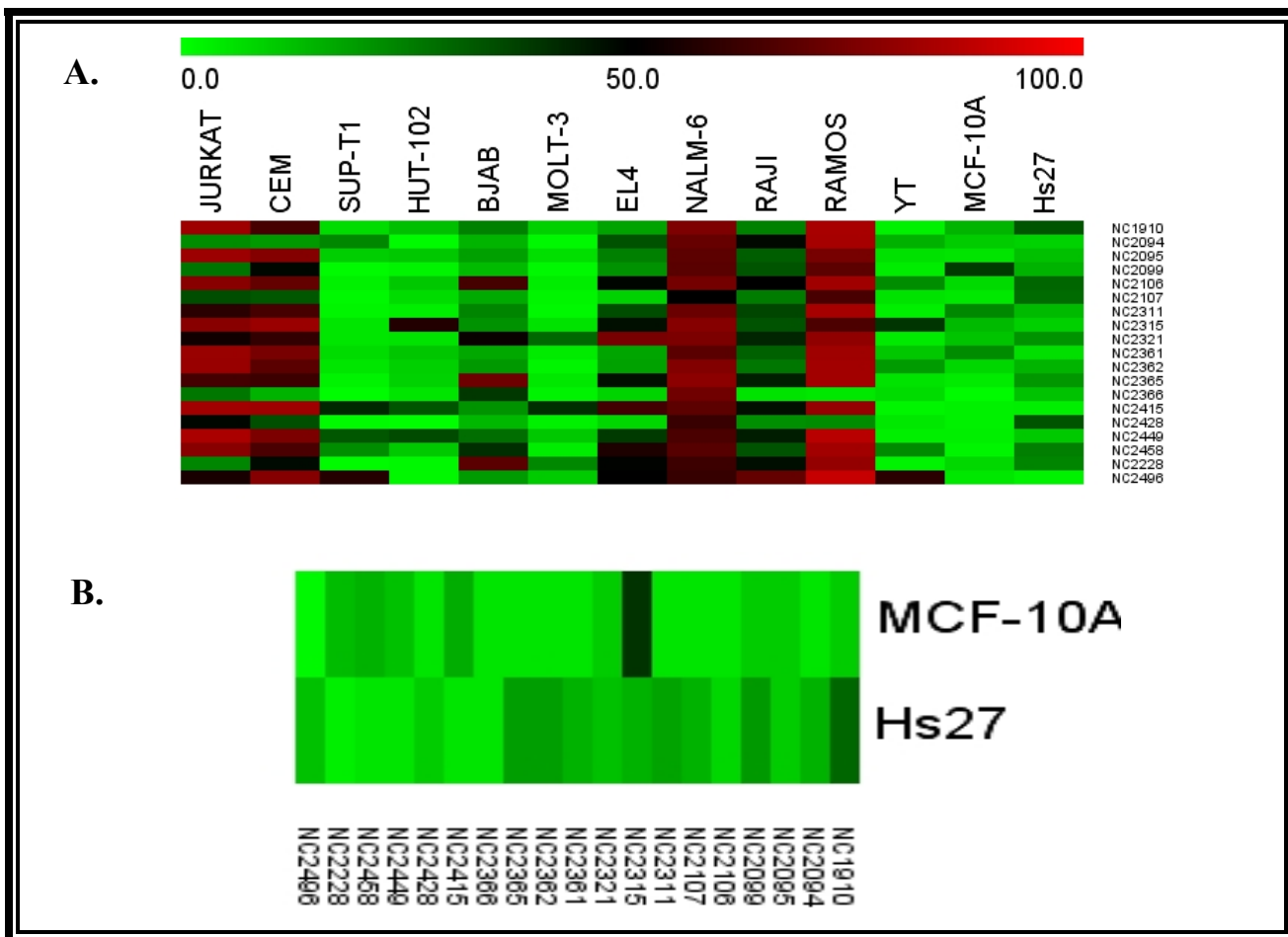


Figure 3.6: Proposed cell death mechanism of NC2496.

From apoptosis, caspases, ELISA, westernblots, and qRT-PCR assays the cell death mechanism of NC2496 was elucidated to occur through downstream and upstream apoptotic effectors involving TNFR.

3.5 Appendix



S. Fig. 3.1: Discovery of cytotoxic curcumin analogues against hematological malignancies.

A. The cytotoxic potential of 19 curcumin analogues was studied in 13 cell lines by DNS. The compounds were tested at a final concentration of 1 μ M and incubated for 20 hrs. The red color represents higher percentage of cytotoxicity (100%); black 50%, and green lower cytotoxicity (0%). Distinctively, Jurkat, CCRF-CEM, Nalm-6, and Ramos cell lines were highly affected by the compounds. B. MTS screen assay was carried out in Hs27 and MCF-10A cell lines. The analogues were tested at a final concentration of 1 μ M and incubated for 72 hrs. Black color represents around 50% percentage of anti-proliferation and green low percentage of death. NC2496 was selected because we were focused on those analogues without cytotoxic effects on

non-cancerous cell lines, but with potent and broad cytotoxic effects on various blood cancerous cells. MeV software was used to construct the heat maps.

S. Table 3.1: Regulation of anti-apoptotic and apoptotic genes by NC2496.

Anti-apoptotic Genes	Fold regulation (Normalized over DMSO)					
	4 hrs		8 hrs		12 hrs	
BCL2L1	2.89	±1.16	2.22	±0.67	1.62	±0.47
IGF1R	2.76	±3.36	3.19	±0.72	1.61	±1.37
AKT1	2.48	±0.71	2.18	±0.66	1.50	±0.29
XIAP	2.11	±0.61	1.23	±0.62	1.21	±0.24
NAIP	2.00	±0.51	1.46	±0.52	1.14	±0.54
BAG1	1.61	±0.30	1.25	±0.66	1.16	±0.06
NFKB1	1.56	±0.46	1.93	±0.54	0.97	±0.50
BNIP3L	1.55	±0.06	1.49	±0.82	1.12	±0.16
BFAR	1.46	±0.22	-1.09	±1.54	1.12	±0.16
BIRC3	1.38	±0.11	2.07	±0.58	1.00	±0.68
BIRC2	1.35	±0.52	1.15	±0.62	1.28	±0.19
BNIP2	1.32	±0.00	1.62	±0.64	1.20	±0.40
TNFRSF1B	1.33	±0.22	-1.05	±0.66	1.89	±1.05
NOL3	1.23	±0.05	1.71	±0.62	1.18	±0.12
BRAF	0.80	±1.62	1.11	±0.65	1.00	±0.24
ABL1	0.57	±1.69	1.71	±0.59	1.40	±0.27
BIRC6	0.37	±1.70	1.74	±0.67	0.90	±0.35
BNIP3	0.33	±1.24	1.44	±0.62	1.33	±0.26
BCL2	0.24	±2.19	2.26	±0.57	0.96	±0.19
BCL2L2	0.13	±1.62	1.60	±0.70	1.34	±0.06
RIPK2	-0.23	±2.74	-1.80	±1.31	0.60	±0.09
BAG3	-0.54	±1.63	-2.78	±2.45	1.37	±1.39
BCL2A1	-1.24	±4.78	-3.48	±0.00	0.16	±0.19
MCL1	-1.49	±0.23	-2.00	±0.98	1.01	±0.56

BIRC5	-1.71	±0.20	1.32	±0.79	1.25	±0.06
-------	-------	-------	------	-------	------	-------

Continuation of Table 3.1

Apoptotic Genes	Fold regulation (Normalized over DMSO)					
	4 hrs		8 hrs		12 hrs	
CD27	3.52	±1.52	1.74	±0.80	1.74	±0.00
CASP2	2.66	±0.40	2.51	±0.62	1.28	±0.49
TNFRSF25	2.41	±1.20	1.93	±0.73	1.59	±0.00
CIDEB	2.58	±1.04	2.07	±0.65	1.15	±0.11
CASP8	2.25	±0.67	1.65	±0.60	1.43	±0.68
CASP10	2.14	±0.54	1.80	±0.61	1.35	±0.33
BAD	1.96	±0.67	1.77	±0.65	1.76	±0.34
FAS	1.91	±0.08	1.49	±0.63	1.11	±0.57
TP53	1.66	±2.75	1.49	±0.59	1.14	±0.17
CASP3	1.44	±0.37	1.15	±0.55	0.82	±0.42
TRAF3	1.76	±0.27	1.32	±0.57	1.18	±0.12
APAF1	2.74	±0.51	2.93	±0.84	1.59	±1.07
BCL2L11	2.01	±0.23	2.38	±0.61	1.62	±0.54
TRAF2	1.93	±0.72	2.11	±0.70	1.62	±0.47
TNFRSF10B	1.84	±0.31	2.38	±0.72	1.20	±0.35
FADD	1.73	±0.38	3.36	±0.76	1.65	±1.23
TNFSF8	1.72	±0.74	1.07	±0.64	1.72	±0.89
TNF	1.65	±0.31	4.07	±0.55	1.81	±0.61
CFLAR	1.60	±0.24	2.11	±0.66	1.43	±0.61
CASP6	1.48	±0.06	1.11	±0.90	1.36	±0.27
CASP7	1.45	±0.56	1.97	±0.58	1.87	±0.18
CYCS	1.43	±0.62	2.00	±0.59	1.64	±0.32
DAPK1	1.42	±5.69	3.48	±1.40	1.88	±1.53
NOD1	1.36	±0.17	2.00	±0.62	1.34	±0.51
TNFRSF21	1.36	±0.16	1.65	±0.60	1.23	±0.83
BCL10	1.29	±0.05	2.42	±0.86	1.07	±0.36

LTBR	1.24	±0.19	2.38	±0.54	1.29	±0.37
CD40LG	1.19	±0.20	2.04	±0.70	1.19	±0.06
TP53BP2	1.16	±0.19	1.97	±0.58	1.14	±0.85
CASP9	1.15	±0.13	1.19	±1.62	1.25	±0.18
BAX	1.13	±0.18	2.14	±0.76	1.28	±0.19
CD70	1.13	±0.14	-1.68	±1.28	0.90	±0.46
TNFRSF1A	0.86	±1.74	2.07	±0.59	1.54	±0.59
DFFA	0.58	±1.39	1.27	±0.59	1.20	±0.00
TRADD	0.57	±1.69	3.08	±0.64	2.02	±1.44
TNFSF10	0.53	±4.0	1.74	±0.51	1.29	±0.31
LTA	0.50	±1.94	1.57	±0.58	0.99	±0.51
CRADD	0.44	±1.42	1.25	±0.89	1.39	±0.14
IL10	0.27	±2.51	-3.48	±0.00	2.82	±3.48
CASP1	0.15	±2.44	-1.19	±0.91	0.85	±0.25
PYCARD	-0.31	±2.61	-1.19	±1.02	0.92	±0.18
CIDEA	-0.38	±1.47	-2.30	±0.88	2.06	±2.37
TNFRSF10A	-0.38	±1.58	-2.69	±0.43	2.07	±2.23
TNFRSF9	-0.38	±1.42	-2.93	±0.50	1.90	±2.24
TNFRSF11B	-0.38	±1.42	-3.48	±0.00	2.23	±2.64
CASP5	-0.38	±1.42	-3.48	±0.00	2.68	±3.17
CASP14	-0.38	±1.42	-2.83	±0.60	2.50	±2.96
FASLG	-0.44	±2.32	-2.00	±0.54	2.46	±2.44
BCL2L10	-0.47	±1.47	-3.48	±0.00	3.62	±4.29
CD40	-0.62	±2.31	-4.00	±0.00	2.08	±2.46
HRK	-0.65	±1.45	-1.83	±1.20	0.97	±0.41
CASP4	-1.18	±0.15	-1.30	±0.92	1.09	±0.61
BID	-1.20	±0.05	-1.23	±0.80	0.94	±0.18
GADD45A	-1.27	±0.16	1.41	±0.82	1.18	±0.29
BAK1	-1.80	±0.51	-1.41	±1.25	1.11	±0.79
AIFM1	-1.16	±0.24	1.25	±0.68	1.03	±0.20
TP73	-0.74	±1.66	2.83	±0.61	1.93	±0.09

DIABLO	0.47	±1.42	1.34	±0.56	1.34	±0.07
BIK	0.62	±1.44	1.25	±0.67	1.46	±0.28

S. Table 3.2: Regulation of apoptotic and anti-apoptotic genes by NC2496^a.

Unigene	Refseq	Symbol	Description	Fold Change	
				Jurkat	Nalm-6
Hs.431048	NM_005157	ABL1	C-abl oncogene 1, non-receptor tyrosine kinase	1.71	-2.14
Hs.424932	NM_004208	AIFM1	Apoptosis-inducing factor, mitochondrion-associated, 1	1.25	-1.23
Hs.525622	NM_005163	AKT1	V-akt murine thymoma viral oncogene homolog 1	2.18	1.32
Hs.552567	NM_001160	APAF1	Apoptotic peptidase activating factor 1	2.93	2.14
Hs.370254	NM_004322	BAD	BCL2-associated agonist of cell death	1.77	1.23
Hs.377484	NM_004323	BAG1	BCL2-associated athanogene	1.25	-1.74
Hs.523309	NM_004281	BAG3	BCL2-associated athanogene 3	0.36	2.46
Hs.485139	NM_001188	BAK1	BCL2-antagonist/killer 1	0.71	1.32
Hs.624291	NM_004324	BAX	BCL2-associated X protein	2.14	1.15
Hs.193516	NM_003921	BCL10	B-cell CLL/lymphoma 10	2.42	1.87
Hs.150749	NM_000633	BCL2	B-cell CLL/lymphoma 2	2.26	1.00
Hs.227817	NM_004049	BCL2A1	BCL2-related protein A1	0.29	1.15
Hs.516966	NM_138578	BCL2L1	BCL2-like 1	2.22	-1.74
Hs.283672	NM_020396	BCL2L10	BCL2-like 10 (apoptosis facilitator)	0.29	1.15
Hs.737004	NM_006538	BCL2L11	BCL2-like 11 (apoptosis facilitator)	2.38	1.15
Hs.735863	NM_004050	BCL2L2	BCL2-like 2	1.60	1.23
Hs.435556	NM_016561	BFAR	Bifunctional apoptosis regulator	0.92	1.00
Hs.591054	NM_001196	BID	BH3 interacting domain death agonist	0.81	-1.15
Hs.475055	NM_001197	BIK	BCL2-interacting killer (apoptosis-inducing)	1.25	-1.15
Hs.731943	NM_001166	BIRC2	Baculoviral IAP repeat containing 2	1.15	1.87
Hs.127799	NM_001165	BIRC3	Baculoviral IAP repeat containing 3	2.07	-1.52
Hs.744872	NM_001168	BIRC5	Baculoviral IAP repeat containing 5	1.32	2.00
Hs.150107	NM_016252	BIRC6	Baculoviral IAP repeat containing 6	1.74	2.14
Hs.592515	NM_004330	BNIP2	BCL2/adenovirus E1B 19kDa interacting protein 2	1.62	1.15
Hs.144873	NM_004052	BNIP3	BCL2/adenovirus E1B 19kDa interacting protein 3	1.44	-78.79
Hs.131226	NM_004331	BNIP3L	BCL2/adenovirus E1B 19kDa interacting protein 3-like	1.49	-1.23
Hs.600998	NM_004333	BRAF	V-raf murine sarcoma viral oncogene homolog B1	1.11	-1.41
Hs.2490	NM_033292	CASP1	Caspase 1, apoptosis-related cysteine peptidase	0.84	1.15
Hs.5353	NM_001230	CASP10	Caspase 10, apoptosis-related cysteine peptidase	1.80	2.00
Hs.466057	NM_012114	CASP14	Caspase 14, apoptosis-related cysteine peptidase	0.35	1.15
Hs.368982	NM_032982	CASP2	Caspase 2, apoptosis-related cysteine peptidase	2.51	1.15
Hs.141125	NM_004346	CASP3	Caspase 3, apoptosis-related cysteine peptidase	1.15	-1.32
Hs.138378	NM_001225	CASP4	Caspase 4, apoptosis-related cysteine peptidase	0.77	1.07
Hs.213327	NM_004347	CASP5	Caspase 5, apoptosis-related cysteine peptidase	0.29	1.15
Hs.654616	NM_032992	CASP6	Caspase 6, apoptosis-related cysteine peptidase	1.11	-1.15
Hs.9216	NM_001227	CASP7	Caspase 7, apoptosis-related cysteine peptidase	1.97	1.00
Hs.599762	NM_001228	CASP8	Caspase 8, apoptosis-related cysteine peptidase	1.65	34.30
Hs.329502	NM_001229	CASP9	Caspase 9, apoptosis-related cysteine peptidase	1.19	1.52
Hs.355307	NM_001242	CD27	CD27 molecule	1.74	1.52

Hs.472860	NM_001250	CD40	CD40 molecule, TNF receptor superfamily member 5	0.25	1.15
Hs.592244	NM_000074	CD40LG	CD40 ligand	2.04	2.30
Hs.715224	NM_001252	CD70	CD70 molecule	0.59	1.15
Hs.731912	NM_003879	CFLAR	CASP8 and FADD-like apoptosis regulator	2.11	1.52
Hs.249129	NM_001279	CIDEA	Cell death-inducing DFFA-like effector a	0.44	1.15
Hs.708040	NM_014430	CIDEB	Cell death-inducing DFFA-like effector b	2.07	1.32
Hs.591016	NM_003805	CRADD	CASP2 and RIPK1 domain containing adaptor with death domain	1.25	6.06
Hs.617193	NM_018947	CYCS	Cytochrome c, somatic	2.00	1.62
Hs.693441	NM_004938	DAPK1	Death-associated protein kinase 1	3.48	2.00
Hs.484782	NM_004401	DFFA	DNA fragmentation factor, 45kDa, alpha polypeptide	1.27	1.74
Hs.169611	NM_019887	DIABLO	Diablo, IAP-binding mitochondrial protein	1.34	1.07
Hs.86131	NM_003824	FADD	Fas (TNFRSF6)-associated via death domain	3.36	-1.32
Hs.244139	NM_000043	FAS	Fas (TNF receptor superfamily, member 6)	1.49	1.74
Hs.2007	NM_000639	FASLG	Fas ligand (TNF superfamily, member 6)	0.50	1.15
Hs.80409	NM_001924	GADD45A	Growth arrest and DNA-damage-inducible, alpha	1.41	-2.46
Hs.87247	NM_003806	HRK	Harakiri, BCL2 interacting protein (contains only BH3 domain)	0.55	-1.32
Hs.714012	NM_000875	IGF1R	Insulin-like growth factor 1 receptor	3.19	1.23
Hs.193717	NM_000572	IL10	Interleukin 10	0.29	1.15
Hs.36	NM_000595	LTA	Lymphotoxin alpha (TNF superfamily, member 1)	1.57	3.48
Hs.1116	NM_002342	LTBR	Lymphotoxin beta receptor (TNFR superfamily, member 3)	2.38	1.15
Hs.632486	NM_021960	MCL1	Myeloid cell leukemia sequence 1 (BCL2-related)	0.50	2.83
Hs.654500	NM_004536	NAIP	NLR family, apoptosis inhibitory protein	1.46	2.30
Hs.618430	NM_003998	NFKB1	Nuclear factor of kappa light polypeptide gene enhancer in B-cells 1	1.93	-1.15
Hs.405153	NM_006092	NOD1	Nucleotide-binding oligomerization domain containing 1	2.00	2.00
Hs.513667	NM_003946	NOL3	Nucleolar protein 3 (apoptosis repressor with CARD domain)	1.71	24.25
Hs.499094	NM_013258	PYCARD	PYD and CARD domain containing	0.84	-1.32
Hs.103755	NM_003821	RIPK2	Receptor-interacting serine-threonine kinase 2	0.55	-1.00
Hs.241570	NM_000594	TNF	Tumor necrosis factor	4.07	2.00
Hs.213467	NM_003844	TNFRSF10A	Tumor necrosis factor receptor superfamily, member 10a	0.37	1.74
Hs.521456	NM_003842	TNFRSF10B	Tumor necrosis factor receptor superfamily, member 10b	2.38	-2.30
Hs.81791	NM_002546	TNFRSF11B	Tumor necrosis factor receptor superfamily, member 11b	0.29	1.15
Hs.279594	NM_001065	TNFRSF1A	Tumor necrosis factor receptor superfamily, member 1A	2.07	-36.76
Hs.256278	NM_001066	TNFRSF1B	Tumor necrosis factor receptor superfamily, member 1B	0.95	1.15
Hs.443577	NM_014452	TNFRSF21	Tumor necrosis factor receptor superfamily, member 21	1.65	-3.48
Hs.462529	NM_003790	TNFRSF25	Tumor necrosis factor receptor superfamily, member 25	1.93	1.00
Hs.86447	NM_001561	TNFRSF9	Tumor necrosis factor receptor superfamily, member 9	0.34	1.15
Hs.478275	NM_003810	TNFSF10	Tumor necrosis factor (ligand) superfamily, member 10	1.74	1.52
Hs.494901	NM_001244	TNFSF8	Tumor necrosis factor (ligand) superfamily, member 8	1.07	-1.00
Hs.740601	NM_000546	TP53	Tumor protein p53	1.49	1.00
Hs.523968	NM_005426	TP53BP2	Tumor protein p53 binding protein, 2	1.97	1.07
Hs.192132	NM_005427	TP73	Tumor protein p73	2.83	1.15
Hs.460996	NM_003789	TRADD	TNFRSF1A-associated via death domain	3.08	1.32
Hs.522506	NM_021138	TRAF2	TNF receptor-associated factor 2	2.11	-64.00
Hs.510528	NM_003300	TRAF3	TNF receptor-associated factor 3	1.32	1.15
Hs.736565	NM_001167	XIAP	X-linked inhibitor of apoptosis	1.23	-1.23
Hs.534255	NM_004048	B2M	Beta-2-microglobulin	1.02	1.32
Hs.544577	NM_002046	GAPDH	Glyceraldehyde-3-phosphate dehydrogenase	1.00	1.00

^a Jurkat and Nalm-6 cells were incubated for 8 hrs with 1 μ M NC2496 and 1% V/V DMSO. DMSO and GAPDH were utilized for normalization purposes. Values show in black

represent a fold regulation of ~1, blue values represent downregulation, and red values represent upregulation.

S. Table 3.3: Primers designed for RT-PCR confirmation.

Primer	Sequence (5' → 3')	Gene	Template
DAPK1_F	CACGACGTCTACTCACAGGC	DAPK-1	mRNA exon pos. 4397
DAPK1_R	ATGGCGAGAAGGCACCCAGTC	DAPK-1	mRNA exon, pos. 4530
TNF- α _F	GAG GCC AAG CCC TGG TAT GA	TNF	mRNA exon pos. 731
TNF- α _R	TGAGTCGGTCACCCTTCTCC	TNF	mRNA exon pos. 800
FADD_F	GAA GAA GAC CTG TGT GCA GCA	FADD	mRNA exon pos. 577
FADD_R	GCTGTGTAGATGCCTGTGGT	FADD	mRNA exon pos. 988
TRADD1_F	TACGAGCGCGAGGGACTGTA	TRADD	mRNA exon pos. 846
TRADD1_R	GGTGAGCTCGTTCTCCTCGA	TRADD	mRNA exon pos. 965
GAPDH-R	GGA AGG ACT CAT GAC CAC AGT	GAPDH	mRNA exon pos.687
GAPDH-F	CAG GGA TGA TGT TCT GGA GAG	GAPDH	mRNA exon pos. 799

R= reverse, F=forward

Summary and conclusions

The apparition of a first mutation and further cell growth dysregulation is considered the initiation of cancer. Environmental factors such as the intromission of virus, bacteria, chemical agents, radiation, and cellular factors like replication errors among others can contribute to mutations in the DNA by interfering with its correct expression. Additional mutations in the DNA along the time, formation of new blood vessels, and cooperation among different factors lead to cancer progression. From these interrelated events is stated that cancer is considered a broad group of pathologies involving dysregulated cell proliferation, invasion, metastasis, along with other conditions.

The earlier in stage cancer is detected and treated the better prognosis, because spreading of mutated cells and organ damage is reduced. Thus, anti-cancer therapies are designed to reduce invasion and spread of mutated cells. These therapies involve targeted and non-targeted chemotherapeutic agents. The last, kill cancerous cells and also non-malignant cells with chances of causing toxicity. While targeted therapies are more directed against cancerous cells. Same occurs with radiation therapy which can result harmful and not specific, yet new approaches are being investigated to address specificity. Another strategy for the removal of compromised tissue is surgery which have shown to be very effective to remove tumors, but it cannot be applied for all types of cancers, such as in the case of leukemia.

The discovery of novel anti-cancer therapies is always desired to reduce statistics and developing resistance to current treatments. Thus, additional search of therapies have led to the isolation and screen of compounds derived from plants and natural sources. In this way, curcumin (derived from the roots of turmeric) have been identified as an anti-cancer agent with low toxicity towards normal cells. *In vivo* testing of curcumin however have show low bioavailabilty reducing curcumins potential. Thus, to overcome this disadvantage curcumin analogues have been designed. During the past years, I have being dedicated to research several curcumin analogues, thus characterizing one lead analogue specific against hematological malignancies. These lead curcumin analogue was found able to induce selective cytotoxicity at low micromolar concentration towards hematological malignancies as confirmed by cytotoxicity assays. Further characterization of this analogue apport findings in where it induces cell death through TNF- α , cell death receptor mediated apoptosis, and expression of a tumor suppressor protein. Compared to curcumin or EF-24, this analogue promises better cytotoxicity towards lymphoma and leukemia, sensitizing these malignancies to apoptosis *via* intrinsic and extrinsic pathways and not depending only on one *via* to affect cancerous cells. Further research should be conducted to study wether if this analogue causes DNA demethylation for the expression of this tumor suppressor protein, since it is well-known that this gene coding for this suppressor protein is frequently methylated in hematological cancers. Further molecules can be designed from this lead analogue in the expectation of finding even more potent analogues.

In conclusions, curcumin analogues share characteristics related to curcumin's molecule, but being a new class of molecules they apport additional features against cancer. Different from

EF-24, our lead analogue is more apoptotic and this could imply better response and reduced inflammation. More molecules can be exploited and derivatives of derivatives can be synthesized in order to find even better anti-cancer compounds. These results support the results of others and that we can not be wrong to ascribe cytotoxic properties to curcumin and its derivatives.

References

1. Olszewski, M.M., *Concepts of Cancer from Antiquity to the Nineteenth Century*. UTMJ, 2010. 87(3): p. 181-186.
2. Retief, F.P. and L. Cilliers, *Tumours and cancers in Graeco-Roman times*. S Afr Med J, 2001. 91(4): p. 344-8.
3. Pray, L., *Discovery of DNA Structure and Function: Watson and Crick*. Nature Education, 2008. 1(1).
4. Jacob, F. and J. Monod, *Genetic regulatory mechanisms in the synthesis of proteins*. J Mol Biol, 1961. 3: p. 318-56.
5. Mu, X.J., et al., *Analysis of genomic variation in non-coding elements using population-scale sequencing data from the 1000 Genomes Project*. Nucleic Acids Res, 2011. 39(16): p. 7058-76.
6. Knudson, A.G., *Two genetic hits (more or less) to cancer*. Nat Rev Cancer, 2001. 1(2): p. 157-62.
7. Gordon, G.M. and W. Du, *Conserved RB functions in development and tumor suppression*. Protein Cell, 2011. 2(11): p. 864-78.
8. Hajdu, S.I.V., M.S. , *A Note from History: The Use of Tobacco*. . Annals of Clinical & Laboratory Science., 2010. . 40(2): p. 178-181.
9. Brown, J.R. and J.L. Thornton, *Percivall Pott (1714-1788) and chimney sweepers' cancer of the scrotum*. Br J Ind Med, 1957. 14(1): p. 68-70.
10. Fujiki, H., *Gist of Dr. Katsusaburo Yamagiwa's papers entitled "Experimental study on the pathogenesis of epithelial tumors" (I to VI reports)*. Cancer Sci, 2014. 105(2): p. 143-9.
11. Rask-Nielsen, R., *On the susceptibility of the thymus, lung, subcutaneous and mammary tissues in strain street mice to direct application of small doses of four different carcinogenic hydrocarbons*. Br J Cancer, 1950. 4(1): p. 108-16.
12. Lijinsky, W. and P. Shubik, *Benzo(a)Pyrene and Other Polynuclear Hydrocarbons in Charcoal-Broiled Meat*. Science, 1964. 145(3627): p. 53-5.
13. Muller, H.J., *The Production of Mutations by X-Rays*. Proc Natl Acad Sci U S A, 1928. 14(9): p. 714-26.
14. Stocks, P. and J.M. Campbell, *Lung cancer death rates among non-smokers and pipe and cigarette smokers; an evaluation in relation to air pollution by benzpyrene and other substances*. Br Med J, 1955. 2(4945): p. 923-9.
15. Doll, R., et al., *Mortality in relation to smoking: 50 years' observations on male British doctors*. BMJ, 2004. 328(7455): p. 1519.
16. Berwald, Y. and L. Sachs, *In vitro transformation of normal cells to tumor cells by carcinogenic hydrocarbons*. J Natl Cancer Inst, 1965. 35(4): p. 641-61.
17. Rous, P., *A transmissible avian neoplasm. (Sarcoma of the common fowl) by Peyton Rous, M.D., Experimental Medicine for Sept. 1, 1910, vol. 12, pp.696-705*. J Exp Med, 1979. 150(4): p. 738-53.
18. Shope, R.E., *A Filtrable Virus Causing a Tumor-Like Condition in Rabbits and Its Relationship to Virus Myxomatousum*. J Exp Med, 1932. 56(6): p. 803-22.
19. Gross, L., *The fortuitous isolation and identification of the polyoma virus*. Cancer Res, 1976. 36(11 Pt 1): p. 4195-6.

20. Fan, H., *Cell transformation by RNA viruses: an overview*. *Viruses*, 2011. 3(6): p. 858-60.
21. Fan, H. and C. Johnson, *Insertional oncogenesis by non-acute retroviruses: implications for gene therapy*. *Viruses*, 2011. 3(4): p. 398-422.
22. Thun, M.J., et al., *The global burden of cancer: priorities for prevention*. *Carcinogenesis*, 2010. 31(1): p. 100-10.
23. Marshall, B.J. and H.M. Windsor, *The relation of Helicobacter pylori to gastric adenocarcinoma and lymphoma: pathophysiology, epidemiology, screening, clinical presentation, treatment, and prevention*. *Med Clin North Am*, 2005. 89(2): p. 313-44, viii.
24. Davis, G.L., et al., *Hepatocellular carcinoma: management of an increasingly common problem*. *Proc (Bayl Univ Med Cent)*, 2008. 21(3): p. 266-80.
25. Burd, E.M., *Human papillomavirus and cervical cancer*. *Clin Microbiol Rev*, 2003. 16(1): p. 1-17.
26. Wroblewski, L.E., R.M. Peek, Jr., and K.T. Wilson, *Helicobacter pylori and gastric cancer: factors that modulate disease risk*. *Clin Microbiol Rev*, 2010. 23(4): p. 713-39.
27. Polk, D.B. and R.M. Peek, Jr., *Helicobacter pylori: gastric cancer and beyond*. *Nat Rev Cancer*, 2010. 10(6): p. 403-14.
28. Bottenstein, J.E. and G.H. Sato, *Growth of a rat neuroblastoma cell line in serum-free supplemented medium*. *Proc Natl Acad Sci U S A*, 1979. 76(1): p. 514-7.
29. Lengauer, C., K.W. Kinzler, and B. Vogelstein, *Genetic instabilities in human cancers*. *Nature*, 1998. 396(6712): p. 643-9.
30. Albertson, D.G., et al., *Chromosome aberrations in solid tumors*. *Nat Genet*, 2003. 34(4): p. 369-76.
31. Singleton, B.K., C.S. Griffin, and J. Thacker, *Clustered DNA damage leads to complex genetic changes in irradiated human cells*. *Cancer Res*, 2002. 62(21): p. 6263-9.
32. Papamichos-Chronakis, M. and C.L. Peterson, *Chromatin and the genome integrity network*. *Nat Rev Genet*, 2013. 14(1): p. 62-75.
33. Rowley, J.D., *Chromosome translocations: dangerous liaisons revisited*. *Nat Rev Cancer*, 2001. 1(3): p. 245-50.
34. Kowarsch, A., et al., *Correlated mutations: a hallmark of phenotypic amino acid substitutions*. *PLoS Comput Biol*, 2010. 6(9).
35. Ferguson, K.M., *Structure-based view of epidermal growth factor receptor regulation*. *Annu Rev Biophys*, 2008. 37: p. 353-73.
36. Hubbard, S.R., M. Mohammadi, and J. Schlessinger, *Autoregulatory mechanisms in protein-tyrosine kinases*. *J Biol Chem*, 1998. 273(20): p. 11987-90.
37. Zhang, Z., et al., *EGFR-mutated lung cancer: a paradigm of molecular oncology*. *Oncotarget*, 2010. 1(7): p. 497-514.
38. Storlazzi, C.T., et al., *Gene amplification as double minutes or homogeneously staining regions in solid tumors: origin and structure*. *Genome Res*, 2010. 20(9): p. 1198-206.
39. Lee, E.Y., et al., *Inactivation of the retinoblastoma susceptibility gene in human breast cancers*. *Science*, 1988. 241(4862): p. 218-21.
40. Das, P.M. and R. Singal, *DNA methylation and cancer*. *J Clin Oncol*, 2004. 22(22): p. 4632-42.

41. Ehrlich, M., *DNA hypomethylation in cancer cells*. Epigenomics, 2009. 1(2): p. 239-59.
42. Hoffmann, M.J. and W.A. Schulz, *Causes and consequences of DNA hypomethylation in human cancer*. Biochem Cell Biol, 2005. 83(3): p. 296-321.
43. Morey, S.R., et al., *DNA methylation pathway alterations in an autochthonous murine model of prostate cancer*. Cancer Res, 2006. 66(24): p. 11659-67.
44. Ehrlich, M., *DNA methylation in cancer: too much, but also too little*. Oncogene, 2002. 21(35): p. 5400-13.
45. Goetz, S.E., et al., *Hypomethylation of DNA from benign and malignant human colon neoplasms*. Science, 1985. 228(4696): p. 187-90.
46. Hoeijmakers, J.H., *Genome maintenance mechanisms for preventing cancer*. Nature, 2001. 411(6835): p. 366-74.
47. Swann, J.B. and M.J. Smyth, *Immune surveillance of tumors*. J Clin Invest, 2007. 117(5): p. 1137-46.
48. Schreiber, R.D., L.J. Old, and M.J. Smyth, *Cancer immunoediting: integrating immunity's roles in cancer suppression and promotion*. Science, 2011. 331(6024): p. 1565-70.
49. Houghton, A.N. and J.A. Guevara-Patino, *Immune recognition of self in immunity against cancer*. J Clin Invest, 2004. 114(4): p. 468-71.
50. Pardoll, D., *Does the immune system see tumors as foreign or self?* Annu Rev Immunol, 2003. 21: p. 807-39.
51. Kaufman, D.S., R.A. Schoon, and P.J. Leibson, *Role for major histocompatibility complex class I in regulating natural killer cell-mediated killing of virus-infected cells*. Proc Natl Acad Sci U S A, 1992. 89(17): p. 8337-41.
52. Trinchieri, G., *Recognition of major histocompatibility complex class I antigens by natural killer cells*. J Exp Med, 1994. 180(2): p. 417-21.
53. Lowe, J., *Modulation of immune responses by the tumor suppressor p53*. BioDiscovery, 2013. 2(8).
54. Xue, W., et al., *Senescence and tumour clearance is triggered by p53 restoration in murine liver carcinomas*. Nature, 2007. 445(7128): p. 656-60.
55. Li, H., et al., *Pharmacological activation of p53 triggers anticancer innate immune response through induction of ULBP2*. Cell Cycle, 2011. 10(19): p. 3346-58.
56. Siegel, R., et al., *Cancer statistics, 2014*. CA Cancer J Clin, 2014. 64(1): p. 9-29.
57. Biemar, F. and M. Foti, *Global progress against cancer-challenges and opportunities*. Cancer Biol Med, 2013. 10(4): p. 183-6.
58. Liang, X.J., et al., *Circumventing tumor resistance to chemotherapy by nanotechnology*. Methods Mol Biol, 2010. 596: p. 467-88.
59. Morrison, R., et al., *Targeting the mechanisms of resistance to chemotherapy and radiotherapy with the cancer stem cell hypothesis*. J Oncol, 2011. 2011: p. 941876.
60. Steinmetz, K.A. and J.D. Potter, *Vegetables, fruit, and cancer prevention: a review*. J Am Diet Assoc, 1996. 96(10): p. 1027-39.
61. Byers, T. and G. Perry, *Dietary carotenes, vitamin C, and vitamin E as protective antioxidants in human cancers*. Annu Rev Nutr, 1992. 12: p. 139-59.
62. Zhang, S.M., et al., *Intakes of fruits, vegetables, and related nutrients and the risk of non-Hodgkin's lymphoma among women*. Cancer Epidemiol Biomarkers Prev, 2000. 9(5): p. 477-85.

63. Woods, J.A., et al., *Exercise and cellular innate immune function*. Med Sci Sports Exerc, 1999. 31(1): p. 57-66.
64. Kruijssen-Jaarsma, M., et al., *Effects of exercise on immune function in patients with cancer: a systematic review*. Exerc Immunol Rev, 2013. 19: p. 120-43.
65. Frye, S.V., *Drug discovery in academic institutions*. Hematology Am Soc Hematol Educ Program, 2013. 2013: p. 300-5.
66. Ahmad, N., et al., *Differential antiproliferative and apoptotic response of sanguinarine for cancer cells versus normal cells*. Clin Cancer Res, 2000. 6(4): p. 1524-8.
67. Wilken, R., et al., *Curcumin: A review of anti-cancer properties and therapeutic activity in head and neck squamous cell carcinoma*. Mol Cancer, 2011. 10: p. 12.
68. Shehzad, A., F. Wahid, and Y.S. Lee, *Curcumin in cancer chemoprevention: molecular targets, pharmacokinetics, bioavailability, and clinical trials*. Arch Pharm (Weinheim), 2010. 343(9): p. 489-99.
69. Park, W., et al., *New perspectives of curcumin in cancer prevention*. Cancer Prev Res (Phila), 2013. 6(5): p. 387-400.
70. Prasad, S., A.K. Tyagi, and B.B. Aggarwal, *Recent developments in delivery, bioavailability, absorption and metabolism of curcumin: the golden pigment from golden spice*. Cancer Res Treat, 2014. 46(1): p. 2-18.
71. Wang, Y.J., et al., *Stability of curcumin in buffer solutions and characterization of its degradation products*. J Pharm Biomed Anal, 1997. 15(12): p. 1867-76.
72. Anand, P., et al., *Bioavailability of curcumin: problems and promises*. Mol Pharm, 2007. 4(6): p. 807-18.
73. Adams, B.K., et al., *EF24, a novel synthetic curcumin analog, induces apoptosis in cancer cells via a redox-dependent mechanism*. Anticancer Drugs, 2005. 16(3): p. 263-75.
74. Thomas, S.L., et al., *EF24, a novel curcumin analog, disrupts the microtubule cytoskeleton and inhibits HIF-1*. Cell Cycle, 2008. 7(15): p. 2409-17.
75. Das, U., et al., *3,5-Bis(benzylidene)-1-[3-(2-hydroxyethylthio)propanoyl]piperidin-4-ones: a novel cluster of potent tumor-selective cytotoxins*. J Med Chem, 2011. 54(9): p. 3445-9.
76. Dimmock, J.R., et al., *Synthesis and cytotoxic evaluation of mesna adducts of some 1-aryl-4,4-dimethyl-5-(1-piperidino)-1-penten-3-one hydrochlorides*. Pharmazie, 1995. 50(7): p. 449-53.
77. A.B. Okey, P.A.H., *Principles of Medical Pharmacology*. 7 ed. 2007: ELSEVIER, Toronto.
78. Dimmock, J.R. and W.G. Taylor, *Evaluation of nuclear-substituted styryl ketones and related compounds for antitumor and cytotoxic properties*. J Pharm Sci, 1975. 64(2): p. 41-9.
79. Chen, G. and D.J. Waxman, *Role of cellular glutathione and glutathione S-transferase in the expression of alkylating agent cytotoxicity in human breast cancer cells*. Biochem Pharmacol, 1994. 47(6): p. 1079-87.
80. Tsutsui, K., et al., *Chemosensitization by buthionine sulfoximine in vivo*. Int J Radiat Oncol Biol Phys, 1986. 12(7): p. 1183-6.
81. Howard, E.W., et al., *Evidence of a novel docetaxel sensitizer, garlic-derived S-allylmercaptocysteine, as a treatment option for hormone refractory prostate cancer*. Int J Cancer, 2008. 122(9): p. 1941-8.

82. Das, S., et al., *Bis[3,5-bis(benzylidene)-4-oxo-1-piperidinyl]amides: a novel class of potent cytotoxins*. ChemMedChem, 2011. 6(10): p. 1892-9.
83. Das, S., et al., *Dimeric 3,5-bis(benzylidene)-4-piperidones: a novel cluster of tumour-selective cytotoxins possessing multidrug-resistant properties*. Eur J Med Chem, 2012. 51: p. 193-9.
84. Das, S., et al., *Novel 3,5-bis(arylidene)-4-piperidone dimers: potent cytotoxins against colon cancer cells*. Eur J Med Chem, 2013. 64: p. 321-8.
85. Hansch C, L.A., *Substituent constants for correlation analysis in chemistry and biology*. 1979, John Wiley and Sons: New York. p. 49.
86. Rydzewski, R.M., *Real World Drug Discovery*. 2008, Oxford: Elsevier.
87. M. Suffness, T.D., *Methods of Cancer Research*. Vol. XVI. 1979, New York: Academic Press.
88. Sheskin, D., *Handbook of parametric and nonparametric statistical procedures*. 4 ed. 2004, London: Chapman & Hall/CRC-Taylor & Francis Group.
89. Goel, A., A.B. Kunnumakkara, and B.B. Aggarwal, *Curcumin as "Curecumin": from kitchen to clinic*. Biochem Pharmacol, 2008. 75(4): p. 787-809.
90. Rahman, M.A., *Caspase-family and apoptosis: an overview of therapeutic targets in cancer treatment*. Novel Science International Journal of Pharmaceutical Sciences, 2012. 1(9-1).
91. E.H. Kerns, L.D., *Drug-like Properties: Concepts, Structure Design and*

Methods: from ADME to Toxicity Optimization

2008, Burlington, MA: Elsevier.

92. P. Artursson, K.P., K. Luthman, *Advanced Drug Delivery Reviews*. Vol. 46. 2001: Elsevier. 27-43.
93. *Statistical Package for Social Sciences*, S.f.W. 2005: Chicago, US.
94. Elie, B.T., et al., *Water Soluble Phosphane-Gold(I) Complexes. Applications as Recyclable Catalysts in a Three-component Coupling Reaction and as Antimicrobial and Anticancer Agents*. Eur J Inorg Chem, 2009. 2009(23): p. 3421-3430.
95. Baraldi, P.G., et al., *Design, synthesis, and biological evaluation of new 8-heterocyclic xanthine derivatives as highly potent and selective human A2B adenosine receptor antagonists*. J Med Chem, 2004. 47(6): p. 1434-47.
96. C. Lema, A.V.-R., R.J. Aguilera, *Differential Nuclear Staining assay for high-throughput screening to identify cytotoxic compounds*. Current Cellular Biochemistry, 2011. 1.
97. Varela-Ramirez, A., et al., *Cytotoxic effects of two organotin compounds and their mode of inflicting cell death on four mammalian cancer cells*. Cell Biol Toxicol, 2011. 27(3): p. 159-68.
98. Santiago-Vazquez, Y., et al., *Novel 3,5-bis(arylidene)-4-oxo-1-piperidinyl dimers: structure-activity relationships and potent antileukemic and antilymphoma cytotoxicity*. Eur J Med Chem, 2014. 77: p. 315-22.
99. Ravindran, J., S. Prasad, and B.B. Aggarwal, *Curcumin and cancer cells: how many ways can curry kill tumor cells selectively?* AAPS J, 2009. 11(3): p. 495-510.
100. Shanmugam, R., et al., *A noncanonical Flt3ITD/NF-kappaB signaling pathway represses DAPK1 in acute myeloid leukemia*. Clin Cancer Res, 2012. 18(2): p. 360-9.

101. Wang, W.J., et al., *DAP-kinase induces apoptosis by suppressing integrin activity and disrupting matrix survival signals*. J Cell Biol, 2002. 159(1): p. 169-79.
102. Huang, Y., et al., *Evaluating DAPK as a therapeutic target*. Apoptosis, 2014. 19(2): p. 371-86.
103. Cohen, O., E. Feinstein, and A. Kimchi, *DAP-kinase is a Ca²⁺/calmodulin-dependent, cytoskeletal-associated protein kinase, with cell death-inducing functions that depend on its catalytic activity*. EMBO J, 1997. 16(5): p. 998-1008.
104. Kalvakolanu, D.V. and P. Gade, *IFNG and autophagy: a critical role for the ER-stress mediator ATF6 in controlling bacterial infections*. Autophagy, 2012. 8(11): p. 1673-4.
105. Wu, B., et al., *DAPK1 modulates a curcumin-induced G2/M arrest and apoptosis by regulating STAT3, NF-kappaB, and caspase-3 activation*. Biochem Biophys Res Commun, 2013. 434(1): p. 75-80.
106. Dimopoulos, K., P. Gimsing, and K. Gronbaek, *The role of epigenetics in the biology of multiple myeloma*. Blood Cancer J, 2014. 4: p. e207.
107. Sanchez-Cespedes, M., et al., *Gene promoter hypermethylation in tumors and serum of head and neck cancer patients*. Cancer Res, 2000. 60(4): p. 892-5.
108. Dansranjav, T., et al., *E-cadherin and DAP kinase in pancreatic adenocarcinoma and corresponding lymph node metastases*. Oncol Rep, 2006. 15(5): p. 1125-31.
109. Hasegawa, M., et al., *Patterns of gene promoter methylation in squamous cell cancer of the head and neck*. Oncogene, 2002. 21(27): p. 4231-6.
110. Michie, A.M., et al., *Death-associated protein kinase (DAPK) and signal transduction: regulation in cancer*. FEBS J, 2010. 277(1): p. 74-80.
111. Kissil, J.L., et al., *DAP-kinase loss of expression in various carcinoma and B-cell lymphoma cell lines: possible implications for role as tumor suppressor gene*. Oncogene, 1997. 15(4): p. 403-7.
112. Ng, M.H., *Death associated protein kinase: from regulation of apoptosis to tumor suppressive functions and B cell malignancies*. Apoptosis, 2002. 7(3): p. 261-70.
113. Ishak, D.H., et al., *A bismuth diethyldithiocarbamate compound promotes apoptosis in HepG2 carcinoma, cell cycle arrest and inhibits cell invasion through modulation of the NF-kappaB activation pathway*. J Inorg Biochem, 2014. 130: p. 38-51.
114. Zhang, J., et al., *Death-associated protein kinase 1 is an IRF3/7-interacting protein that is involved in the cellular antiviral immune response*. Cell Mol Immunol, 2014. 11(3): p. 245-52.
115. Raval, A., et al., *Downregulation of death-associated protein kinase 1 (DAPK1) in chronic lymphocytic leukemia*. Cell, 2007. 129(5): p. 879-90.
116. Chuang, M. and A.D. Chisholm, *Insights into the functions of the death associated protein kinases from C. elegans and other invertebrates*. Apoptosis, 2014. 19(2): p. 392-7.
117. Lai, M.Z. and R.H. Chen, *Regulation of inflammation by DAPK*. Apoptosis, 2014. 19(2): p. 357-63.
118. Jin, Y., E.K. Blue, and P.J. Gallagher, *Control of death-associated protein kinase (DAPK) activity by phosphorylation and proteasomal degradation*. J Biol Chem, 2006. 281(51): p. 39033-40.

119. Matsuzaki, H., et al., *Bikunin inhibits lipopolysaccharide-induced tumor necrosis factor alpha induction in macrophages*. Clin Diagn Lab Immunol, 2004. 11(6): p. 1140-7.
120. Elesa, C.R., et al., *Inhibition of p38 MAPK suppresses inflammatory cytokine induction by etoposide, 5-fluorouracil, and doxorubicin without affecting tumoricidal activity*. PLoS One, 2008. 3(6): p. e2355.
121. Tse, B.W., K.F. Scott, and P.J. Russell, *Paradoxical roles of tumour necrosis factor-alpha in prostate cancer biology*. Prostate Cancer, 2012. 2012: p. 128965.
122. Naude, P.J., et al., *Tumor necrosis factor receptor cross-talk*. FEBS J, 2011. 278(6): p. 888-98.
123. Takada, H., et al., *Role of SODD in regulation of tumor necrosis factor responses*. Mol Cell Biol, 2003. 23(11): p. 4026-33.
124. Jiang, Y., et al., *Prevention of constitutive TNF receptor 1 signaling by silencer of death domains*. Science, 1999. 283(5401): p. 543-6.
125. van Horsen, R., T.L. Ten Hagen, and A.M. Eggermont, *TNF-alpha in cancer treatment: molecular insights, antitumor effects, and clinical utility*. Oncologist, 2006. 11(4): p. 397-408.
126. Deng, G.M., *Tumor necrosis factor receptor pre-ligand assembly domain is an important therapeutic target in inflammatory arthritis*. BioDrugs, 2007. 21(1): p. 23-9.
127. Lu, H.F., et al., *Curcumin induces apoptosis through FAS and FADD, in caspase-3-dependent and -independent pathways in the N18 mouse-rat hybrid retina ganglion cells*. Oncol Rep, 2009. 22(1): p. 97-104.
128. Zheng, L., et al., *Competitive control of independent programs of tumor necrosis factor receptor-induced cell death by TRADD and RIP1*. Mol Cell Biol, 2006. 26(9): p. 3505-13.
129. Au, P.Y. and W.C. Yeh, *Physiological roles and mechanisms of signaling by TRAF2 and TRAF5*. Adv Exp Med Biol, 2007. 597: p. 32-47.
130. Schutze, S., V. Tchikov, and W. Schneider-Brachert, *Regulation of TNFR1 and CD95 signalling by receptor compartmentalization*. Nat Rev Mol Cell Biol, 2008. 9(8): p. 655-62.
131. Blackwell, K., et al., *TRAF2 phosphorylation modulates tumor necrosis factor alpha-induced gene expression and cell resistance to apoptosis*. Mol Cell Biol, 2009. 29(2): p. 303-14.
132. Festjens, N., et al., *RIP1, a kinase on the crossroads of a cell's decision to live or die*. Cell Death Differ, 2007. 14(3): p. 400-10.
133. Yoo, H.J., et al., *DAPk1 inhibits NF-kappaB activation through TNF-alpha and INF-gamma-induced apoptosis*. Cell Signal, 2012. 24(7): p. 1471-7.
134. Micheau, O. and J. Tschopp, *Induction of TNF receptor I-mediated apoptosis via two sequential signaling complexes*. Cell, 2003. 114(2): p. 181-90.
135. Helal, M., et al., *Mitochondrial dysfunction contributes to the cytotoxicity of some 3,5-bis(benzylidene)-4-piperidone derivatives in colon HCT-116 cells*. Bioorg Med Chem Lett, 2013. 23(4): p. 1075-8.
136. Boyum, A., *Isolation of mononuclear cells and granulocytes from human blood. Isolation of mononuclear cells by one centrifugation, and of granulocytes by combining centrifugation and sedimentation at 1 g*. Scand J Clin Lab Invest Suppl, 1968. 97: p. 77-89.

137. Lema, C.V.-R., A.; Aguilera, RJ, *Differential nuclear staining assay for high-throughput screening to identify cytotoxic compounds*. *Current Cellular Biochemistry*, 2011. 1(1): p. 1-14.
138. Kerbel, R.S., *Inhibition of tumor angiogenesis as a strategy to circumvent acquired resistance to anti-cancer therapeutic agents*. *Bioessays*, 1991. 13(1): p. 31-6.
139. Martin-Villalba, A., E. Llorens-Bobadilla, and D. Wollny, *CD95 in cancer: tool or target?* *Trends Mol Med*, 2013. 19(6): p. 329-35.
140. Deiss, L.P., et al., *Identification of a novel serine/threonine kinase and a novel 15-kD protein as potential mediators of the gamma interferon-induced cell death*. *Genes Dev*, 1995. 9(1): p. 15-30.
141. Inbal, B., et al., *DAP kinase links the control of apoptosis to metastasis*. *Nature*, 1997. 390(6656): p. 180-4.
142. Cohen, O., et al., *DAP-kinase participates in TNF-alpha- and Fas-induced apoptosis and its function requires the death domain*. *J Cell Biol*, 1999. 146(1): p. 141-8.
143. Yamamoto, M., et al., *DAP kinase activity is critical for C(2)-ceramide-induced apoptosis in PC12 cells*. *Eur J Biochem*, 2002. 269(1): p. 139-47.
144. Pelled, D., et al., *Death-associated protein (DAP) kinase plays a central role in ceramide-induced apoptosis in cultured hippocampal neurons*. *J Biol Chem*, 2002. 277(3): p. 1957-61.
145. Ivanovska, J., V. Mahadevan, and R. Schneider-Stock, *DAPK and cytoskeleton-associated functions*. *Apoptosis*, 2014. 19(2): p. 329-38.
146. Benderska, N. and R. Schneider-Stock, *Transcription control of DAPK*. *Apoptosis*, 2014. 19(2): p. 298-305.
147. Raveh, T. and A. Kimchi, *DAP kinase-a proapoptotic gene that functions as a tumor suppressor*. *Exp Cell Res*, 2001. 264(1): p. 185-92.
148. Raveh, T., et al., *DAP kinase activates a p19ARF/p53-mediated apoptotic checkpoint to suppress oncogenic transformation*. *Nat Cell Biol*, 2001. 3(1): p. 1-7.
149. Nam, Y.J., et al., *Inhibition of both the extrinsic and intrinsic death pathways through nonhomotypic death-fold interactions*. *Mol Cell*, 2004. 15(6): p. 901-12.
150. Gustafsson, A.B., et al., *Apoptosis repressor with caspase recruitment domain protects against cell death by interfering with Bax activation*. *J Biol Chem*, 2004. 279(20): p. 21233-8.
151. Koseki, T., et al., *ARC, an inhibitor of apoptosis expressed in skeletal muscle and heart that interacts selectively with caspases*. *Proc Natl Acad Sci U S A*, 1998. 95(9): p. 5156-60.

Vita

Yahaira Santiago Vazquez was born in the municipality of Humacao, located in the eastern coast of Puerto Rico. Before completing her schoolwork at Ana Roque High School in Humacao, Yahaira was awarded for her paint and participation in a contest sponsored by Medtronic and 'Alianza Para Un Puerto Rico Sin Drogas'. In 2002 she was admitted into the University of Puerto Rico at Humacao. She received a Bachelor of Science with a major in Biology, a minor in Microbiology and a component in Pedagogy from the University of Puerto Rico at Humacao on May 2007. During the following three years, she was employed as lab technician and administrative assistant of the Research Initiative for Scientific Enhancement (RISE) Program in the University of Puerto Rico at Humacao. During those years she had the opportunity to participate in workshops, seminars, conferences, symposiums, and teach undergraduate students. In August 2010, she entered the Graduate School of The University of Texas at El Paso. In 2014, an article entitled: "Novel 3,5-bis(arylidene)-4-oxo-1-piperidinyl dimers: Structure activity relationships and potent antileukemic and antilymphoma cytotoxicity" was published.

Permanent address: HC 12 BOX 5626
Humacao, Puerto Rico 00791

This thesis/dissertation was typed by Yahaira Santiago Vazquez.